Analytical process improvement of dried tomato value chain

PhD. Thesis

Main Supervisor: Dr. Yunny Meas Vong-CIDETEQ

Supervisor: Prof. Dr. Uwe Schmidt-HU

Dr. Genaro Soto Zarazúa-UAQ

Dr. Germán Orozco Gamboa-CIDETEQ

Dr. José de Jesús Pérez Bueno-CIDETEQ

To my family.

Acknowledgments

Thanks to the Mexican Council of Science and Technology (CONACYT) and the Council of Science and Technology of the State of Queretaro (CONCYTEQ) for their financial support to carry out this research. Thanks to the support of CONACYT's program Mixed-Scholarships it was possible to fulfill a research stay of 1.5 years to work in collaboration with the Biosystems Division of the Humboldt University of Berlin.

In particular thanks to each of the ones listed below for the following reasons:

Dr. Yunny Meas has been a great tutor who always encourages me to keep working in the research field. His high values, honorability and excellent reputation have been a guide for me.

Prof. Uwe Schmidt accepted me for doctorate with his outstanding team where I learned a good variety of agriculture knowledge.

Dr. Genaro Soto and Dr. Germán Orozco supported me constantly.

The company Nutrimeza supported me a lot with information, knowledge and dried products, especially Lic. Zaldumbide.

Dr. Klaus Gottschalk gave me the opportunity to have a research stay in the Leibniz Institute of Agriculture

Ma. Luisa Colina Irezabal shared a lot of knowledge that helped me understand the drying technology.

Rocío Vidal has always been essential support.

Víctor Rodriguez gave support to find solutions for logistics issues.

My project colleagues Juan Carlos Tapia, Luis Fernando García, Oscar Farias, Carla Uribe, Dolores Castañon and Fernanda Correa whose work is an essential complement of the present research.

Resumen

El presente estudio compara dos casos en ambientes totalmente diferentes: caso A) en Berlin, Alemania y caso B) en Querétaro Mexico.

El proceso de deshidratado de jitomates (*Solanum lycopersicon* L.) es de sumo interes por todos los beneficios que representa en cuanto al manejo del producto en el transpote y distribución, asi como el tiempo de vida y disponibilidad fuera de temporada.

A través de una metodología completa es propuesta una serie de acciones de eficiencia energetica, cambios en la logística, uso de energía renovable, interacciones de agua y energía. La diferencia en tecnología, condiciones ambientales, temporalidad de producción influyen en la necesidad de recursos de energía y agua. Esto deriva en diferentes propuestas de solución de acuerdo al caso. Las acciones exploradas en el desarrollo de ésta investigación son resumidas en:

-Abordar en su totalidad la cadena de valor de deshidratado de jitomate

-Es analizado el acoplamiento de procesos de pre y post cosecha, es decir, cultivo y deshidratado para optimización de consumo de recursos

-Construcción de zonas termodinámicas de operación (temperature, humedad y entalpía) -Evaluar huella de agua y de carbon

-Destacar la relevancia del efecto de la temporalidad en los recursos necesarios para implementar mejoras de proceso

-El empleo de energía renovable para dar valor agregado al producto

-Aplicar interacciones entre sub procesos de las cadenas de valor

-Diseñar y probar un sistema de deshidratado solar

Los resultados derivan en mejores atributos quantitativos de la cadena de valor, así como referencia de mejores prácticas en el sector agropecuario.

Abstract

In the present research the drying value chain is analyzed in terms of water and energy consumption. Two case studies in two different environments are compared: case A) in Berlin, Germany, and case B) in Queretaro, Mexico.

The drying process of tomatoes (*Solanum lycopersicon* L.) is of main interest due to the benefits of the impact on transport and distribution, as well on shelf life and product availability off-season.

Through a complete methodology a set of actions concerning energy efficiency, changes in logistics, use of renewable energy, water, and energy interactions is proposed. Different technology, ambient conditions and production seasonality influence energy and water need. As such, different solution proposals are derived according to each case. The actions explored in the development of this research are located in:

- Tackling the complete tomato drying value chain.

- Analysis of the coupling of pre- and post-harvest processes, namely growing and drying respectively, for resource consumption optimization.

- Constructing thermodynamic operation zones (temperature, humidity and enthalpy).

- Water and carbon footprint evaluation.

- Highlighting the relevance of the seasonal effect on resources needed for implementing process improvements.

- Using renewable energy and energy efficiency to add value to the product.

- Applying interaction between sub-processes in the value chains.

- Designing and testing a solar drying system.

Results from these derive in better quantitative attributes of the drying value chain, as well as a reference for best practices in the agribusiness sector.

Table of contents

Acknowledgments 4

Resumen 5

Abstract 6

Table of contents 7

Table of figures 11

Tables 14

Nomenclature 15

Chapter 1

1.1 Introduction to drying supply chains 17

1.2 Status of research 18

1.3 Relevance 18

1.4 Problem statement, research questions and hypotheses 20

1.5 Objectives and methodology 21

1.6 Outline of the thesis 22

Chapter 2

Stage 1: Base case of drying process value chain 24

2.1 Drying value chain 25

2.2 Dried tomato value chain sub-processes 26

2.2.1 Nutritional value of dried tomato 26

2.2.2 Quality standards for a dried product 27
2.2.2.1 Moisture content 28
2.2.2.2 Colour 29
2.2.2.3 Nutritional value 29
2.3 Two case studies 30
2.3.1 Case study A: Berlin 31
2.3.2 Case study B: Queretaro 32
2.4 Generalities of unitary processes 34
2.4.1 Growing in greenhouses 34
2.4.2 Harvest and transport 36
2.4.3 Drying 37
2.4.3.1 Drying kinetics 38
2.4.3.2 Energy consumption due to environment 41
2.4.3.3 Mass and energy balance (macrolevel) 45
2.4.3.4 Intermittent drying 45
2.4.3.5 Solar drying 46
2.4.3.6 Thermodynamic states calculation 47
2.4.3.7 Simulation 53
2.4.3.8 Control design 54
Chapter 3
Stage 2. Pre-benchmarking 57
3.1 Case study A: *reference* value chain 58
3.1.1 Data compilation 58
3.1.2 Comparison with current practice 61
3.1.2.1 Production and crop residues 61

3.1.2.2 Water flow 61
3.1.2.3 Energy flow and associated CO_2 emissions 63
3.1.3 Indicators 65
3.1.2.4 Statistical analysis 66
3.1.3.1 Production and residues 66
3.1.3.2 Water footprint 67
3.1.3.3 Carbon footprint 68
3.2 Case B: *baseline* drying simulation 71
3.2.1 Data compilation 71
3.2.2.1 Batch and time dependent heat flow 73
3.2.3 New performance indicators 77
3.2.3.1 Exergy in the drying process 77
3.2.3.2 Exergy in greenhouses 79
Chapter 4
Stage 3. Interaction analyses 81
4.1 Case A: heat exchange 81
4.2 Case B: exergy and energy 84
Chapter 5
Stage 4 and 5: implementation strategy and post-benchmarking 90
5.1 Case A: *collector* value chain 91
5.1.1 Implementation strategy 91
5.1.2 Post-benchmarking 92
5.1.2.1 Water and energy measurements impact 94
5.1.2.2 Energy measurements impact 98

5.2 Case B: *solar dryer* 103
5.2.1 Implementation strategy 103
5.2.2 Post-benchmarking 104
5.2.2.1 Drying experimental prototype 104
5.2.3 Test under case B conditions 111
5.2.3.1 Temperature and relative humidity profiles 112
5.2.3.2 Exergy and energy 118
5.2.3.3 Product quality 121
5.3 Economic evaluation 126
5.3.1 Cost and community 128
Chapter 6
6.1 General conclusions 130
6.2 Further research 132
Appendix 1. Basic concepts used for drying 133
Appendix 2. Tools 134
Mollier diagrams 134
Sankey diagrams 135
Matlab tool 135
Appendix 3. Statistiscs 136
Appendix 4. Values of parameters 138
Appendix 5. Complementary images 140
References 142

Table of figures

Fig. 1 Thesis outline 23
Fig. 2 General drying value chain 26
Fig. 3 Growing in greenhouses 34
Fig. 4 Drying process steps 38
Fig. 5 Drying kinetics of tomato(3 repetitions) 40
Fig. 6 Characteristic drying curve of a market tomato (3 repetitions) 40
Fig. 7 Diffusion mechanism of tomato drying. T=60°C, hr=20%, v_a=0.85 ms^{-1} 41
Fig. 8 Mollier diagram of an industrial conventional drying process at 85°C, hr 3% 43
Fig. 9 Mollier diagram of different drying energy consumption due to humidity 44
Fig. 10 Solar heater and drying chamber 47
Fig. 11 Schematic of the equations used for the solar drying simulation 55
Fig. 12 Schematic of the simulation of heating air in the solar dryer 55
Fig. 13 Schematic of the simulation in the drying chamber 56
Fig. 14 Mollier diagram: ambient (triangles), reference greenhouse (diamonds) and air heater (circles). 60
Fig. 15 Water content in the tomato produce from the reference greenhouse 67
Fig. 16 Water flow for the *reference* configuration 69
Fig. 17 Water flow per kilogram of tomato 72
Fig. 18 Temperature profiles for a winter day (D1) 74
Fig. 19 Temperature profiles for a spring day (D2) 74
Fig. 20 Moisture content (M) and air absolute humidity (ω3) in the drying process of a winter day (D1) 75
Fig. 21 Moisture content (M) and air absolute humidity (ω3) in the drying process of a spring day (D2) 75

Fig. 22 Heat load for a winter day (D1) from solar heater (Q2), in the greenhouse without heating/cooling (Q4) and with heating/cooling (to set point) 76
Fig. 23 Heat load of a spring day (D2) from solar heater (Q2), in the greenhouse without heating/cooling (Q4) and with heating/cooling (to set point) 76
Fig. 24 Exergy on a winter day (D1). Ambient conditions (ex2), exhaust air (ex3) and within the greenhouse (ex4) 80
Fig. 25 Exergy on a spring day D2. Ambient conditions (ex2), exhaust air (ex3) and within the greenhouse (ex4)..... 80
Fig. 26 Schematic of the energy interaction for the Berlin case..... 82
Fig. 27 Temperature and energy availability from the storage tank..... 83
Fig. 28 Schematic interactions growing in greenhouse drying (states)..... 85
Fig. 29 Absolute humidity on a winter day (D1) at the dryer outlet (ω3), within the greenhouse (ω4) and from the mixing (ω5)..... 87
Fig. 30 Absolute humidity on a spring day (D2) at the dryer outlet (ω3), within the greenhouse (ω4) and from the mixing (ω5)..... 87
Fig. 31 Temperature and relative humidity on a winter day (D1) within the greenhouse (T4, hr4) and from the mixing (T5, hr5) 88
Fig. 32 Temperature and relative humidity on a spring day (D2) within the greenhouse (T4, hr4) and from the mixing (T5, hr5) 88
Fig. 33 Water content considering tomato 94.6%, leaves 84% and stems 86% moisture content 94
Fig. 34 Water flow for the *collector* configuration 96
Fig. 35 Comparison of greenhouse transpiration and ventilation..... 96
Fig. 36 Comparison of fresh water and plant uptake per month in greenhouses 97
Fig. 37 Energy flow interaction for a coupled system..... 100
Fig. 38 Temperature and energy availability from the storage tank..... 101
Fig. 39 Array of the drying system..... 108

Fig. 40 a) Detail of the resistance inside the storage tank and b) heat exchanger 108
Fig. 41 a) Air circulation system and b) air deflector 109
Fig. 42 a) Parts of the drying chamber and b) tray trolley with wheels 109
Fig. 43 Trajectory lines from the air inlet 110
Fig. 44 Velocity distribution of flow 110
Fig. 45 Partially charged dryer 22 kg *28.01.2015* 113
Fig. 46 End of the test partially charged dryer *29.01.2015* 113
Fig. 47 Temperature and humidity inside the drying chamber for 4 days. Starting at 10 am 114
Fig. 48 Adjustment for temperature results 114
Fig. 49 Result of run with empty load for a span of 10 hours *21.01.2015*. Starting at 4pm 116
Fig. 50 Temperature (T3) and absolute humidity (ω3) inside the drying chamber on *25.06.2015* 116
Fig. 51 Humidity (Hr3) trend inside the drying chamber *25.06.2015*. The main curve is split and displaced to the left. The first part corresponds to the measurement 117
Fig. 52 Exergy use potential from the drying air inside the drying chamber ... 117
Fig. 53 Mollier diagram for test *25.06.2015* ambient conditions (T1) and inside drying chamber (T3) 119
Fig. 54 Energy from solar source (Q1) and effectively used in air heating (Q3), test *25.06.2015* 120
Fig. 55 The efficiency obtained from the solar resource and the real heating of the air, test *25.06.2015* 120
Fig. 56 Drying process comparison of solar and oven conditions, test *25.06.2015* 123
Fig. 57 Lycopene content in the solar drying process, test *25.06.2015* 123
Fig. 58 Acidity of the dried tomatoes, test *25.06.2015* 124

Fig. 59 Brix grades of dried tomatoes, test *25.06.2015* 124
Fig. 60 Vitamin C content of dried tomatoes, test *25.06.2015* 125
Fig. 61 Colour of dried tomatoes in its values (L) (a*) (b*), test *25.06.2015* .. 125
Fig. 62 Payback time of *solar dryer* proposal 128

Tables

Table 1. Main resources case: industrial conventional drying at 85°C, Hr 3%, case: solar drying 40°C Hr 10% 20
Table 2. Case study characteristics: Berlin 31
Table 3. Case study characteristics: Queretaro 33
Table 4. Thermodynamic states in *reference* greenhouse 59
Table 5. Water footprint (L kg^{-1} tomato) for *reference* process configuration... 69
Table 6. Energy flow (MJ kg^{-1} tomato) of the *reference* drying value chain 70
Table 7. Water (L kg^{-1}) and carbon footprint (kg CO_2 kg^{-1}) of the *reference* drying value chain 70
Table 8. Water added per plant per day [89] 72
Table 9. Thermal energy interaction 83
Table 10. Thermodynamic states in *collector* greenhouse 93
Table 11. Water consumption for the *collector* value chain 97
Table 12. Energy requirement for drying (tomato classes B+C) in the *collector* value chain 100
Table 13. Energy flow (MJ kg^{-1} tomato) of the *collector* drying value chain .. 101
Table 14. Water and carbon footprint of the *collector* value chain 102
Table 15. Electricity requirements of *solar dryer* 111
Table 16. Characteristics of the photovoltaic system 112
Table 17. General characteristics of test A 25.06.2015 112
Table 18. Energy distribution in the system 126

Table 19. Economics of solar energy system. Values of 08.07.2015 in Mexican economy. 127

Nomenclature

Δz Distance between trays (m)

Δx Distance between two points in the dryer (m)

ρ Density (kg m^{-3})

θ Latitude (°)

a,b,k Diffusion model constants

BER Blossom end rot

C_p Specific heat (kJ kg^{-1} K^{-1})

ex Exergy (kJ kg^{-1} dry air)

F Amount of fresh product (kg)

h Enthalpy (kJ kg^{-1} dry air)

h_{cv} Convective heat transfer coefficient ($Wm^{-2}K^{-1}$)

hr Relative humidity (%)

I_g Solar radiation (Wm^2)

L Length (m)

M Moisture (kg kg^{-1}, d.s.)

m_a Mass flow rate of air (kg s^{-1})

P Pressure (h Pa)

Q Heat flow (MJ)

Q_{ah} Energy of rejected air heating (MJ)

Q_{sh} Energy for heating solids from ambient temperature to the drying air temperature (MJ)

Q_{we} Energy for water evaporation (MJ)

S Entropy (kJ kg^{-1})

T Temperature (°C)

t Time (h)

T_{wb} Wet bulb temperature (°C)

X Moisture content referred to wet basis (%)

Y Ambient humidity (kg kg^{-1} dry air)

ω Absolute humidity (kg water kg^{-1} dry air)

Subscripts

1 State 1 ambient condition

2 State 2 outlet air heater, inlet to the drying chamber

3 State 3 outlet drying chamber

4 State 4 greenhouse conditions

5 State 5 hypothetical mixing from drying

c cover

r receiver

a air

i at i time

l,w liquid water

p product

v vapor

am ambient

e,0 equilibrium, initial

f final

Chapter 1

1.1 Introduction to drying supply chains

The term *dehydration* refers to the removal of moisture from a material with the primary objective of reducing microbial activity and product deterioration [1].

The drying process value chain is definitely the most used post-harvest operation necessary for conservation of fruit and vegetables. In addition, the reduced weight and bulk of dehydrated products decreases packaging, handling and transportation costs [2]. Nonetheless, drying is highly energy intensive because almost 99% of applications involve the removal of water [3], where the latent heat of vaporization is 2500 kJ kg^{-1} at 0°C.

The close relationship between water and energy consumption in the food sector [4], has an impact not only on the final product price but also on resource management. Therefore, the implementation of process efficiency improvements and renewable energy supply is of positive economic and environmental relevance.

An approximate estimate indicates that about 20% of the world fruit and vegetable production is subjected to drying; more than 50% is consumed as fresh, 20% as frozen, 5% as canned and 5% as pickled [5]. It is difficult to estimate the energy consumption for food drying in the agrifood sector due to the large variety of physical and thermal characteristics of products, quality requirements and used technologies; a reported estimation was 12% in England and 27% in France ([6], [7]).

Currently, in a commercial dryer, the energy required to evaporate 1 kg of moisture from a product ranges from 3.5 to 7.0 MJ [8]; the water to be removed for one ton of fresh product is 50 L for each 5% of desired moisture content reduction.

1.2 Status of research

Most studies report drying as a unit process; they show that energy efficiency is not very high since 85% of installations for industrial processes involve inefficient convective dryers [3], in which exergy efficiency is low mainly due to irreversibility, such as exhaust wet air, low isolation of dryer walls, and within the product itself [9]. However, increasing efficiency has an economical impact. The price of input resources along the value chain for extending product shelf life, which is worth optimization studies, can also lead to positive environmental impact as well as economic savings. In addition, issues such as availability of water resources, plus energy and grid systems integration, are common in the field-agribusiness sector of developing countries.

Process improvement is mainly triggered by quality, safety, environmental considerations or economic potentials [10]. There has been an increasing trend in recent years to tackle problems such as process integration or energy interaction for optimization of resource use of whole value chains, while studies in the past focused solely on unit scale processes.

Additionally, an important point to keep in mind is that agriculture has a strong correlation with seasonal factors; thus, any process evaluation or improvement should include time factors for planning and logistics. Different studies ([11], [12], [13], [14]) imply a high impact of temporal and geographical factors where the carbon and water impact varies depending on whether consumption is in- or off-season.

1.3 Relevance

The focus on drying analysis is taken from the point of view of the dried product, in order to obtain the highest quality of delivered items as possible. However, drying is also a subject of attention since a huge quantity of energy is needed to fulfill the drying level purpose due to the high latent heat of

evaporation of water. Thus it is relevant to use renewable energy as well as energy efficiency measures and heat recovery systems in drying processes. Solar thermal energy for drying is a proven technology that has been applied to different products and loads ([15], [16], [17]) where the final benefits are determined by design and operation conditions. However, as Ímre [17] states, there are intrinsic temporal and geographical factors, which can only be economically useful if the drying application can be matched to the specific incident solar radiation characteristics. Using only solar thermal energy has the disadvantage that the available sunny hours are mostly not sufficient to reach the required drying levels. This usually requires backup heating systems to guarantee the right operation conditions in order to avoid tissue damage or variances in the drying level of the product.

Several studies on dryers have demonstrated that the use of solar energy for drying is an interesting alternative when it comes to cost investment and manipulation. In addition, depending of the solar dryer design, solar drying has no significant negative impact on the product's quality ([18], [19]).

However, in general, the reference case used in these studies is open sun drying. In addition, as it is known giving the nature of solar resource, the operation range of solar drying is variable and, in comparison with conventional industrial air drying, operation temperatures are significantly lower.

Required energy is very high when processing product in industrial quantities, but also residual water becomes a significant factor – since drying means to take away the water in fruit and vegetables that in majority have 2.33 to 19 kg kg^{-1} dry solids. Table 1 compares cases for conventional drying and solar conditions; it shows energy consumption (Q), water removed ($m_{w)}$, initial moisture content (M_o) and amount of air needed, (m_a,) to reach 0.10 and 0.43 kg kg^{-1} dry solids of moisture ($M_{f)}$ for different quantities of fresh tomato products that initially had 19 kg kg^{-1} dry solids.

Table 1. Main resources case: industrial conventional drying at 85°C, Hr 3%, case: solar drying 40°C Hr 10%

Drying of tomato (9 hr)	Case 1		Case 2	
$m_{f,}$ final mass of dried product (kg)	50	50	50	50
F, initial mass of fresh product (kg)	958	737	958	737
$M_{0,}$ initial moisture content (kg kg^{-1} dry solids)	19	19	19	19
M_f , final moisture content (kg kg^{-1} dry solids)	**0.43**	**0.1**	**0.43**	**0.1**
$m_{a,}$ air mass required (kg)	12160	9199	41750	31585
$m_{w,}$ water removed (kg)	908	687	908	686
Energy for water evaporation (kWh)	610	462	619	487

1.4 Problem statement, research questions and hypotheses

Tomato is one of the major and most important agriculture products worldwide; its high moisture and susceptive tissue nature make it a target product for the pursuit of constant post-harvest value chain process improvement. Water scarcity in agriculture zones and the high energy consumption of the tomato drying value chain leads to state the following research questions:

1. How can the water and energy consumption along the value chain be reduced considering two cases of temporal and location conditions?

2. What is the quantitative impact of water and energy consumption reduction?

From these are derived the following hypotheses:

a) Water and energy consumption along the value chain can be reduced by water and energy interactions, recycling methods and use of renewable energy.

b) Along the value chain, water consumption can be reduced by at least 30% and energy consumptions by at least 30%, with variations according to temporal and location conditions.

1.5 Objectives and methodology

The hypotheses and research questions are translated in the two objectives:

1. Find ways to reduce water and energy consumption along the value chain addressed to two different temporal and location conditions

2. Assess the quantitative impact of water and energy consumption reduction

To reach these objectives **the unified methodology for thermal energy efficiency improvement** developed by Mateos Espejel et al. [10] is used, where the target is **energy enhancement through interactions of the utility and process systems**. This methodology was elaborated for industrial chemical processes, where several flow processes interfere. However, for process integration at a value chain level, the methodology was selected for its inclusive feature which can implement and compare in a clear way the introduced process improvements.

The general aspects of the stages used in this work are listed as follows:

Stage 1. Base case: the data gathering, master diagram, systems analysis and computer simulation take place.

Stage 2. Pre-benchmarking: the data compilation, comparison to the current practice, new performance indicators (energy and exergy) and targeting are carried out.

Stage 3. Interaction analysis: is comprised of steps 1) internal heat recovery; 2) water reutilization; 3) elimination of non isothermal mixing; 4) energy upgrading; 5) condensate recovery; and, 6) energy conversion.

Stage 4. Implementation strategy: is the development of the energy improvement measurements where the limiting factors are mainly economic.

Stage 5. Post-benchmarking: where finally the improvement in energy efficiency of the current processes is assessed.

Each of the stages is described in a more complete and detailed way at the beginning of the section of the presented work where it is developed.

Stage 1 of the methodology is applied for the general case of value chain; consequently, **stages 2 to 5** are developed to compare **two case studies** (case A and case B) under different temporal and location conditions. It is important to mention that for each of the cases, different steps from the methodology are applied according to decisions taken to solve each of the specific problems.

1.6 Outline of the thesis

Fig. 1 displays the working structure and schematic synthesis of this research, where:

Chapter 1 has the overall introduction to the problematic of drying value chains and the interest driving this study. The research description is also stated.

Chapter 2 includes **stage 1** of the followed methodology where the reference base case of the studied value chain is described. The unit processes or sub-processes are defined and a state of art of each item is given. In addition, the description of the two case studies is stated.

Chapter 3 contains **stage 2** which includes the data compilation, comparison with the base case and the steps applicable for each specific case study.

Chapter 4 tackles **stage 3** of the methodology, covering the proposed energy interaction for each of the case studies.

Chapter 5 reports **stage 4** with the implementation strategy and **stage 5** with the evaluation of the derived measures in the post-benchmarking situation.

Chapter 6 is comprised of the final remarks of the research: conclusions and further research.

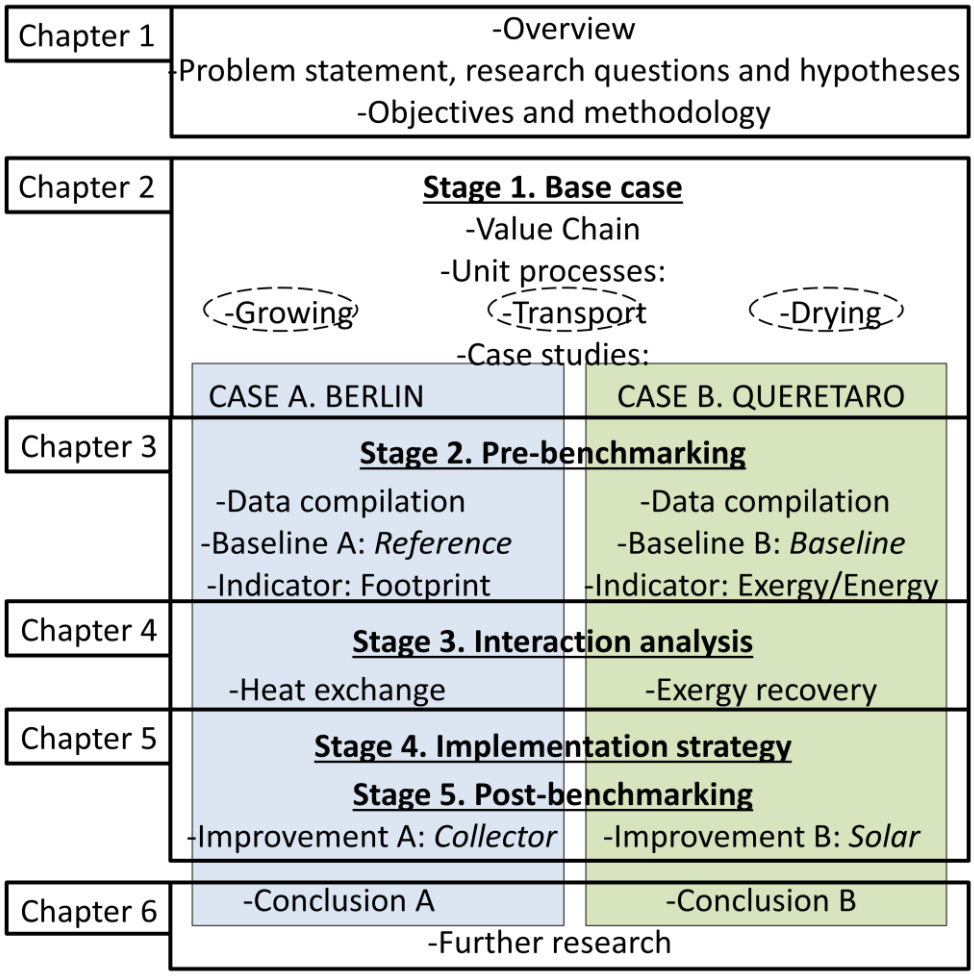

Fig. 1 Thesis outline

Chapter 2

Stage 1: Base case of drying process value chain

The definition of the base case is fundamental in the process analysis and it consists of developing the utility systems, the process diagram and the overall balances. Additionally, for any energy study is important to build a representative computer simulation to assess the impacts of possible process modifications [20]. The base case represents the current steady state of all process units. The procedures that define it are:

Master diagram, the general drying value chain is described as a starting point, consequently the specific tomato value chain steps are defined to identify and set the sub-process on which the research is going to be focused. In parallel, the specific flow diagrams are sketched.

Data gathering, all system operational characteristics are identified and the thermal and water performance data are collected from the data acquisition measuring devices for the time span of interest. When working with solar thermal applications it is important to describe the trends in two ways: i) throughout the day; and ii) throughout the year.

Systems analysis, the general state of the art of the unitary processes which comprise the value chain are described with a focus on their energy consumption. This is used to identify and work further on all value chain improvements, simulation and energy interaction.

Computer simulation, the detailed simulation in a Matlab^{TM} environment is limited to the drying process given that it is the main part of the drying value chain employed in the work.

2.1 Drying value chain

The generic drying value chain of fruit and vegetables could be described with Fig. 2 where seven sub-processes take place. The growing of the products take place either in open fields or in different technology levels of protected agriculture systems. Depending on the product to be dried some steps are skipped, such as washing, disinfection or thermal pre-treatments, and some others steps are added, such as different drying stages/processes where different drying levels are reached depending of product-specific operations. The size of product pieces or slices is one of the key factors influencing drying quality. For industrial levels the highest possible storage shelf life of products is sought.

Huge quantities of resources are related to water manipulation-transformation in the identified nine sub-processes of the fruit and vegetables drying value chain: starting with the water used for irrigation in fields and greenhouses, water input for washing and disinfection, then the cost of moving that water within the product from production zones to processing clusters; in addition, and as mentioned, a lot of energy is invested in removing water from products in low efficiency drying processes. It is remarkable that the resources needed are higher while higher the specific targets of shelf life, appearance, and final moisture or nutraceutical requirements in the quality of the product. If we analyze the high level value chain and add in all the irreversibility factors the total efficiency becomes even lower, besides water and fuel requirements being high.

Once operational conditions and the best configuration are set by the unitary processes to meet quality needs, it becomes feasible when the whole value chain for fruits and vegetables is observed to link sub-processes for reducing time, transport, water and energy consumption by using recovery systems and renewable energy.

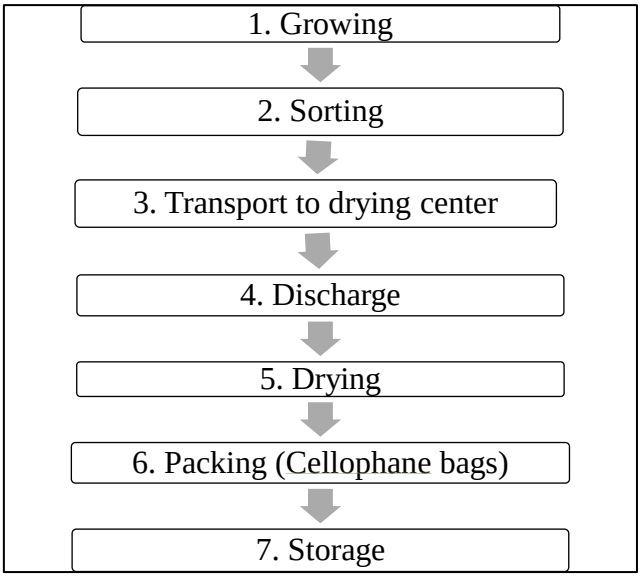

Fig. 2 General drying value chain

2.2 Dried tomato value chain sub-processes

This work focuses specifically on the detailed evaluation of sub-processes **1. Growing in greenhouses** and **5. Drying** (Fig. 2) based on the fact that both display similar characteristics to be improved:

1) **high thermal energy requirement** to fulfill the operation conditions to obtain best product quality,

2) **different seasonal/time trends** and

3) the need to **reduce transportation** energy.

2.2.1 Nutritional value of dried tomato

Several scientific studies have shown that the nutritional value of tomato could be enhanced through different types of processing ([21] [22], [23]).

In the case of air drying, it has been determined that product degradation may be decreased with the combination of milder temperatures and reduced residence time [24]. Additionally, a study from Chang et al. [25] reports the effects on

tomato´s antioxidant properties and against the notion that processed fruit has lower nutritional value than fresh fruit, as their results indicated the drying process increases parts of the total flavonoids, total phenolics and lycopene contents.

2.2.2 Quality standards for a dried product

Drying affects the physical properties of a product, changing its size, shape, colour and texture; also many chemical and enzymatic conversions take place.

From the complete research of Augustus Leon et al. [15], it is summarized that quality assessment of dried products usually includes assessment of **1) sensory, 2) nutritional parameters** and **3) rehydration capacity**.

Product sensory quality assessment is a combination of different senses of perception from the potential consumer, including: appearance judged by the eye, e.g. colour, size, shape, uniformity and absence of defects; sense of taste, e.g. sweet, sour, salty and bitter; and flavour perception involving the senses of taste, smell and feel [15].

As St. George et al. [26] summarize, the major biologically active compounds in tomatoes are carotenoids, ascorbic acid, folate, polyphenols and vitamins A and E. However, drying generally affects the nutritive value of food due to the potential of enzyme-catalyzed reactions, non-enzymatic and Maillard reactions, protein denaturation and nutrient loss like vitamins A and C.

The rehydration ratio is the capacity of the dried product to recover its original volume. In this work this characteristic lies outside of the study since dried tomato itself is the final product, and it is not used as a feed resource for other food processes.

Thus, the considered factors in this work to evaluate the quality of the dried tomato are: 1) **moisture content;** 2) **colour;** and 3) **nutritional value** in terms of lycopene content, ascorbic acid and total phenolics.

2.2.2.1 Moisture content

The main parameter in food dehydration processes is the moisture content (M) in the form of molecules of water expressed in (kg water kg^{-1} dry solids (d.s.)). A related concept is water activity (a_w) or the equilibrium relative humidity [27] which is defined as the ratio of the equilibrium vapour pressure within the product to the saturation vapour pressure. When water activity is reduced it interrupts microbial growth or spore germination. Usual values of dried fruit with a moisture content of 0.22-0.39 kg kg^{-1} d.s. have water activity of 0.7-0.8 while dried vegetables with 0.16–0.31 kg kg^{-1} d.s. have water activities of 0.7-0.77 [5].

Within a product, the initial mass of the fresh product F (kg) equals the final dried mass of the product m_f (kg dry solids or kg, d.s.) plus the mass of the water m_w (kg water). The moisture content could be expressed in dry basis (M) referring to the dried solids, or in percentage (X) referring to the wet basis – or product mass (F). Definitions are described as follows:

$$F = m_f + m_w \quad (1)$$

$$M = \frac{m_w}{m_f} = \frac{F - m_f}{m_f} \quad (2)$$

$$M_{wb} = \frac{m_w}{F} = \frac{F - m_f}{F} \quad (3)$$

$$X = 100\, M_{wb} \quad (4)$$

The balance of the air drying process, Eq. (1), is complemented with the air mass m_a (kg) which is the same at the beginning and the end of the process; however at the end it is present as mixture of wet air.

$$F + m_a = m_f + m_w + m_a \quad (5)$$

2.2.2.2 Colour

Evaluation of colour is one of the first quality attributes a consumer perceives in any food and it influences other attributes, such as flavor – change of colour is generally accompanied by flavour changes.

Changes of colour derived from air drying are a combination of both enzymatic and non-enzymatic browning, Maillard reactions and the degradation of lycopene ([28], [29]).

Colour assessment is based on the tridimensional colour space CIE L*a*b* specified by the International Commission on Illumination, where L is the lightness of the color, a* indicates the red-green position and b* indicates the blue-yellow position. This space in cylindrical coordinates is determined by the hue (h°), and chroma (C*), which are described as

$$h° = tan^{-1}(\frac{b^*}{a^*}) \quad (6)$$

$$C^* = \sqrt{a^{*2} + b^{*2}} \quad (7)$$

Usually the value of a* is related to the lycopene content. In a comparative study from Shi et al. [30], progressive deterioration of overall colour quality with lowered values of (a*) and (L*) in the conventional air drying process was found. Gómez-Gómez [31], presents results from slices of tomato dried at 60°C and 1.2 ms^{-1} with values of L*=34.12, a*=20.49, b*=29.05, C= 35.55 and h=54.8 (from values of fresh sample of L*=37.52, a*=18.18, b*=15.37).

Unadi et al. [32], established a scale to determine the quality of dried product based in chromaticity, where values >20 determine an excellent quality, values of 17 to 20 a very good quality, from 14 to <17 a good quality and <14 a poor quality.

2.2.2.3 Nutritional value

Lycopene is the main carotenoid present in tomato and is responsible for its colour; the ascorbic acid is the biologically active form of vitamin C and the phenolic compounds are a group of 8000 secondary metabolites from which polyphenols are produced in tomato.

The oxidation and isomerization of lycopene are complex processes depending on many factors, such as moisture, oxygen availability, low water activity, high temperatures, instability of metallic ions like Cu or Fe, presence of pro- and antioxidants, and lipids ([30],[33]). The lycopene content from dried tomatoes with standard humidity may reach 50-70 mg per 100 g product [34]. The study of Gómez-Gómez [31], presents results in fresh tomato of 34.9±0.15 mg/ 100 g total solids and, after air drying at 60°C and 1.2 ms airflow, of 30.6±1.5 mg/ 100 g total solids.

The loss of ascorbic acid is dependent on the presence and type of heavy metals, such as copper and iron, light, water activity level in the product, dissolved oxygen, and the temperature of drying. The losses of ascorbic acid during drying have been between 10% and 50% [27]. The study of Gómez-Gómez [31], presents results in fresh tomato of 360.7±1.1 mg $(100\ g\ total\ solids)^{-1}$ and, after air drying at 60°C and 1.2 ms^{-1} airflow, of 263±0.7 mg $(100\ g\ total\ solids)^{-1}$.

Regarding total phenolics, a value of 99.81±14.91 mg EAG $(100g\ total\ solids)^{-1}$, and after drying a loss of 9.5%, was found in fresh tomatoes [31].

2.3 Two case studies

Due to the broad variation of conditions for the drying value chain two opposite cases have been selected. The main differences of these are the climatologic conditions and the technology used. In a complex combination, the weather, technology, seasonality, practices and resource availability are compared.

Solutions and improvements can never be generalized. As in most cases, one of the main concerns and eligibility of solutions derived for already established

processes is less investment. By following the methodology, this work reflects how the problems in the two cases are tackled and lead to different possible solutions. The steps from the followed methodology were selected according to data availability and technological performance.

2.3.1 Case study A: Berlin

The main characteristics of the case study are summarized in Table 2.

Table 2. Case study characteristics: Berlin

Description	Cold and humid
Ambient conditions:	T=12°C, Hr=68.5% (year average)
Latitude:	52° 31’
Atmospheric pressure:	1015 mB
Sunlight hours:	May: 14 h, Jun.: 15 h, Jul.: 16 h, Aug.: 15 h, Sep.: 14 h and Oct.: 12 h.
Greenhouse	
Season:	April-May to October-November
Description:	High tech
Wall material:	Glass
Characteristics:	High humidity, variation of sunshine hours and low irradiation
Energy problems:	High heating requirements
Drying process	
Season:	April-May to November
Characteristics:	High humidity, variation of sunshine hours and low irradiation

The studied system is the established and ongoing “Low Energy Greenhouse” (ZINEG- ZukuftsInitiative NiedrigEnergy Gewächshaus) project. The ZINEG German macro project (2009-2014) was sponsored by the Federal Ministry for Environment, Nature Conservation and Nuclear Safety and the Rentenbank

managed by the Federal Ministry of Food and Agriculture, with assistance of the Federal Agency for Agriculture and Food. The presented treatment of data is with the approval of Prof. Uwe Schmidt, responsible for the project based in the Humboldt University of Berlin.

This project comprises a high technological greenhouse with the objective of reducing fossil fuel consumption. When the growing process is joined with the post-harvest process, it is possible to reach better results, i.e. the energy collected from growing at the ZINEG project is used for the post-harvest process.

This case study is addressed to appraise and compare the water and carbon footprints in the tomato drying value chain reflecting the temporal variation during the season due to the broad and continuous measurement of data. The analysis is done during the whole season in order to draw the trend for during the year. The daily basis was not selected because there is variation in a day's duration, which complicates a comparison. Hence the trend should be described per month given that whatever the average value is it will have a considerable variation among days. Two process conditions are compared in the growing phase.

This section of research is reported in the published paper in the Journal of Cleaner Production: **Water and carbon footprint improvement for dried tomato value chain** under reference DOI 10.1016/j.jclepro.2015.05.007 [35].

2.3.2 Case study B: Queretaro

The main characteristics of the case study are summarized in Table 3.

This case study research is sponsored by the Council of Science and Technology of the State of Queretaro CONCyTEQ (Project number: M0016- 175136) in the macro project Mixed Funds (FOMIX-2011-02): **Capacity, technologies and innovation development for renewable energy use in the agribusiness sector of Queretaro state**. ("Desarrollo de capacidades, tecnologías e innovación para

el aprovechamiento de energías renovables en el sector agroindustrial del Estado de Querétaro") in its Sub-project A: Dryer.

The scope of this section is the use of renewable energy in the food production value chains to improve energy use in the agribusiness sector; it tackles the problem of scarcity of energy and water in agriculture zones.

The improvement of the added value of dried products is studied with a solar assisted dryer either by reduction of energy cost or by the better drying quality.

The analysis is made theoretically to estimate changes of air temperature and humidity, but focused on its dependence on environmental conditions during the day, which is a key issue of solar energy resource.

Table 3. Case study characteristics: Queretaro

Description:	Semidesert
Ambient conditions:	T=18.9°C, Hr=56% (year average)
Latitude:	20° 36'
Atmospheric pressure:	810 mB
Sunlight hours:	Jan.: 11 h, Feb.: 11 h, Mar.: 12 h, Apr.: 12 h, May: 13 h, Jun.:13 h, Jul.: 13 h, Aug.: 12 h, Sep.: 12 h, Oct.: 11 h., Nov.:11 h and Dec.: 10 h
Greenhouse	
Season:	Whole year
Description:	Low-medium tech
Wall material:	Plastic
Characteristics:	Low humidity and high temperatures during day, scarcity of water resources
Energy problems:	Cooling requirements
Drying process	
Season:	Whole year
Characteristics:	Relative low ambient humidity, length of sunshine hours with low variation and high irradiation

As a complementary solution the use of the drying exhaust's wet air, potentially water, for circulating back to the growing process is analyzed. Previous studies evidence that exergy is lost within exhausted wet air from the drying process. In addition, high energy requirements for meeting heating and cooling necessities for optimal conditions of crops growing within greenhouses are reported. But, such conditioning systems are usually not able to control and maintain the required humidity levels affecting the quality of crop growth [36].

This section of research is reported and presented in the published paper in the Energy Procedia Journal: **Energy interaction of sub processes in drying value chain using exergy waste. Study case: drying and greenhouse growing of tomato** under reference DOI:10.1016/j.egypro.2014.10.135 [37].

2.4 Generalities of unitary processes

Initially, the analyzed value chain is described on the level of the unit processes that encompass it. The state of art of main characteristics and problems regarding resources needed for growing in greenhouses, transport and drying are presented in the following sections.

2.4.1 Growing in greenhouses

Fig. 3 depicts the considered steps within the growing process. In this work, growing in glass greenhouses is studied.

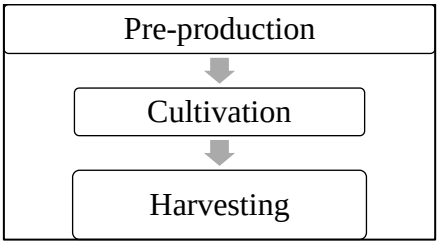

Fig. 3 Growing in greenhouses

According to Pimentel D. and Pimentel M. H. [38], the total required energy input in the United States is 32.4 million kcal ha^{-1} (including labour, machinery, fertilizers, pesticides, electricity, transportation, irrigation, etc.) just in the tomato production phase.

The worldwide tomato production is reported by the FAOSTAT as 159,347,031 tons [39], and as a consequence, for this amount of product any quantity of related resources becomes significant.

In the tomato production phase, two priority hotspots for reducing greenhouse gas (GHG) emissions are: transportation in field production and artificial heating in modern greenhouses [40].

A successful greenhouse production system is a result of overall strategic management [41]; starting with the proper location of the amenity according to the needs of the crop to be grown, and to the availability of water, land, roads, energy, markets and labour supply. Usually high energy usage for heating systems is required; for the extensive variety of types, crop growth and technology used in greenhouses it is difficult to fix values, but as a reference, for 11.5 m^2 the heat load is 4.5 kW and for a 7.5 ha it is specifically 7.5 MW [36], and 1500 $MJm^{-2}year^{-1}$ ([42],[43]). A research project called Greenhouse as energy source was based on the hypothesis that the excess of heat that enters during summertime by solar radiation could be captured using a closed greenhouse environment and reused during winter, or as otherwise needed, obtaining about 50% of primary energy savings [43].

With a variation of weather conditions such as solar radiation, ambient temperature, relative humidity and day-night presence, a plant will show different values of water uptake, CO_2 fixation, light reception, leaf transpiration, photosynthesis, fruit production, etc. throughout its growing process; this impacts on the nutritional content of the product as the antioxidant components (total phenolics, antioxidant activity, ascorbic acid and lycopene content) of

tomatoes vary considerably with the changes in environmental conditions within greenhouses ([14], [44]).

Like light and temperature, humidity is also an important factor for achieving high quality crop yield. Its impact is mainly on leaf size and light interception, photosynthesis and dry matter production, either by affecting leaf area development or by changing the stomatal conductance [45] .

Humidity control is very important. According to ASHRAE, relative humidity should be between 60-70% inside the greenhouses. Relative humidity above 40% would avoid water stress. Values below that of 20% could wilt plants [46], due to a higher rate of evaporation or plant water stress which enhances potential crop transpiration and xylem water flux and, therefore, the import of calcium ions into leaves; in combination with high radiation, water loss may exceed water uptake. On the other hand, relative humidity above 80% leads to fungal, leaf necrosis, calcium deficiencies and soft and thin leaves; it can also hamper pollination in fruit vegetables [47]. Jolliet and Bailey [48], report an optimal value of 70-75% hr for greenhouses. Transpiration is the major process contributing to accumulation of water vapour [49], and in practice there is a feedback effect on transpiration on the inside temperature, which affects transpiration and so on.

2.4.2 Harvest and transport

Once the products are harvested, a sorting process takes place to classify the products according to marketable standards. Some products are designated to be sold as fresh products, while some are selected for post-harvest processes, e.g. drying. On average 6.3% of produce does not conform to quality requirements, depending on the season, and is separated as residue [13]. In the case of drying processes, the products are transported to the post-harvest processing site; in the case of tomatoes 5% usually perish during transport [11]. Within the whole

value chain, the transportation, especially over long distances, becomes a significant factor for the linkage of pre- and post-harvest processes.

During transportation, especially the distances to be covered are of major influence for energy consumption on the supply chain level. One side is the transportation performance described by the mass of the freight transported over a specific distance, and also the impact of greenhouse gas emissions [50].

2.4.3 Drying

Extending the shelf life of foods is not the only objective of the drying process; it is however the most important. Other objectives for controlled fruit and vegetable drying are to add value to off-season sales, to reduce the product seasonality, to improve transportability, to reduce the costs of transport, to improve storage capability and to reduce nutritional fluctuations [51].

Fortunately, a lot of research has already been done on the drying process, which is used for levering the value process. The performance of the hot air drying process depends mainly on the drying conditions (air temperature, air humidity, air velocity and tomato slice thickness) and on the product characteristics (moisture content and material structure), which Mujumudar [3], classifies as external and internal conditions. The former are those sought to be controlled to obtain the best dried product quality; the latter are directly related to the pre-harvest conditions during the growing phase (Fig. 2). The coupling of both is what drives the drying mechanism and which yields the characteristic drying kinetics or drying rate curve.

Drying thermal efficiency is also influenced by other factors, such as heat fluxes supplied and exhausted number of internal heating zones, material pre-heating, recycled air ratio, fractional air saturation, etc. As outlet air conditions are close to saturation, energy efficiency is increased [6].

Though temperature level is limited by technological and economic reasons, an excessive temperature can provoke adverse effects such as ‘heat damage’ of

heat-sensitive constituents (e.g. deactivation of enzymes or deterioration of proteins) and generation of carcinogenic substances, browning, shrinkage, ‘case hardening, irreversible loss of ability to rehydrate, loss of volatile constituents or changes in moisture distribution within the product [52]. However, even if air drying temperatures in the constant drying rate are above 60°C, depending on the humidity level of the air and on thermodynamic properties, the wet bulb temperature could remain below 40°C, which avoids vitamins and carotenoids being destroyed before the critic moisture content is reached. On the other hand, high air humidity reduces the driving force leading to slower drying; plus condensation may occur on the dryer wall and downstream equipment.

The first step in the considered drying process (Fig. 4) is the slicing, followed by pre-treatment to avoid microbiological growth development. Here, tomato slices are submerged in a 2% citric acid ($C_6H_8O_7$) solution for periods of 3 to 4 minutes. After this procedure, the slices are distributed on meshes which, when done manually to reduce product damage, is time consuming for industrial quantities; then the meshes are collected inside the air convection dryer. Finally, discharge occurs; the dried products are then packed and stored.

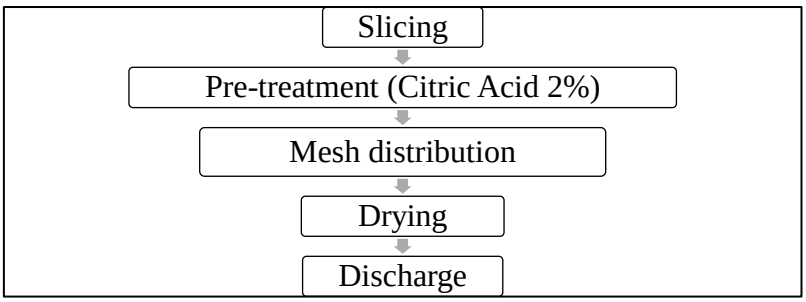

Fig. 4 Drying process steps

2.4.3.1 Drying kinetics

Drying of food particles is a complex problem involving simultaneous mass and energy transport in a hygroscopic, shrinking system. Air drying curves have two well-defined periods: a constant rate period and a falling rate period.

The constant rate period is characterized by almost free water evaporation from the surface of the solid which is governed by external heat and mass transfer rates and is thus not dependent on the material being dried [53].

However, as Hawlader et al. [54] indicate, some materials present only the falling rate period which occurs when the surface water no longer exists, thus the water to be evaporated comes from within the structure and must be transported to the surface. Changes in structure, such as case hardening and shrinkage, could derive from different falling rate regions.

As such, the falling rate period is an extremely complex phenomenon where the equations that represent the mass transfer demand additional calculations if the effect of shrinkage and the dependence of diffusivity with water content and temperature are to be taken into account [53].

Regarding tomato, Doymaz [55], reports that all the drying processes of his experiment occurred in falling rate drying periods and the drying process was mainly controlled by diffusion mechanisms. Hawlader et al. [54], state that tomato is considered hygroscopic with an inner wall structure resembling a fibrous material while the pulpous areas containing the seeds resemble a non-porous material.

The experimental drying curve obtained for tomato Saladett at a constant temperature 60°C, relative ambient humidity of 20% and airflow of 0.85ms^{-1} are shown in Fig. 7 and Fig. 8. From this experimental data it is possible to define the mass transfer mechanism of a product when plotting the log $\frac{M-M_e}{M_c-M_e}$ vs. time (t) [56]; in this way, when curves as observed in Fig. 9 are obtained, diffusion is the mechanism of water mass transfer in the tomato tissue for the falling drying rate. When diffusion is the mechanism of the falling drying rate, the geometry of the product has a considerable impact on the drying time. Initially, slices of tomato take a cylindrical form which the equation to determine the drying time is Eq. (8). However, in this time calculation there is uncertainty because the

radius of the tomato slices depends on time and because the determination of equilibrium moisture is not simple in the case of tomato:

$$t_d = \frac{r^2}{5.78 D_m} \ln\left(\frac{0.642(M_c - M_e)}{(M_f - M_e)}\right) \quad (8)$$

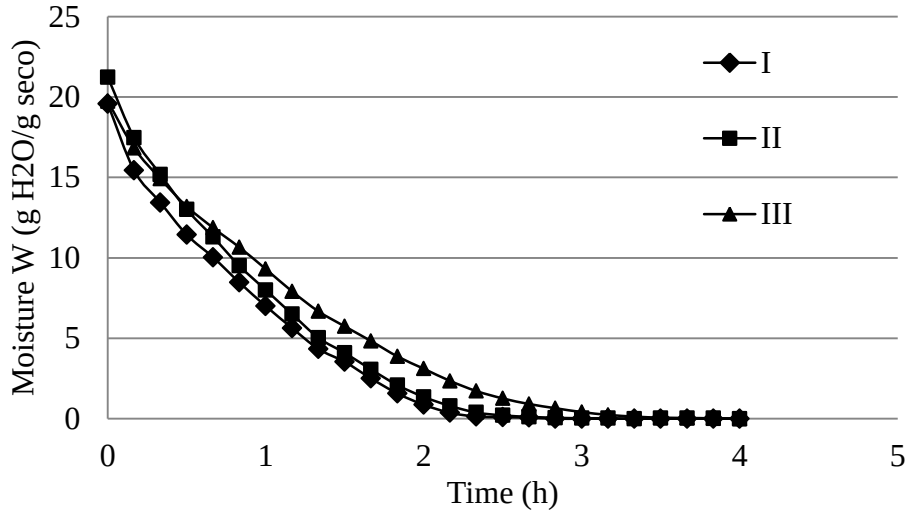

Fig. 5 Drying kinetics of tomato(3 repetitions)

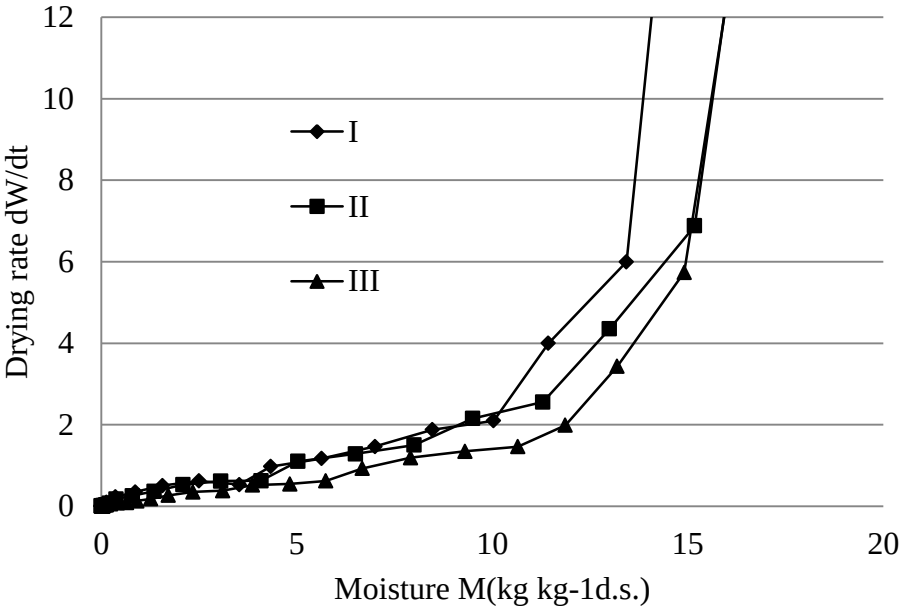

Fig. 6 Characteristic drying curve of a market tomato (3 repetitions)

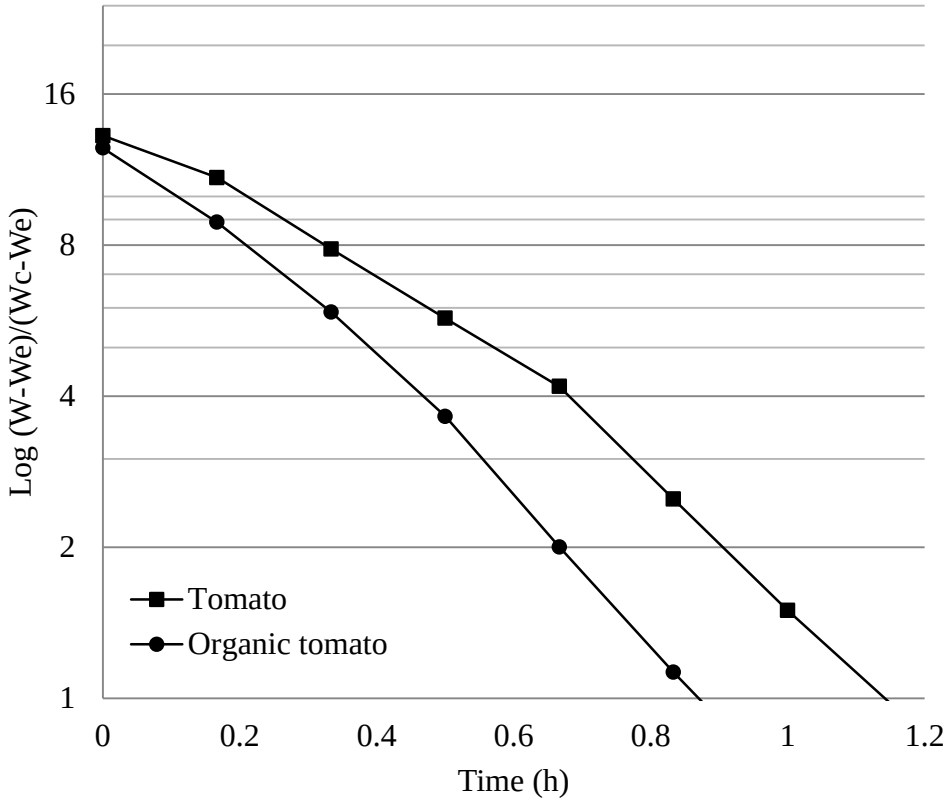

Fig. 7 Diffusion mechanism of tomato drying. T=60°C, hr=20%, v_a=0.85 ms^{-1}

2.4.3.2 Energy consumption due to environment

In the drying process the amount of water plays a key role, whether the water is within the product as moisture content, or in the air as humidity.

The maximum rate at which water can be extracted by the airflow from the product is called by Jannot the evaporative capacity [57], which can be increased by either dehumidifying (decreasing its relative humidity) or heating the air (increasing its moisture holding capacity) [15]. In addition, the equilibrium moisture content is a function of air humidity and temperature [58].

Thus, the humidity level influences the energy needed to raise the air temperature or the energy needed to move the air with mechanical devices.

Nevertheless, Krokida et al. [59], reported no significant impact on the drying times for tomato.

In general, the air conditions for the drying process represented in the Mollier diagram (see **Appendix 1**) in Fig. 8 include the following: **1) ambient conditions** that determine inlet air properties depending on the location of the dryer device; 2) **outlet of air heater** where it is necessary to increase the air temperature and reduce its relative humidity – the difference of enthalpy is the amount of energy transferred before entering the drying chamber; and **3) outlet of drying chamber**, at which point the dry air has removed the product's water, the temperature is decreased and the relative humidity increased again.

The enthalpy of the air h, considering the absolute humidity ω (g kg^{-1} dry air) is:

$$h = 1006.9T + \omega[2512131 + 1552.4\,T_a] \quad (12)$$

Considering a 60°C temperature requirement, in Fig. 9, it is observed that the energy requirement to raise the air temperature from ambient conditions for the two cases (Table 2 and Table 3) is 48.89 kJ kg^{-1} for Berlin while for Queretaro it is 42 kJ kg^{-1}. However, the reached relative humidity of the air in Berlin is 4.8% while in Queretaro it is 6.1%; when no dehumidification occurs the air will have different relative humidity because of the different amount of absolute humidity.

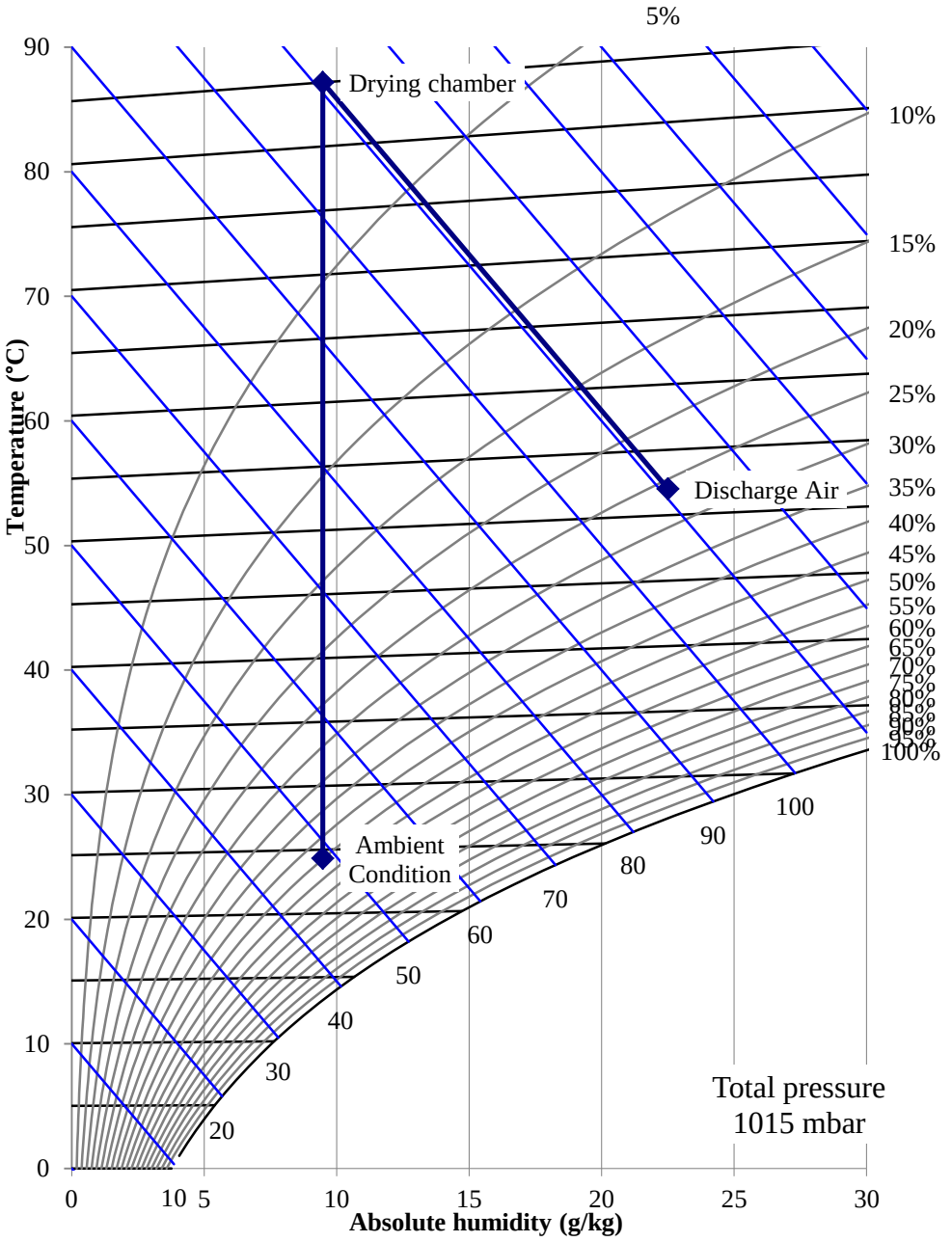

Fig. 8 Mollier diagram of an industrial conventional drying process at 85°C, hr 3%

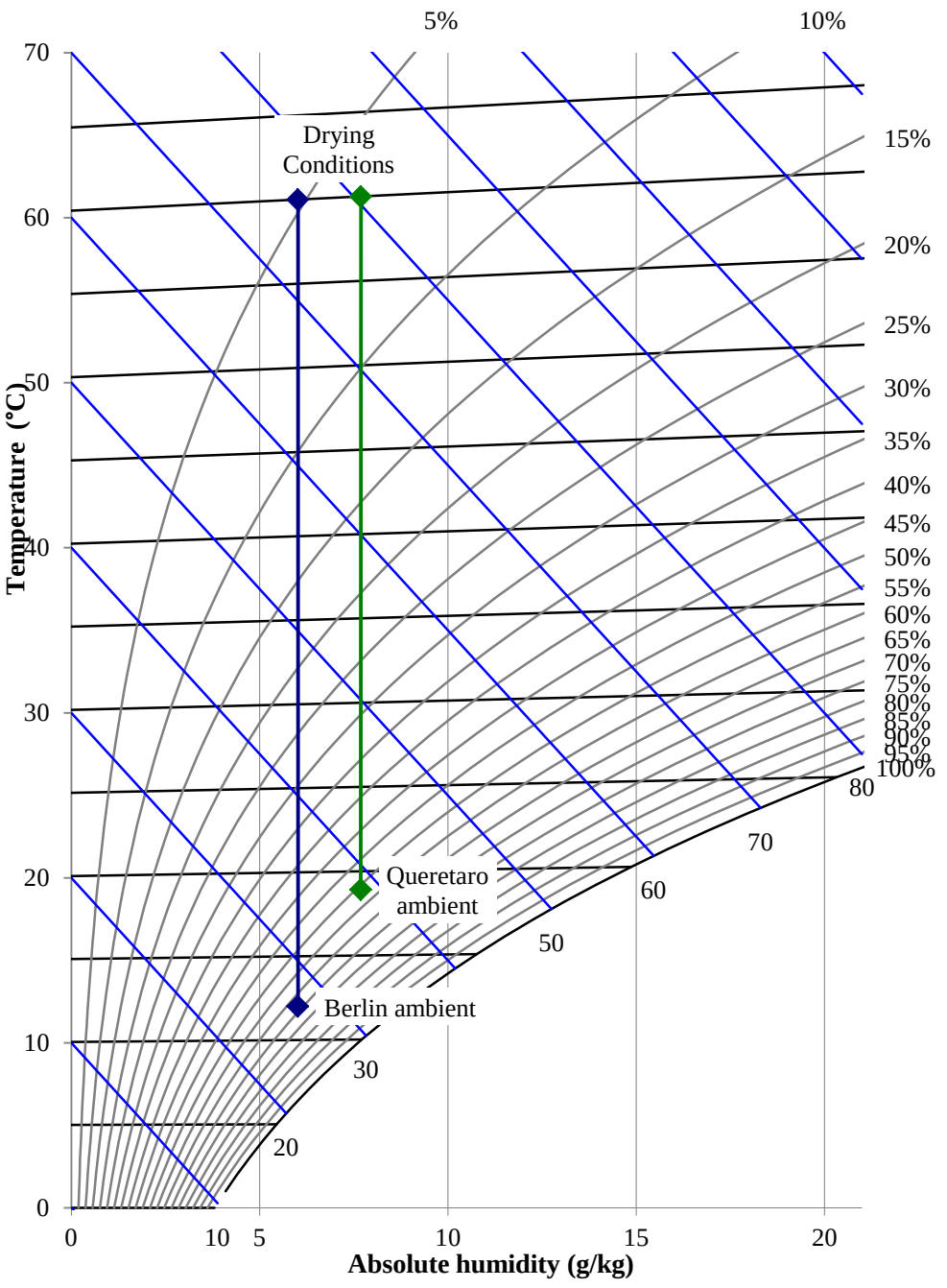

Fig. 9 Mollier diagram of different drying energy consumption due to humidity

2.4.3.3 Mass and energy balance (macrolevel)

The drying energy required from the air heater, according to Maroulis et al. [60], (adjusted to batch dryer), is given by the addition of the three terms in Eq. (9), Eq. (10) and Eq. (11). Where Q_{we} in Eq. (9) estimates the energy for water evaporation, Q_{sh} in Eq. (10) gives the energy for heating solids from ambient temperature to the drying air temperature, and Q_{ah} in Eq. (11) is the energy of rejected air heating. Within these, F (kg) is the amount of fresh product, M (kg kg^{-1} d.s) is the moisture content, Δh (kJ kg^{-1} dry air) is the enthalpy change, cp (kJ kg^{-1} K^{-1}) is the specific heat, T (°C) is the temperature and Y (kg kg^{-1}dry air) is the ambient humidity. The sub-index l refers to liquid, 0 to initial, f to final, p to product and v to vapour.

$$Q_{we} = F(M_0 - M)\left[\Delta h \quad - \left(c_{pl} - c_{pv}\right)T_a\right] \tag{9}$$

$$Q_{sh} = F\left(c_{ps} - M_0 c_{pl}\right)[T_a - T_{am}] \tag{10}$$

$$Q_{ah} = \dot{m}_a\left(c_{pa} - Y_0 c_{pv}\right)[T_a - T_{am}] \tag{11}$$

In the studied case this energy is supplied partly by solar energy and partly by the auxiliary system. The air drying temperature is set at 60°C to ensure drying homogeneity and to avoid tissue and essential components damage. The final dried tomato moisture is required to be 0.43 kg kg^{-1}, d.b.

2.4.3.4 Intermittent drying

Intermittent drying is the technological solution for increasing energy efficiency via lower specific energy consumption, higher effectiveness and lower electrical energy for driving a fan [17]. According to Chua et al. [61] and Mujumdar [3], this strategy is based on a controlled supply of thermal energy that varies periodically with time; in the falling rate period, this break time requires essentially no heat supply [62], to allow the product to redistribute the tissue temperature and moisture content. This offers better energy efficiency because

of reduced heat input, a shorter effective drying time and lower air consumption, in addition to improved product quality as a result of the lower material temperature [6].

A simulation made by Bon and Kudra [63], of intermittent drying reveals that energy consumption is reduced between 2.3% to 6.3% while also reducing drying time or lowering the average temperature and, with this, the average enthalpy of the product by up to 23% [6]. In regards to product quality, Chua et al. [61], found that colour changes can be reduced by using different temperature profiles.

2.4.3.5 Solar drying

"The Handbook of Industrial Drying" [64] dedicates a chapter to solar drying [17], which describes the state of this art and is used as reference in this regard.

The well known advantages of solar drying related to energy resource are that it is renewable, freely available and non-polluting. However, its main disadvantage is that the intensity of incident radiation is a function of time (creating its intrinsic periodic character and variation). This is tackled only with the use of an auxiliary energy source such as a complement of energy storage devices, which often demands proper control strategies. Additionally, the low energy density of solar radiation requires the use of large collector surfaces.

Thus, Ímre [17] summarizes that for the drying process the nature of solar radiation requires the implementation of means such as: heat stores, auxiliary energy sources, control systems and large surface solar collectors that increase investment costs. One way to reduce the costs of solar collectors is to strive for a cheap, simple construction, low power, short life, and comparatively low efficiency. Another possibility is to incorporate multipurpose construction, for instance, integrating the collector into the roof structure. On the other hand, there are high-efficiency, high power, long life, expensive dryers which are

characterized not only by an integrated structure but also by integration in an energy system involving processes other than drying.

2.4.3.6 Thermodynamic states calculation

For the drying phase, the used solar dryer performance was modeled by Hossain et al. [65], and proved with respect to temperature prediction [18], and applied to estimate absolute and relative humidity [37].

The solar dryer consists of a solar air heater with a glass cover and an aluminum reflector; the flow passes by forced convection perpendicularly through the product in five meshes of the drying chamber; humidified air comes out in the upper section of the drying chamber. The schematic of the system used is depicted in Fig. 10.

The drying process starts from ambient conditions, the air is heated up, which decreases its relative humidity, and once in the drying chamber its humidity is raised while the temperature decreases. The main phenomenon to study is the water mass transference to the drying air through time.

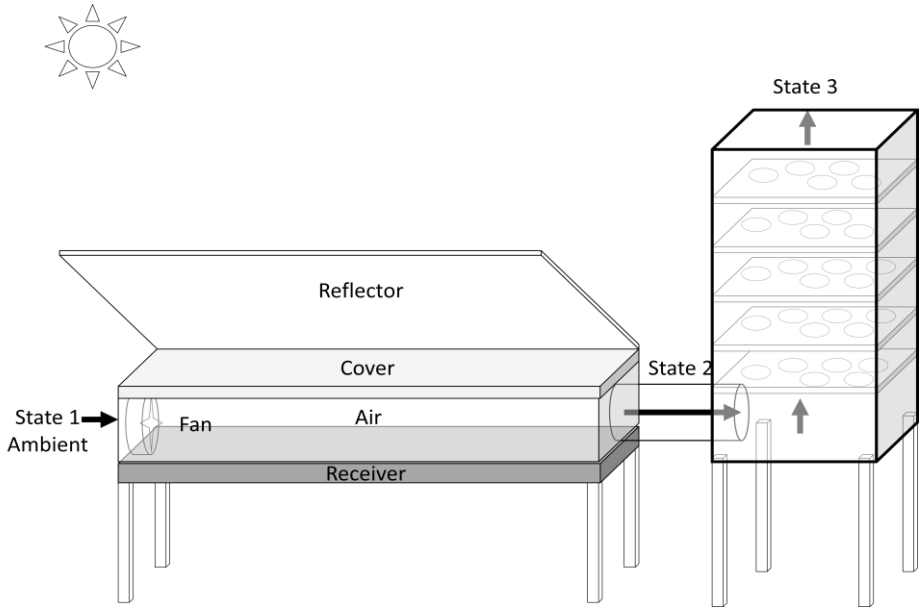

Fig. 10 Solar heater and drying chamber

All the parameters were calculated to determine the condition of the air at the inlet of the drying chamber from a numeric simulation of an already validated mathematic model according to Hossain et al. [65]. The reported thermal efficiency ranged from 25% to 62%, reaching maximum temperatures for drying air of 55°C. Each solar dryer unit has a receiving area of 4.5 m^2, uses a 0.75 kW air blower and has a capacity of 50 kg fresh tomato (in halves). With the assumption that the number of units of used dryers is not limited the monthly produce of tomato determines it.

The thermodynamic states of the solar air heater were predicted using the ambient conditions (temperature, irradiation, sunshine hours and relative humidity) as inputs to estimate the increment of air temperature $\Delta T_{a,1\text{-}2}$ (associated with a decrement of relative humidity) at the outlet of the air heater. The obtained temperature values are used to estimate energy requirements to process the monthly amount of fresh tomatoes in slices of 0.01 m. The amount of dry air and energy required to take the product to M_f =0.43 kg kg^{-1} d.s. moisture level is calculated by mass balance.

For the phenomena inside the drying chamber and for model simplification the following assumptions were considered by [65]:

1) airflow is one dimensional; 2) the heat flow is parallel to the direction of airflow; 3) air properties do not change within the air gaps; 4) contribution to the energy and moisture balances from the rate of air properties are negligible; and 5) outlet air temperature and relative humidity of the collector is the same as inlet dryer temperature and relative humidity. Each tray is considered one single layer and the total numbers of layers are assumed to be made of a deep bed. This physically based model is developed by a set of partial differential equations: continuity equation, drying rate equation, mass balance equation, heat balance equation and heat transfer equation.

With this context, the mathematical model previously developed, described by main equations (10) to (34), is adapted and applied in this work for simulation.

State 1: Ambient conditions

Ambient temperature (T_{am}) and ambient relative humidity (Hr_{am}) are taken from the data measuring systems $T_1 = T_{am}$; $Hr_1 = Hr_{am}$. Saturation vapour pressure, vapour pressure and absolute humidity (ω) are evaluated by î

$$p_{vs} = 6.11 * 10^{\left(\frac{7,5*T_1}{(Ta+273)}\right)} \quad (10)$$

$$p_v = p_{vs} Hr \quad (11)$$

$$\omega_1 = 0.622 \frac{p_v}{P} \quad (12)$$

State 2: Air heater outlet

The heat (Q) transmitted by absorption ($_{absor}$), convection ($_{conv}$), radiation ($_{rad}$) and reflection ($_{ref}$) in the energy balance on the glass cover (**see Appendix 4**) is,

$$Q_{absor,c} - Q_{conv,c-am} - Q_{conv,c-a} - Q_{rad,c-s} + Q_{rad,r-c} - Q_{ref,c-am} + Q_{ref,r-c} = 0 \quad (13)$$

The equations of Q are substituted in terms of its components where *h* is the heat transfer coefficient, A(m) is the area, ρ is the reflection, Γ is the capture fraction, ρ the reflectance, τ the transmittance cover, α absorptivity of receiver, θ (°) latitude, β(°) Beta

$$\alpha E A_c - h_{conv,c-am} A_c (T_c - T_1) - h_{conv,c-a} A_c (T_c - T_a) - h_{rad,c-s} A_c (T_c - T_s) + h_{rad,r-c} A_c (T_r - T_c) - \Gamma \rho_c E A_c + \Gamma \rho_r E A_r = 0 \quad (14)$$

Where the area of cover and receiver (absorber plate) are the same it follows that the temperatures are determined by

$$T_c = \frac{h_{conv,c-am}T_1 + h_{conv,c-a}T_a + h_{rad,c-am}T_1 + h_{rad,r-c}T_r + E(\alpha_c + \Gamma\rho_r - \Gamma\rho_c)}{h_{conv,c-am} + h_{conv,c-a} + h_{rad,c-out} + h_{rad,r-c}} \quad (15)$$

In a similar way, the energy balance on the receiver is

$$Q_{absor,r} - Q_{conv,r-am} - Q_{conv,r-a} - Q_{rad,r-c} - Q_{ref,r-c} = 0 \quad (16)$$

Substituting the equation for Q yields

$$h_{conv,r-a}A_r(T_r - T_a) + k_{cond}\Delta y A_r(T_r - T_1) + h_{rad,r-c}A_r(T_r - T_c) +$$

$$h_{rad,r-c}A_c(T_r - T_c) - \Gamma\rho_r E A_r = \frac{\tau_c\alpha_r E}{1-(1-\alpha_r)\rho_r}A_r \quad (17)$$

$$T_r = \frac{\frac{\tau_c\alpha_r E}{1-(1-\alpha_r)\rho_r} + \Gamma\rho E + h_{conv,r-a}T_a + k_{cond}\Delta y T_1 + h_{rad,r-c}T_c}{h_{conv,r-a} + h_{rad,r-c} + k_{cond,r-am}\Delta y} \quad (18)$$

The air temperature change is given by

$$\Delta T_{air} = (B - T_{ai-1})(1 - e^{-A\Delta x}) \quad (19)$$

where

$$E = I_g(1 + \Gamma\rho\sin\beta)\cos\theta \quad (20)$$

$$A = \frac{2Lh_{conv,a}}{m_a c_{ca}} \quad (21)$$

$$B = \frac{T_r + T_c}{2} \quad (22)$$

$$h_{rad,r-c} = \frac{\sigma(T_r^{\,2} + T_c^{\,2})(T_r + T_c)}{\frac{1}{\varepsilon_r} + \frac{1}{\tau_c} + \frac{1}{1-\tau_c} - 2} \quad (23)$$

$$h_{rad,c-am} = \frac{\sigma\left(T_c^{\,2} + T_1^{\,2}\right)\left(T_c + T_1\right)}{\frac{1}{\varepsilon_c} + \frac{1}{\tau_c} - 1} \tag{24}$$

To finally determine the change of air temperature by

$$\Delta T_{a,1-2} = \left(\left(\frac{T_r + T_c}{2}\right) - T_{ai-1}\right)\left(1 - e^{-\left(\frac{2Lh_{cv,a}}{m_a c_{pa}}\right)\Delta x}\right) \tag{25}$$

The absolute humidity from the inlet mass air is evaluated and maintained constantly through the air heater, so the new state of relative humidity is evaluated using the new temperature.

State 3: Drying chamber outlet

At the outlet of the drying chamber the change of air temperature (Eq. 31) and humidity (Eq. 30) will be determined by the change of water mass (Eq. 26) in the product. Constant values for the diffusion model (Eq. 27) are taken from [19], for slices of organic tomato and M_e (Eq. 28) is obtained (Eq. 29) using results from [59].

$$\Delta M = \left[-ae^{-kt}k - (1-a)be^{-bkt}k\right](M_0 - M_e)\Delta t \tag{26}$$

where

$$a = 1.454788 - 0.00393\,T_a + 0.27268\,hr$$

$$b = -0.00016 + 0.00000225\,T_a + 0.000924\,hr$$

$$k = 0.005699 + 0.00000742\,T_a + 0.044428\,hr \tag{27}$$

$$M_e = b_1 e^{\left(\frac{b_2}{273+T}\right)}\left(\frac{a_w}{1-a_w}\right)^{b_3} \tag{28}$$

Where $b1 = 0.000002; b2 = 3796.953; b3 = 0.7665$ (29)

The change of absolute humidity is given by

$$\Delta\omega = \left(\frac{\rho_p}{\dot{m}_a}\right)\left(\frac{\Delta M}{\Delta t}\right)\Delta z \tag{30}$$

The change of the temperature of the product is

$$\Delta Tp = \frac{2\left(T_a - T_p\right) + \rho_p\left(\frac{\Delta M}{\Delta t}\right)\left[\frac{2A}{h_{cv}} + \frac{D\,\Delta z}{\dot{m}_a\, C}\right]}{1 + \left(\frac{\rho p}{\Delta t}\right)\left[\frac{2B}{h_{cv}} + \frac{\Delta z}{\dot{m}_a\, C}(B + C_{pl}\,\Delta M)\right]} \tag{31}$$

where

$$A = L_p + C_{pw}T_a - C_{pl}T_p$$

$$B = C_{pp} + C_{pl} * M_i$$

$$C = C_{pa} + C_{pw} * (\omega - (\rho_p\,\Delta z\,\Delta M)/(\dot{m}_a\,\Delta t))$$

$$D = L_a + C_{pw}T_a - C_{pl}T_p \tag{32}$$

The change of air temperature in the drying chamber is described by

$$\Delta T_{a,2-3} = \frac{\frac{\rho_p\,\Delta z}{\dot{m}_a \Delta t}\left[\left(-\Delta T_p\left(C_{pp} + C_{pl}\,(M + \Delta M)\right) + \Delta M\left(C_{pw}T_a + L_a - C_{pl}\,T_p\right)\right]}{C_{pa} + C_{pw}\,\omega - \left(C_{pw}\frac{\rho_p}{\dot{m}_a}\right)\Delta z\left(\frac{\Delta M}{\Delta t}\right)} \tag{33}$$

Since in this experiment there are no means to know the initial values of the product temperature according to Ímre and Mujumdar ([17], [3]), the temperature of the material during the constant rate period approximates to the wet bulb temperature (T_{wb}) and remains practically constant. In the falling rate period the temperature of the material will approximate the dry bulb temperature. Even though tomato presents no constant drying rate period, during the first five minutes of the drying it is considered that the product temperature corresponds to the wet bulb temperature calculated according to Stull, R. [66], using Eq. (34) (temperature range -20 to 50°C)

$$T_{wb} = T_a \arctan\left[0.151\,977(hr + 8.313\,659)^{\frac{1}{2}}\right] + arctan(T_a + hr) - arctan(hr - 1.676331) + 0.00391838(hr)^{\frac{3}{2}} arctan(0.023101hr) - 4.686\,035 \quad (34)$$

2.4.3.7 Simulation

This work presents results of a Matlab™ Simulink™ program using the mathematical model for a solar dryer developed by M. A. Hossain, K. Gottschalk and B. M. A. Amer [65], in the Leibniz Institute of Agricultural Engineering Potsdam-Bornim.

Nevertheless, as Zhen-Xiang G. and Mujumdar A. [67] summarized regarding the availability of drying software, the main characteristics of drying simulations are **1) complexity of calculations; 2) difficulties in modeling solids;** and **3) limited market** and **lack of replicability.** During drying, the product loses moisture to the air and the air gains moisture from the product. Therefore, both the product and air properties (temperature, humidity, moisture content, etc.) are continuously changing in a coupled system.

The analysis of the drying process is divided into: 1) the air heater; and 2) the drying chamber. Fig. 11 represents these two processes with reference to the equations used; Fig. 12 depicts the variables involved for the calculation of the outlet air temperature from the solar air heater; and in Fig. 13 the relationships between variables in a simultaneous drying system are shown.

From these figures it can be observed how the temperature of the air is related to the changes of the cover and receiver temperature (Fig. 12). The air passes through the air heater and for each increment of distance travelled the air temperature is calculated from the previous temperature increment. The calculated outlet air temperature is then the input for the drying chamber.

The temperature of the air impacts the temperature of the product which influences the water mass transfer to the air and also the equilibrium moisture of

the product, which then effects changes in the drying level of the product (Fig.13). With this, the mass transfer of the product's moisture to the air modifies the air humidity, which impacts the drying potential. The results from this simulation are shown in the following sections.

2.4.3.8 Control design

Control actions in the drying operation maintain the required operational parameters. Generally these are comprised of: 1) a sensor to measure the actual value of the parameter to be controlled; 2) the control device which commands intervention, if necessary; and 3) the element which executes the command of the controller [17]. The main control actions are:

1. Temperature control of working mediums.
2. Relative humidity control.
3. Mass flow rate control of flowing mediums.
4. Switch in and out devices (e.g., fans, humidifiers, valves or dampers, auxiliary heaters) when the limit values of some parameters occur.
5. Control of charging the thermal storage of the system.
6. Control of the rate of drying.
7. Control of the recirculation.
8. Control of the intermittent drying process.

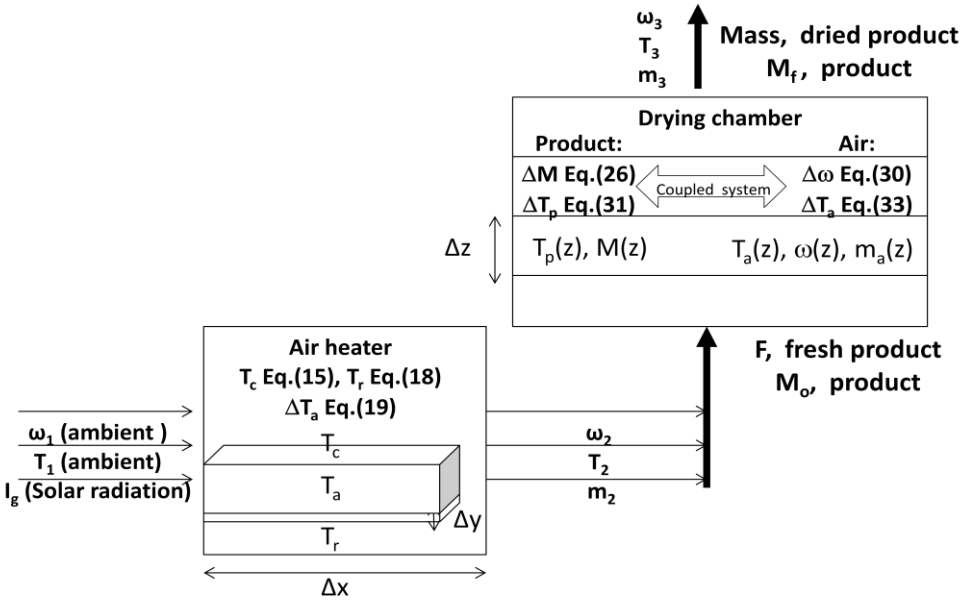

Fig. 11 Schematic of the equations used for the solar drying simulation

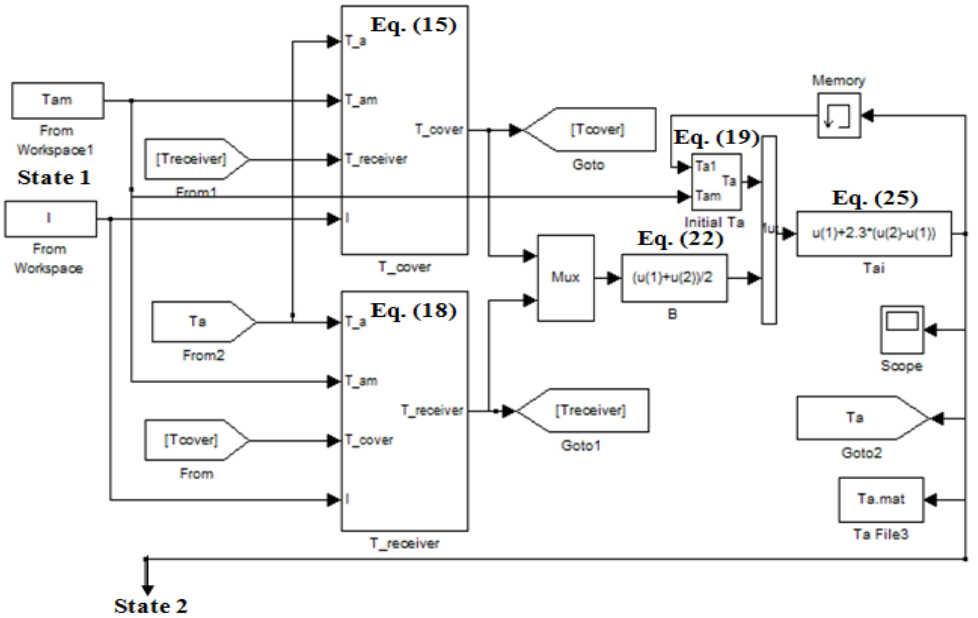

Fig. 12 Schematic of the simulation of heating air in the solar dryer

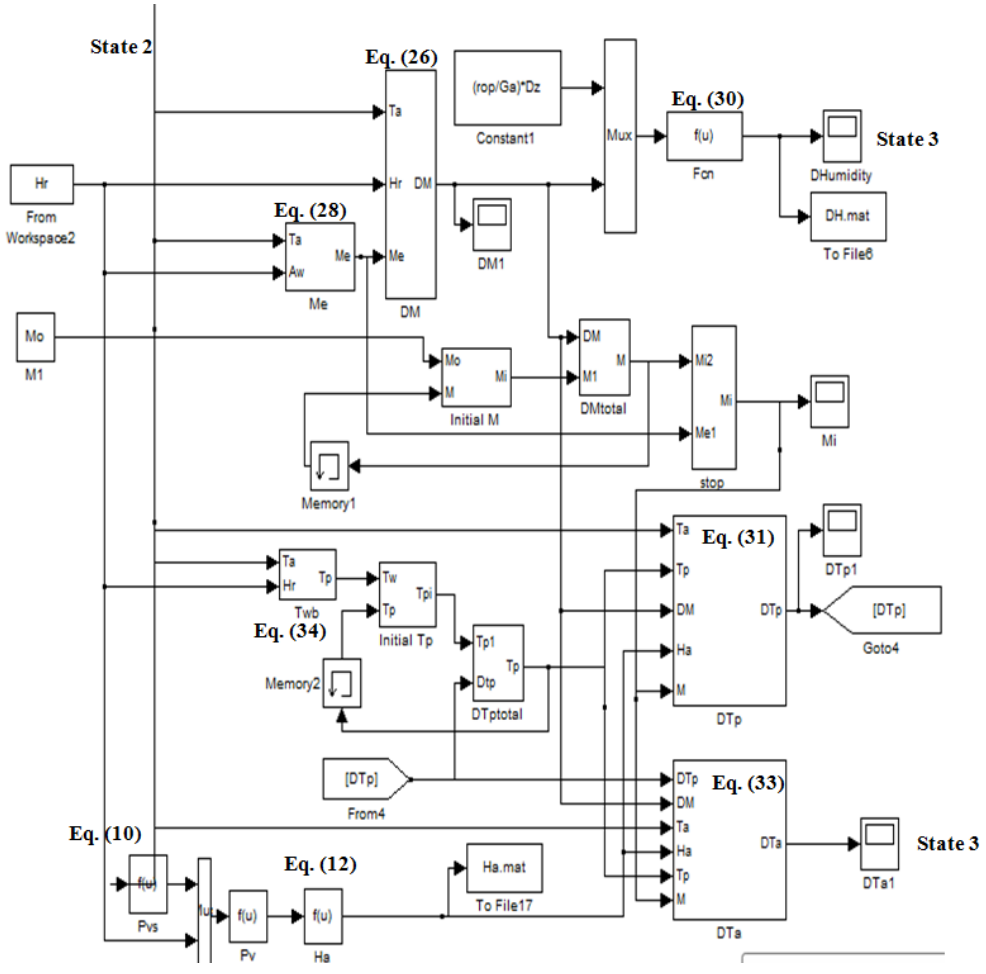

Fig. 13 Schematic of the simulation in the drying chamber

Chapter 3

Stage 2. Pre-benchmarking

This stage has the objectives of identifying the process inefficiencies and to establish guidelines to develop effective enhancement measures [20]. At the end of this stage, it will be possible to estimate the savings that can be obtained, while the means by which they could be implemented are found at the next stage [10].

Data compilation: the input and output resources (water, energy, products and wastes) for dried tomato production as well as the target operation conditions are defined. System characteristics are collected. Water flows are classified and energy flows are split according to the energy source.

Comparison to the current practice: the amount of resources needed and the inefficiencies in the current value chain practice are evaluated. The selected key performance indicators are water footprint, carbon footprint and exergy waste. The specific drying section is evaluated in detail for the exergy losses in the process. In order to link the growing and drying processes, the kilogram of fresh tomato is the analyzed operational unit. The likely improvements of water and energy consumption are identified.

New performance indicators (energy and exergy indicators): the performance indicators are evaluated to quantify the savings that can be achieved before applying the energy enhancement measures [10]. Sankey diagrams (**see Appendix 1**) of the energy and water balances are constructed for the value chain; these also include the waste flows regarding water and residues in order to show the potential for this to be recovered or included in other process steps.

Targeting: the minimum and maximum potential resource savings in the whole value chain are evaluated.

3.1 Case study A: *reference* value chain

The system boundary contemplates cradle-to-gate (pre-farm processes to factory gate) [68], life cycle stages. Inventory analysis is done for the consumption of thermal energy, electricity and water flow; the energy associated with fertilizers, human power and machinery (reported by Hatirli et al. [69], as 27.6%, 8.6% and 2.8% respectively of total energy input) is excluded from the analysis.

The base research was appraised during the growing season of tomatoes (*Solanum lycopersicon* L. cv, Pannovy) in 2011 (March 8th to October 24th) in the ongoing ZINEG system. The experimental full set-up of these systems is described in detail by (Tantau et al. [69]; Dannehl et al. [70]; Schuch et al. [71]; Dannehl et al. [72]). Here the aim is to reduce CO_2 emissions through applying energy saving principles. Parameters such as ambient and operation temperature, radiation, water flow, energy flow, transpiration, tomato production and nutrient solution application are used as inputs for the presented research.

3.1.1 Data compilation

The *reference* value chain is a configuration that follows a conventional sequence of processes, i.e. the products are grown in a greenhouse with ventilated operation and then transported to another location for drying.

The baseline greenhouse, the so-called *reference* greenhouse is a Venlo-glass type of 200 m^2 crop area with a single layer screen (Dannehl et al. [44]; Dannehl et al. [74]) set points of 29°C and RH above 90%.

Table 4 summarizes the greenhouse conditions in the growing phase.

For the analyzed processes, the most important parameters to describe the thermodynamic states of the air are temperature, energy and relative humidity.

Thus, a Mollier diagram is used to visualize the operation zones. Fig. 14 shows the operation zones for the season 2011 from Month 3 to 10 of growing in the *reference* greenhouse (white diamonds) and conditions at the inlet of the drying chamber for the whole year (circles). Also shown are the daily average ambient conditions (triangles). The objective for evaluating the operation zones is to correctly size and design systems and processes.

Table 4. Thermodynamic states in *reference* greenhouse

	Reference	
	Mean value	Standard deviation
Temperature (°C)	22.5	1.3
Absolute humidity (g kg^{-1})	13.1	2.3
Enthalpy (kJ kg^{-1})	55.9	6.6
Relative humidity (%)	75.4	11.4

In the solar air heater the air is heated up from ambient conditions (triangles). By using Eq. (25) from the mathematic model it is possible to calculate the air conditions in the drying chamber (circles). From May (circles-5) to October (circles-10) the drying air temperature at maximum irradiation reaches an average of 44.05°C with temperatures from ~40°C to 48°C, thereby reducing its relative humidity in a range of 20% to 30%. This period, which is when the tomatoes are also actually harvested, provides the best conditions for solar drying given that the lower the relative humidity and the higher the temperature the better the drying potential. From Fig. 14 the need for energy becomes evident to: **i) take the air from ambient condition states to the conditions for tomato growing inside the greenhouse**; and **ii) to heat up the air for the drying process**.

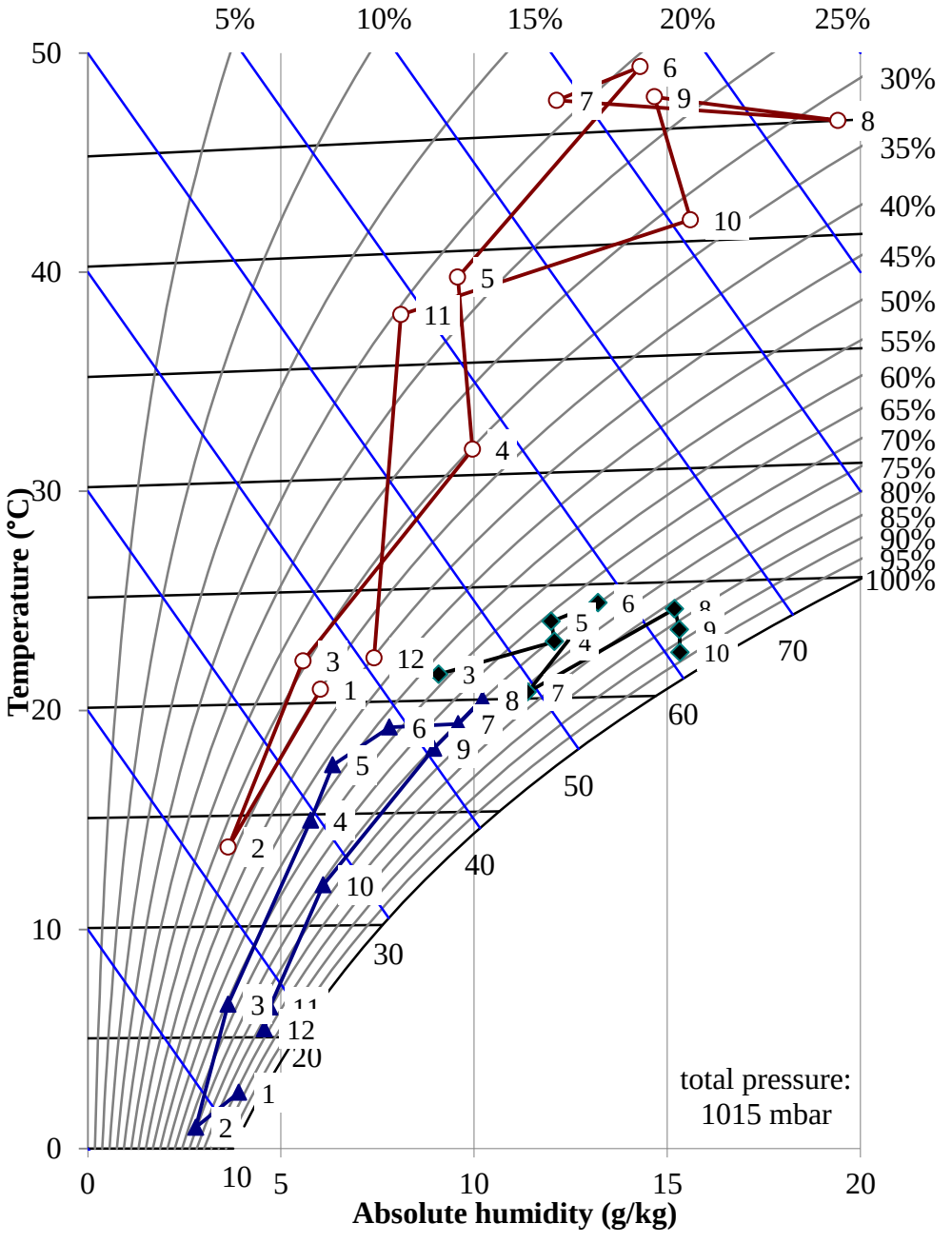

Fig. 14 Mollier diagram: ambient (triangles), reference greenhouse (diamonds) and air heater (circles).

3.1.2 Comparison with current practice

3.1.2.1 Production and crop residues

Production is evaluated weekly and the fruits are classified in 4 classes [74]; class A weight >70 g, class B from 50 g to 70 g, class C <50 g and BER (Blossom End Rot) class. It is considered that all tomato class A production is assigned to be sold as fresh produce. Classes B and C were used for the drying post-harvest process in order to enhance their added value.

The first tomato harvest as well as leaf pruning took place in May. The leaves were pruned once per month to keep the plants healthy [75], and were weighed once; for the rest of the season the values were estimated. At the end of the season, plants without leaves were weighed to make an extrapolation of the total residues considering 400 plants per greenhouse. The dry mass of leaves, fruits and plants was measured to estimate the percentage moisture content in order to calculate the amount of water content.

3.1.2.2 Water flow

The water requirement of the value chain is considered from the total water input to the greenhouse, evaluating how water is transformed within the product throughout the different sub-processes until the drying post-harvest process.

The water flow in the growing stage was measured automatically with a precise volumetric dosing system [74], and all recorded data were accumulated for total water consumption per item. The water content in the drying phase was calculated according to the final drying requirements. Item descriptions are as follows:

- Stored substrate: each greenhouse has 10 rows of tomato plants storing 2600 L of water mixed with nutrient solution in plastic bags (to avoid evaporation) of rockwool slabs substrate; considered to be constant.

- Fresh water: the total input of water measured daily to each greenhouse.

- Rain water: the component of the irrigation water coming from rain; taken from the precipitation data recorded.

- Condensation water: the water condensing either in the glass walls (estimated) or in the finned pipe (measured).

- Re-circulated water: the drain water being re-circulated back into the system.

- Transpiration: obtained from measurements in the leaf chambers (Dannehl et al. ([72], [74]).

- Ventilation: the estimated water lost to the atmosphere through the greenhouse windows is calculated through Eq. (38).

$$ventilation = transpiration - condensation \quad (38)$$

- Production: the solid products are represented solely by the water contained as moisture content within the tomato production (classes A, B, C and BER), pruned leaves and plant residues.

- Evaporation: in the drying process, the main task is to evaporate water from within the tomatoes. This water is contained in the exhaust air.

- Dried product: water content of the final dried product.

Mekonnen and Hoekstra [77], define the blue water footprint as the volume of surface and groundwater consumed (evaporated) as a result of the production of a good; the green water footprint refers to the rainwater consumed. The grey water refers to the volume of fresh water that is required to assimilate the load of pollutants based on existing ambient water quality standards.

For the growing process, the blue water, labeled as fresh water, comes from the public water service given that the ZINEG project is located in the city of Berlin, Germany. The green water is the rain water recovered from the roofs of the collector greenhouse and used for irrigation. The grey water comes from the irrigation circuit that is periodically refreshed to avoid high concentrations of chlorides which influence the presence of BER products. It is considered that the

same amount of fresh water is added to the estimated grey water to reduce its chloride concentration, with no specific limiting values.

From the grey water the original nutrient solution (NS) and from where it is derived is known. The used NS was the same for both greenhouses and the composition was as follows: 175 mg L^{-1} calcium (Ca), 303.28 mg L^{-1} potassium (K), 42 mg L^{-1} magnesium (Mg), 1.50 mg L^{-1} iron (Fe), 692.79 mg L^{-1} nitrate nitrogen (NO3), 117.24 mg L^{-1} phosphate (PO_4), 165.85 mg L^{-1} sulphate (SO_4), 0.20 mg L^{-1} boron (B), 0.03 mg L^{-1} copper (Cu), 0.51 mg L^{-1} manganese (Mn), 0.05 mg L^{-1} molybdenum (Mo) and 0.22 mg L^{-1} sodium (Na) [74]. However, the exact amount of each component within the grey water is unknown given that it is recycled water and only the conductivity is measured and the variable levels not systematically registered. The average value of the conductivity measure was for *collector* 2.3 µScm^{-1} and for *reference* 2.19 µScm^{-1}. The pH for the *collector* was 5.75 and for the *reference* 5.9. The measuring devices used were Hanna Instruments.

For the drying process, the blue water for washing the produce of each greenhouse is considered to be 5 L kg^{-1} of tomato [76], assuming that this amount is added to the actual specific monthly produce; however, usually this process is done per batch according to the recipient's capacity. The grey water is the residue from the batched pre-treatment of 2% citric acid for the sliced tomatoes (0.01 m thickness) using 2.5 L kg^{-1} tomato. Although there is no specific normativity for citric acid concentration, since it is readily biodegradable in aquatic environments [77], this work considers the additional water to take the solution to a concentration of 50 mg L^{-1}.

3.1.2.3 Energy flow and associated CO_2 emissions

According to a report from the National Inventory Report Germany 2014 [78], agricultural activities in 2012 contributed 0.66% of carbon dioxide (CO_2), 0.01% of methane (CH_4) and 0.01% of nitrous oxide (N2O) to the total

emissions (Gg) represented. For its representativeness, the CO_2 GHG is the only indicator used in this work and is limited to electricity and thermal energy; the kg of CO_2 equivalences for electricity and thermal energy using lignite coal are 0.433 and 0.99 kg CO_2 kWh^{-1} ([79], [80], respectively).

By using the emission factor for Germany it would be possible to associate an average value for determining the equivalence per L of water and MWh in CO_2 emissions for the drying process, as Tomás et al. [81], apply for the chemical industry and Gomés et al. [82], for electricity demand and waste treatment. However, the emission factors of agriculture sector activities (together with those of forestry and fisheries) are included in the commercial and institutional sector. This means that the accounting and statistics of drying value chain processes are not precisely represented; worldwide there are reliable reported values but still with country specific applicability.

To estimate the energy balance per month for growing and drying processes, the analysis is divided into the solar contribution and the fossil fuel contribution (split into electricity and heating consumption). The energy flow is measured by using nine magnetic heat meters and two electricity meters [83]. The electricity, for the whole system, is used to drive the heat pump and the circulation pumps.

The drying cluster is considered to be established at 150 km from the ZINEG project; the produce of classes B and C are assumed to be transported in a small truck (1-1.5 tons, speed 60 km h^{-1}) consuming 0.1667 L km^{-1} [11] of diesel with an energy equivalent of 56.31 MJ L^{-1} [12]. Depending on production, the truck is not always used to its maximum capacity. Here the hypothetical energy for transporting only the specific production is reflected.

On positive balance, plants use carbon dioxide for photosynthesis during the growing process. The rate of CO_2 consumption varies with crop, light intensity, temperature, stage of crop development and nutrient level. An average

consumption level is estimated to be between 0.12-0.24 kg ($hr^{-1}100\ m^{-2}$). The higher rate reflects the typical usage for sunny days and a fully-grown crop [84].

The way of measuring CO_2 is taken from the procedure and experiment described by Dannehl [74], where the unit of the measured photosynthesis rate is mol $s^{-1}m^{-2}$.

The photosynthesis equation is as follows:

$$6CO_2 + 6H_2O + light \rightarrow\ C_6H_{12}O_6 + 6O_2 \tag{39}$$

And in terms of mass is:

$$6\ mol\ CO_2\left(\frac{44\ gr\ CO_2}{1\ mol\ CO_2}\right) + 6\ H_2O\left(\frac{18\ gr\ H_2O}{1\ mol\ H_2O}\right) + light \rightarrow\ C_6H_{12}O_6 + 6\ O_2 \tag{40}$$

3.1.3 Indicators

The evaluations of the energy and water balances in the greenhouse growing and drying processes are described independently. All inputs and outputs for the greenhouse growing process were monitored by devices as described in detail by Dannehl et al. and Schuch et al. ([74], [72], [83]). The inputs and outputs for the greenhouse drying process are evaluated in the presented work.

Eq. (41) gives the calculation for the water footprint (L kg^{-1} tomato) and Eq. (42) gives the calculation for the CO_2 footprint (kg kg^{-1} tomato):

$$\left(\frac{Water_{total}}{F_{total}}\right) = \frac{\sum Water_i}{\sum F_i} \tag{41}$$

$$\left(\frac{CO_{2\,total}}{F_{total}}\right) = \frac{\sum CO_{2\,i}}{\sum F_i} \tag{42}$$

where the total season water (L) and CO_2 (kg) are divided by the total season production; F (kg tomato) is the produce which, for growing, comprises the tomato classes A, B, C and, for the drying process, just classes B and C; the index i means at i time (months). In the case of the whole season, the right side

indicates the monthly addition of water and energy divided by the monthly addition of produce.

3.1.2.4 Statistical analysis

The main objective is to compare the monthly amounts of water and energy used to produce a certain amount of tomatoes per greenhouse. Given that a sum of values is not a proper statistical estimator; the statistical proof was gained using the mean values of the parameters that make up each footprint indicator.

Due to the nature of the data collected, one replication of the measurements is considered, representing one season.

The electricity and thermal energy data was taken every 30 seconds, 24 hours a day for 232 days. The energy flow data was split into day and night. The data presented corresponds to the different daily sunshine hours per month, creating different sample sizes according to the month. The z test (p = 0.95) for normal distribution (n >2000) was applied for the thermal energy flows.

The mean water flows per month (n< = 31) were compared using the t-test (p = 0.95). The tomato production was evaluated weekly (n = 4) and the total season production of biomass residues (n = 5) was evaluated using the t-test.

For all tests, the null hypothesis (H_0) of the evaluated parameter is $H_0: \bar{x}_{collector} = \bar{x}_{reference}$

The complete statistical analysis is shown in **Appendix 3**.

3.1.3.1 Production and residues

The measured average moisture levels are: 94.65% for the tomatoes, 84% for the leaves and 86.5% for the stem plants. From these values the water content is represented in Fig. 15.

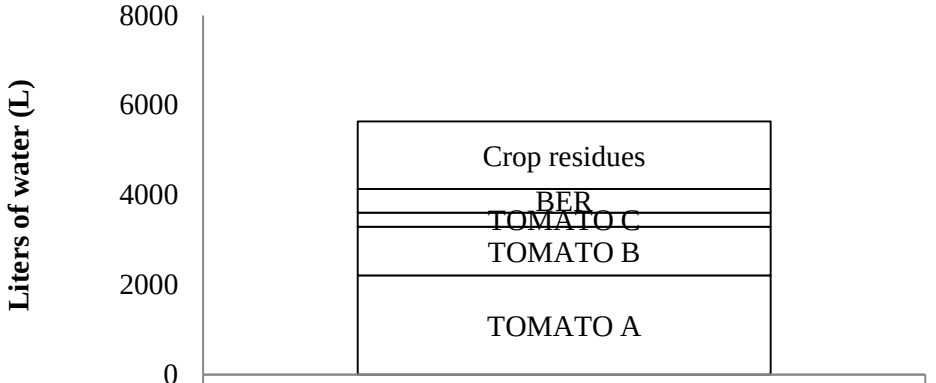

	Reference
Crop residues	1502.78
BER	528.99
TOMATO C	313.53
TOMATO B	1087.62
TOMATO A	2207.69

Fig. 15 Water content in the tomato produce from the reference greenhouse

3.1.3.2 Water footprint

For the *reference* circuit Fig. 16, 100% of input water in the system is blue water. A fraction of the water is used for plant structure biomass formation. 38.6% of water is lost by transpiration, followed by ventilation and an estimated 5% of condensation in glass walls; the transpiration is reduced in greenhouse systems from a 64% average global transfer by vegetation transpiration [85]. The tomato classes B and C reach the processing cluster after transport with 5% losses. During the drying process 1299 L of water are lost to the environment as air humidity and the water content of 107.5 kg of dried tomato at 0.43 kg kg^{-1}, d.b. is 32 L.

Table 5 summarizes the monthly amount of water used in the value chain. For similar tomato growing systems, reported irrigation values are 43 and 24 L kg^{-1} of total blue water consumption for med-tech and hi-tech systems, respectively [40]; 61.85 L m^{-2} [86] and 96.2 L kg^{-1} on average with a standard deviation of 23.1 L kg^{-1} [87].

Regarding both processes, the reported average water footprint for production of fresh tomatoes is 214 L kg^{-1} (green water 108, blue water 63 and grey water 43 L kg^{-1}) and for dried tomato production is 4276 L kg^{-1} (green water 2157, blue water 1265 and grey water 853 L kg^{-1}) [88].

3.1.3.3 Carbon footprint

The main objective of greenhouses is to make use of solar energy and to retain the already gained energy through physical barriers (greenhouse walls). In spite of the fact that the majority of the energy used by the crops is supplied by solar energy, only the energy supplied to greenhouses by artificial means, such as for heating, cooling, irrigation systems and control systems is commonly reported.

The drying energy consumption was determined by using Equations (9), (10) and (11). The monthly energy requirements present variations due to: **i) monthly amount of tomato to be processed** which impacts directly on the amount of required air and water content; **ii) irradiance**, i.e. different maximums per month; and **iii) solar energy irradiation**, i.e. sunshine hours. In Month 7, the production is maximal, so the water to be eliminated is also maximal and the required energy reaches its peak, but at the same time, the average sunshine hours, ambient temperature and irradiance reach their peak.

Table 6 presents the energy consumption for both sub-processes of the drying value chain. The solar contribution to the growing energy is displayed to indicate its relevance, given that the vast majority of energy required for growing is provided by solar. The thermal energy for heating is supplied via ground tubes, blowers and vegetation heaters.

Table 7 shows the water and carbon footprint with a standard deviation for the Reference value chain of 53.2 L kg^{-1} tomato and 23.9 kg CO_2 kg^{-1} of tomato.

The values of the carbon dioxide consumed for the tomato crop are interesting, given that they come directly from measurements [74]. The highest value is in month 5 with 1.52 kg CO_2 kg^{-1} where the tomato produce is starting.

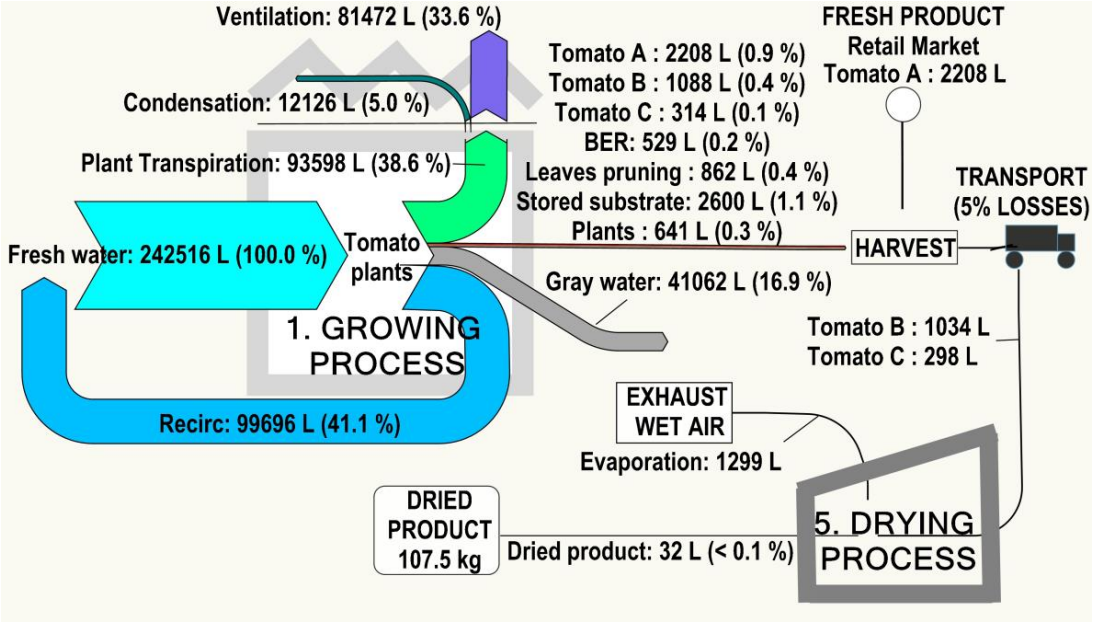

Fig. 16 Water flow for the *reference* configuration

Table 5. Water footprint (L kg^{-1} tomato) for *reference* process configuration

	Month							TOTAL
Reference	5	6	7	8	9	10	End	
1. Growing (L kg^{-1} tomato)								
Blue water	33.4	52.8	69.8	107.4	127.1	77.8		63.6
Grey water	5.6	12.8	29.9	27.8	61.7	47.4		21.5
Crop residues*	0.07	0.09	0.34	0.52	0.64	0.43	0.39	0.63
5. Drying (L kg^{-1} tomato)								
Blue water for washing	5	5	5	5	5	5		5
Grey water	10	10	10	10	10	10		10

* Including leaves, plants and BER

Table 6. Energy flow (MJ kg^{-1} tomato) of the *reference* drying value chain

Reference	Month						
(MJ kg^{-1} tomato)	5	6	7	8	9	10	TOTAL
1. Growing							
Solar Energy	141.32	161.84	164.62	256.28	427.97	232.73	189.89
Thermal Energy	28.77	27.83	52.20	65.67	162.41	215.17	60.38
Electricity *	18.17	23.96	25.46	36.09	83.40	54.01	30.04
3. Transportation							
To drying cluster	11.8	4.2	2.8	7.5	9.6	7.4	
5. Drying (class B+C)							
Thermal Energy	4.30	4.45	4.57	4.63	4.71	4.87	4.58
Electricity	1.00	1.13	1.09	1.14	1.09	0.89	0.96

* Electricity of total ZINEG system, considered equally distributed to reference and collector greenhouse

Table 7. Water and carbon footprint of the *reference* drying value chain

Reference value chain	Month						
	5	6	7	8	9	10	TOTAL
Water foot print							
(L kg^{-1} tomato)	54.0	80.6	114.7	150.2	203.7	140.2	91.0
CO_2 footprint							
(kg CO_2 kg^{-1} tomato)	30.83	31.11	38.01	43.09	75.30	86.37	40.18
CO_2 photosynthesis							
(kg CO_2 kg^{-1} tomato)	1.52	0.46	0.47	0.64	0.59	0.64	0.14
Residual water							
**(L kg^{-1} tomato)	0.38	0.66	1.27	1.39	2.23	1.82	0.97

** Water from greenhouse residues and drying evaporation not reutilized

3.2 Case B: *baseline* drying simulation

The growing phase takes place under the ambient conditions of Central México (latitude 20.6°) in a plastic Gothic type greenhouse of 2500 m^2 without aerial windows and as part of the research project of the Faculty of Biosystems of the Autonomus Queretan University. The growth tomatoes (*Solanum lycopersicon* L.) are Caimán and Saladette varieties; in an 8-month season the productivity of the greenhouses is 20 kg m^{-2} with 3 plants m^{-2}.

A general description of the equipment consists of: a 3HP three-phase pump, fans, extractors, humidity and, temperature sensors. During the daytime the temperature is lowered by the use of fans, but this creates the new problem of low relative humidity. Data availability is limited to the temperature and relative humidity sensors installed in the middle of the greenhouse. The solar radiation and ambient conditions are recorded from the nearby environmental station.

Regarding the drying analysis, this is done using the model simulation from **section 2.3.3.5** to evaluate the potential of the implementation of solar drying systems in the tomato value chain.

3.2.1 Data compilation

In Table 8 the amount of water added to the plants after the transplantation to the harvest phase is reported.

The Sankey diagram shows a representation of the amount of water per kilogram of tomato. The losses were weighed per experimental kilogram of tomato. In proportion, 0.22 L kg^{-1} tomato is lost in the slicing process. This is necessary to emphasize due to the scarcity of reports on losses in water. Given that the analysis is done on a day basis, the yield of the greenhouse is not relevant for the comparison.

Table 8. Water added per plant per day [89]

	Water (per plant per day)	Time (days)
Transplantation	500 mL	14
Vegetative growing	800 mL – 1L	28
Blooming	1L (according to weather)	14
Fruits growing	1.5 – 2 L	14-28
Harvest	2.5 L in soil	163

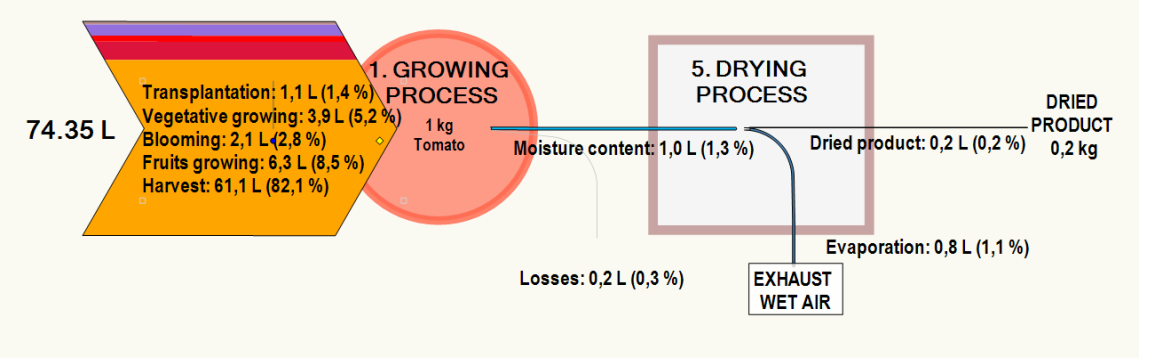

Fig. 17 Water flow per kilogram of tomato

The collected data is taken from **1) ambient conditions; 2) data from the greenhouse; and 3) results from the model simulation.**

The data from the ambient conditions of Querétaro, México over two representative days – 1) **D1 winter** weather (January); and 2) **D2 spring** weather (April) – are shown in Fig. 18 and Fig. 19.

The analyzed greenhouse data is taken from a crop of the Saladett variety of tomato 2198 (91 days transplanted) using a period of 12 hours, from 7 am to 7 pm with time intervals $\Delta t = 0.25$ h.

The model was solved to process 1 ton of fresh tomato in slices of 0.01 m. From the Eq. (25) the results of air temperature change ΔT_a are the input for estimating

ΔM, $\Delta\omega$ and ΔT_p in the Equations (26), (31) and (33). The airflow velocity was considered constant at 0.5 m s^{-1} and airflow mass is considered, depending on temperature and humidity for specific day conditions, to remove 908 kg of water (Table 1) which is desired to be recovering in the greenhouse.

From Fig. 20 and Fig. 21 it is observed that better final drying levels are reached for D2 (~9% w.b.) and, as consequence, more water is mixed with the exhaust air. It is important to mention that the total amount of airflow for D1 is 4:1 of the air required for D2 given that the drying potential of D2 is higher.

3.2.2.1 Batch and time dependent heat flow

According to the methodology proposed by Kemp [90], the greenhouse is considered as a batch process that requires heating or cooling. Fig. 22 and Fig. 23 show the heat load of different sources: 1) *solar greenhouse* curve is the representation of the heat load of the greenhouse air **heated up only by solar radiation** and the surroundings; 2) the *solar heater* trend shows the work load of the airflow **from the drying process**; and 3) the curve labeled as *To set point* indicates the heat load utility **to reach a temperature set point of 27°C**.

As it is observed, values below zero means that cooling is required and above zero indicates heating demand. The total heat load for cooling to reach the set point at 27°C is for D1: 950 MJ and D2: 27470 MJ.

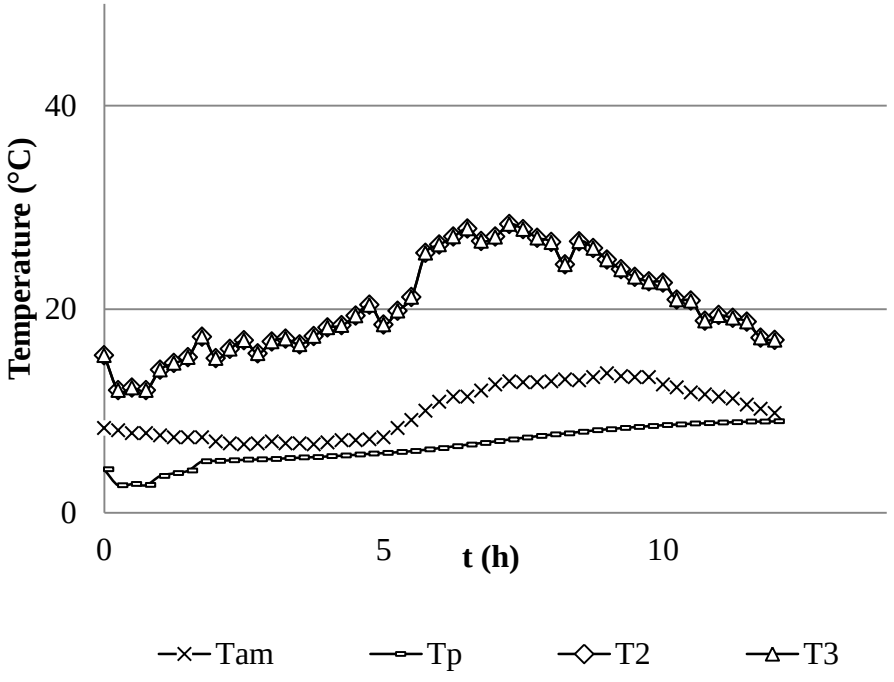

Fig. 18 Temperature profiles for a winter day (D1)

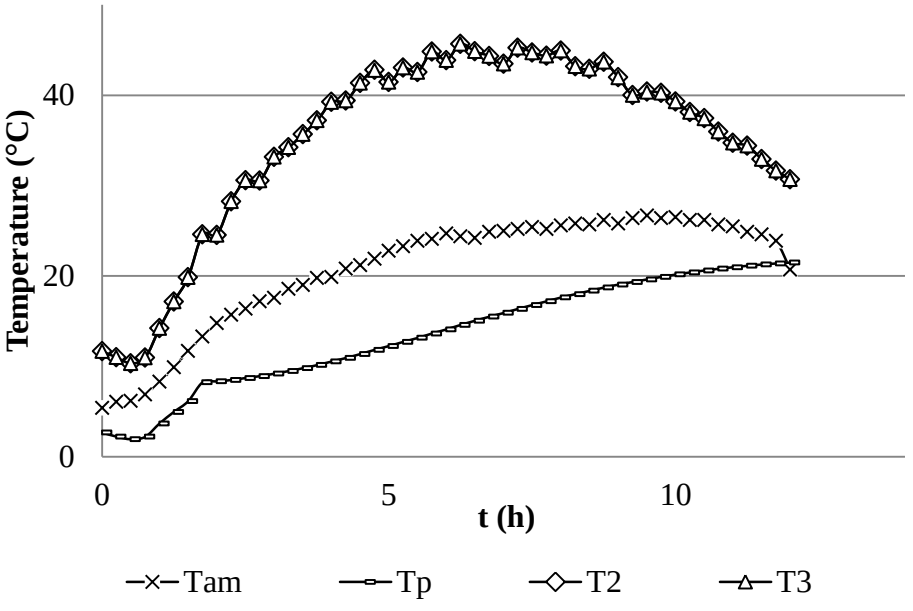

Fig. 19 Temperature profiles for a spring day (D2)

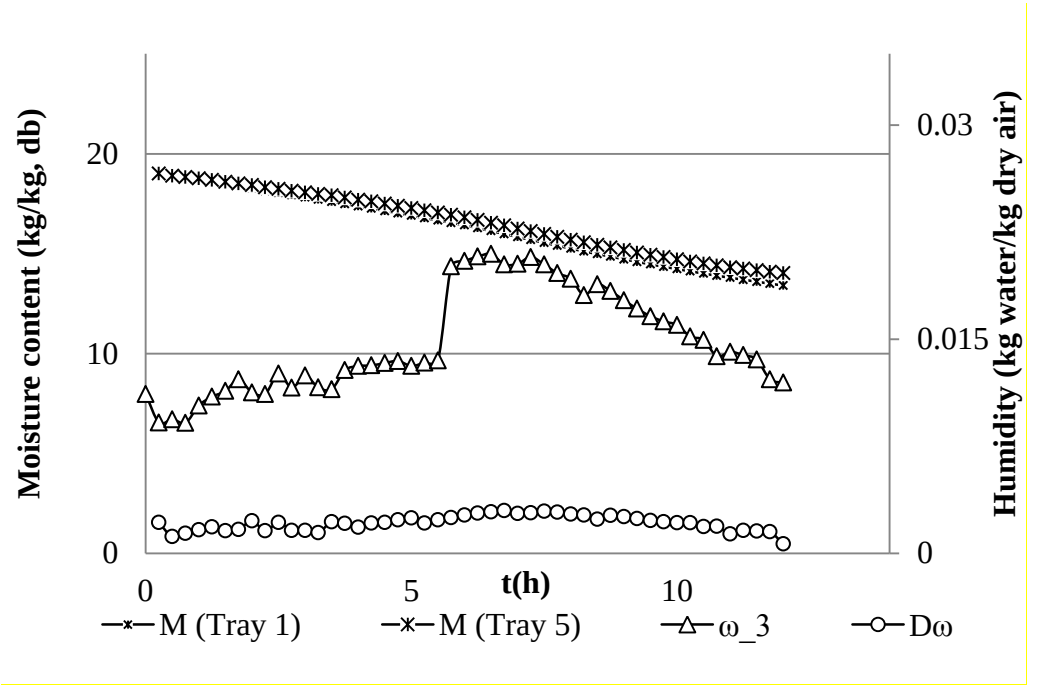

Fig. 20 Moisture content (M) and air absolute humidity (ω3) in the drying process of a winter day (D1)

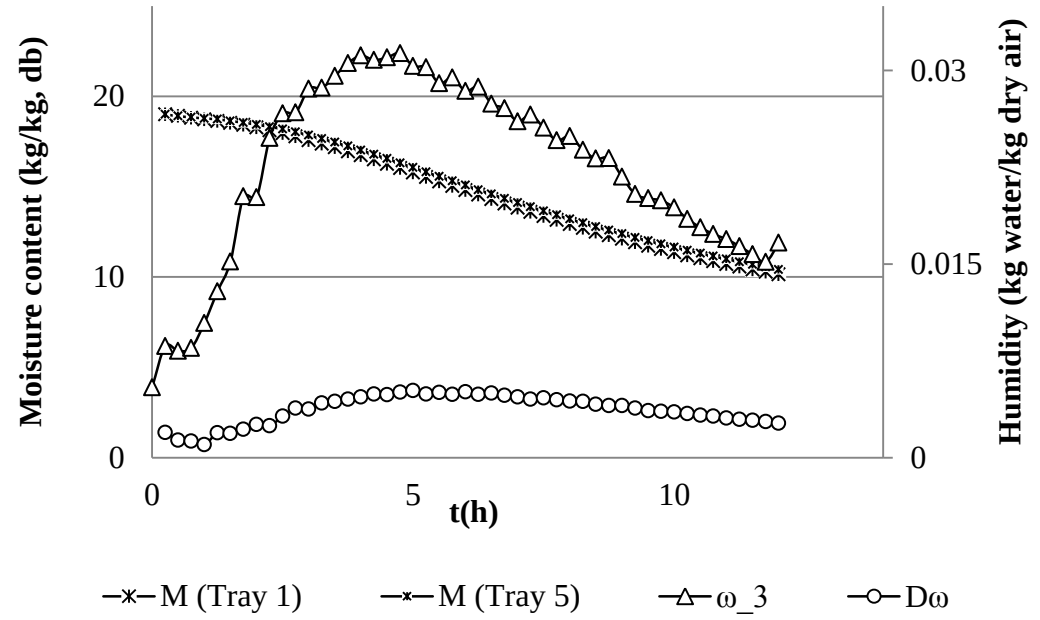

Fig. 21 Moisture content (M) and air absolute humidity (ω3) in the drying process of a spring day (D2)

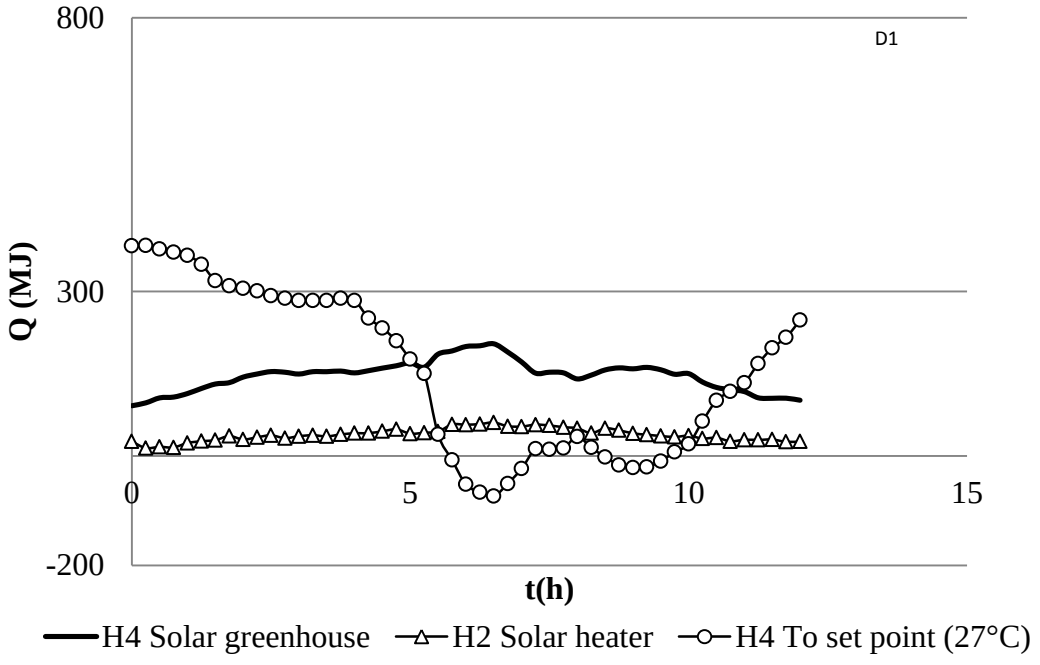

Fig. 22 Heat load for a winter day (D1) from solar heater (Q2), in the greenhouse without heating/cooling (Q4) and with heating/cooling (to set point)

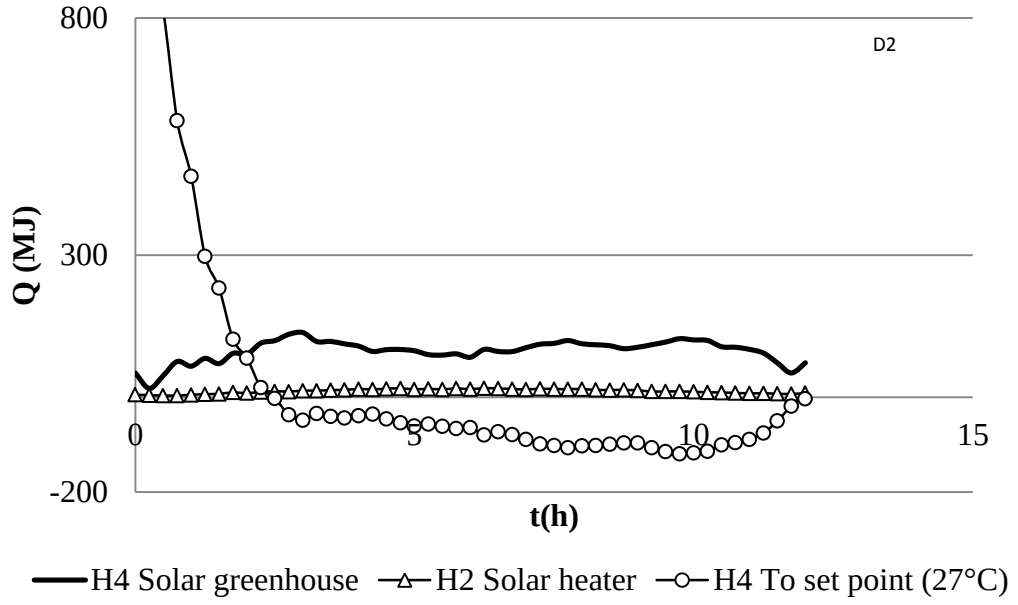

Fig. 23 Heat load of a spring day (D2) from solar heater (Q2), in the greenhouse without heating/cooling (Q4) and with heating/cooling (to set point)

3.2.3 New performance indicators

Exergy is a measure of both the quality and quantity of the energy involved in transformations within a system and the transfers across its boundary. Therefore, the exergy is an indicator of the inefficiencies of a process. Exergy analysis is an approach based on the principle of exergy destruction and exergetic efficiency used to analyze the performance of certain operations or to identify the bottlenecks of a process ([91], [92]).

Szargut et al. [92], mention that to be efficient it is important to utilize energy in quantity and quality that matches the task. They remark that society is inefficient in its use of energy since high temperature or high quality energy sources are used for low temperature processes. Exergy analysis differs from energy/enthalpy analysis; since exergy is destroyed by the processes in the system [42], the analysis permits a better matching of energy sources and uses and has become an essential tool for system design, analysis performance assessment and optimization of thermal system or component levels [9]. Analysis of exergy destruction is a powerful method that can highlight areas of improvement in a system and prevent irreversibilities (exergy destructions).

The general relation for change of exergy for a closed system between two states [93] for a reference state, usually environmental conditions, at T_0 and P_0 is given by:

$$\Delta Ex = (Ex_f - Ex_i) + P_0(v_f - v_i) - T_0(S_f - S_i) \quad (43)$$

3.2.3.1 Exergy in the drying process

Dincer and Rosen [94], presented the research *Exergy analysis of drying processes and systems*, where it is shown that a sizeable amount of exergy is lost with exiting air, even if it is assumed that the wet bulb temperature is reached in the drying process. Also, Cook and Dumont [95], mentioned that 20-40% or even up to 60% of energy is lost by rejected heat. So the airflow rate should be minimal to reduce absolute values of heat carried away with exhaust air. A study

by Sami et al. [96], concluded that airflow increment reduces exergy efficiency of solar collectors; even if the total exergy efficiency is low, the total energy efficiency is high and shows that the maximum energy loss occurs during midday. They also established that exergy is always produced and there is no exergy loss in the solar collector. Another study by Aziz et al. [97], covered heat circulation for algae drying; they worked on the idea of exergy recovery from the evaporated stream which contains a large amount of latent heat that can be utilized for raising the temperature of another fluid, which is sensible heat, and the amount of which is significantly smaller than the one owned in the evaporated stream.

The specific exergy for the flow at the drying inlet is determined by:

$$ex_1 = \left[\left(C_p\right)_a + \omega_1\left(C_p\right)_v\right](T_1 - T_0) - T_0\left\{\left[\left(C_p\right)_a + \omega_1\left(C_p\right)_v\right] ln\left(\frac{T_1}{T_0}\right) - (R_a + \omega_1 R_v) ln\left(\frac{P_1}{P_0}\right)\right\} + T_0\left\{[R_a + \omega_1 R_v] ln\left(\frac{1+1.6078\omega_0}{1+1.6078\omega_1}\right) + 1.6078\ \omega_1 R_a ln\left(\frac{\omega_1}{\omega_0}\right)\right\} \quad (44)$$

The specific exergy for the moist products can be written as

$$ex_p = \left[h_p(T,P) - h_p(T_0,P_0)\right] - T_0\left[s_p(T,P) - s_p(T_0,P_0)\right] \quad (45)$$

The specific exergy for the water content is

$$ex_w = \left[h_f(T) - h_g(T_0)\right] + v_f\left[P - P_g(T)\right] - T_0\left[s_f(T) - s_g(T_0)\right] + T_0 R_v ln\left[\frac{P_g(T_0)}{x_v^0 P_0}\right] \quad (46)$$

The specific exergy at the drying outlet is described as follows:

$$ex_3 = \left[\left(C_p\right)_a + \omega_3\left(C_p\right)_v\right](T_3 - T_0) - T_0\left\{\left[\left(C_p\right)_a + \omega_3\left(C_p\right)_v\right] ln\left(\frac{T_3}{T_0}\right) - (R_a + \omega_3 R_v) ln\left(\frac{P_3}{P_0}\right)\right\} + T_0\left\{[R_a + \omega_3 R_v] ln\left(\frac{1+1.6078\omega_0}{1+1.6078\omega_3}\right) + 1.6078\ \omega_3 R_a ln\left(\frac{\omega_3}{\omega_0}\right)\right\} \quad (47)$$

Fig. 24 and Fig. 25 show the specific exergy of exhaust air after drying for D1 and D2 which were obtained from the used model and applying using Eq. (47) from Dincer and Rosen [94]. The exergy values for D2 are higher than for D1, mainly due to higher energy from the solar resource.

3.2.3.2 Exergy in greenhouses

Bronchart et al. [42], describe that in greenhouses the energy of solar radiation and primary energy input with high exergy content degrades primarily through heat and vapour loss; this is by different physical and biological processes turning into heat at outside temperatures and air at outside concentrations with no exergy content. The impact can be compensated for with exergy input from heating, solar radiation, or both. If the exergy destruction is reduced, the necessary compensation can also be reduced. With regards to the main aim of this work, it is notable that: vapour is a source of exergy, although too much vapour can be harmful for plants. Exergy from vapour is very low cost compared to exergy from heat buffers in aquifer systems. Furthermore, its exergy values (quality) are comparable. The analysis of greenhouse air showed that its exergy value is made up equally of its heat and vapour content. When attempting to save energy, vapour must not be seen as something to get rid of, but as an exergy source.

To estimate the exergy of greenhouse air mass that is heated by solar radiation Eq. (48) is used (Fig. 24 and Fig.25). The reference temperature, T_0 was set as the average of T_{am} for each experimental data set.

$$ex_4 = \left(C_p\right)_v (T_4 - T_{am}) \left(1 - \frac{T_0}{T_4}\right) \quad (48)$$

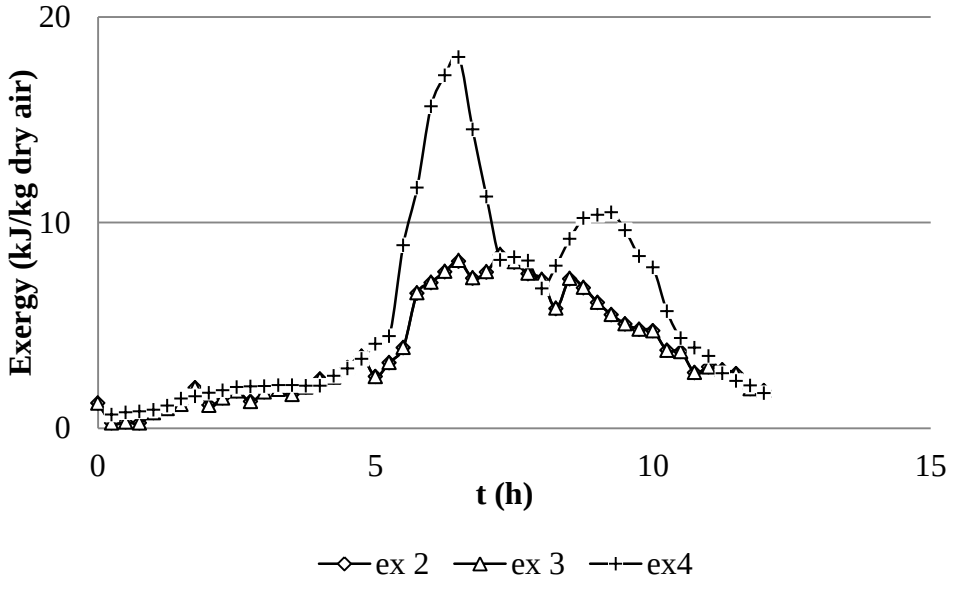

Fig. 24 Exergy on a winter day (D1). Ambient conditions (ex2), exhaust air (ex3) and within the greenhouse (ex4)

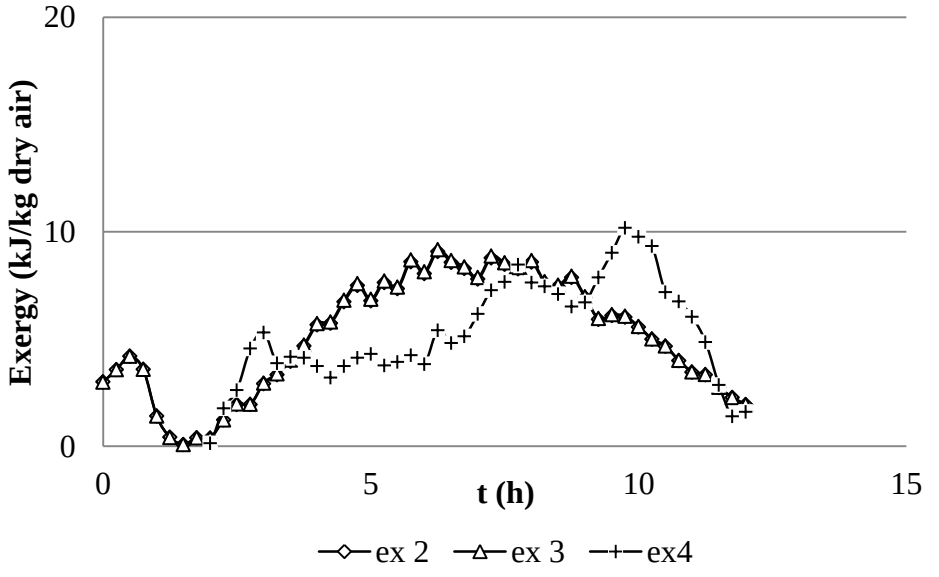

Fig. 25 Exergy on a spring day D2. Ambient conditions (ex2), exhaust air (ex3) and within the greenhouse (ex4)

Chapter 4

Stage 3. Interaction analyses

This stage is comprised of all possible means of efficiency improvement. With regard to the specific problem of this research, it is identified that linking the growing phase with the post-harvest processing in the drying value chain improves the environmental impact of production. Through designing best practices and new energy interaction methods among sub-processes by using thermodynamic operation zones it is feasible to achieve better sizing of equipment and more efficient use of available resources.

For case study A in Berlin the **energy interaction as heat recovery** from the growing phase for use for drying through heat exchangers is applied.

In the case B in Querétaro, the interaction is proposed as a **physical mixture of current flows** to recover exergy and water from the drying process for redelivery to the greenhouse system. By thermodynamic model simulation, humid air from the drying process is retrieved and delivered back to the crops in the greenhouses.

4.1 Case A: heat exchange

The proposed energy interaction is depicted in Fig. 26 where the objective is to recover in the greenhouse the energy from the latent and sensible heat of condensation. A heat pump is then used to raise the water temperature of the storage tank (270000 L) and the whole system benefits from the heating system. In the current process where the ZINEG project has its boundary, the excess energy is exported (especially under summer conditions) to the cooling tower, which simulates a heat consumption unit. In order to use the available energy from the growing phase, the heat exchange interaction with the drying post-

harvest process is theoretically evaluated. For this a second storage tank (300 L) where the water temperature is raised is needed.

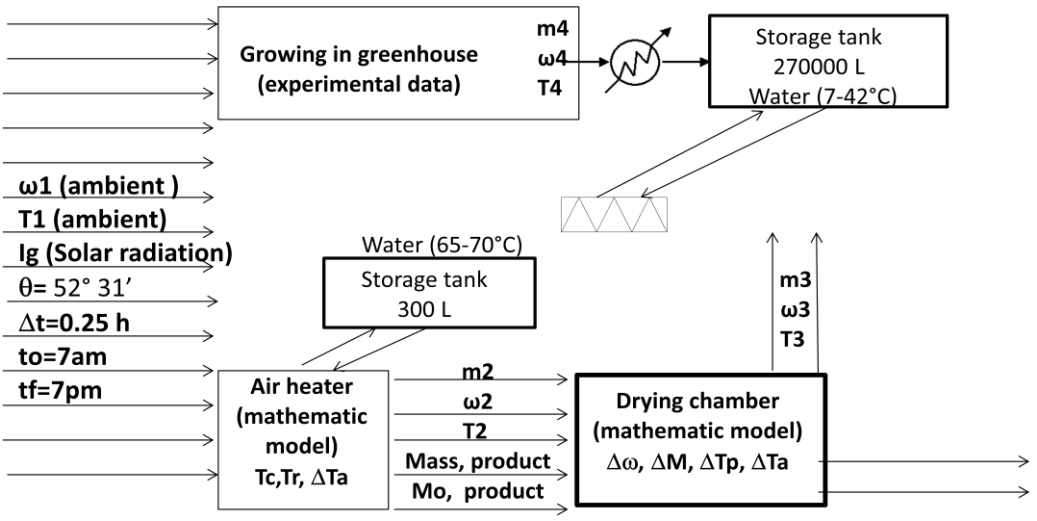

Fig. 26 Schematic of the energy interaction for the Berlin case

Table 9 summarizes the monthly values for the available energy of the storage tank, the used solar energy and the thermal energy for conventional drying of the *reference* case. These values are depicted in Fig. 27 where the energy for *drying reference produce* (crosses) and the *energy available* from the tank (squares) are shown, while the secondary axis shows the average (day and night) temperature of the 270000 L storage tank (dashed-diamonds line). From months 5 to 8 the average temperature is 35°C, in Month 9 the maximum average temperature is 40.7°C. As observed, the total energy sent to the cooling tower is enough for the drying process of tomato produce; however, the enthalpy and exergy would not allow the air temperature to be raised to the 65-70°C required to carry out the drying because the water temperatures in the tank range from 7-42°C. For this reason it is necessary to add auxiliary heating to raise the air temperature, but in whatever case the water that is already heated up is useful for pre-heating or for continued drying throughout the night.

Table 9. Thermal energy interaction

	Month						
Reference	5	6	7	8	9	10	TOTAL
5. Drying (tomato classes B+C) **(GJ)**							
Thermal energy	0.49	1.43	2.17	0.83	0.65	0.88	6.44
TOTAL per month	0.49	1.43	2.17	0.83	0.65	0.88	6.44
Thermal energy heat exchange **(GJ)**							
Storage tank [1]	21.36	17.20	16.27	16.00	24.87	16.72	112.42

[1] 260,000 L temperature max 42°C

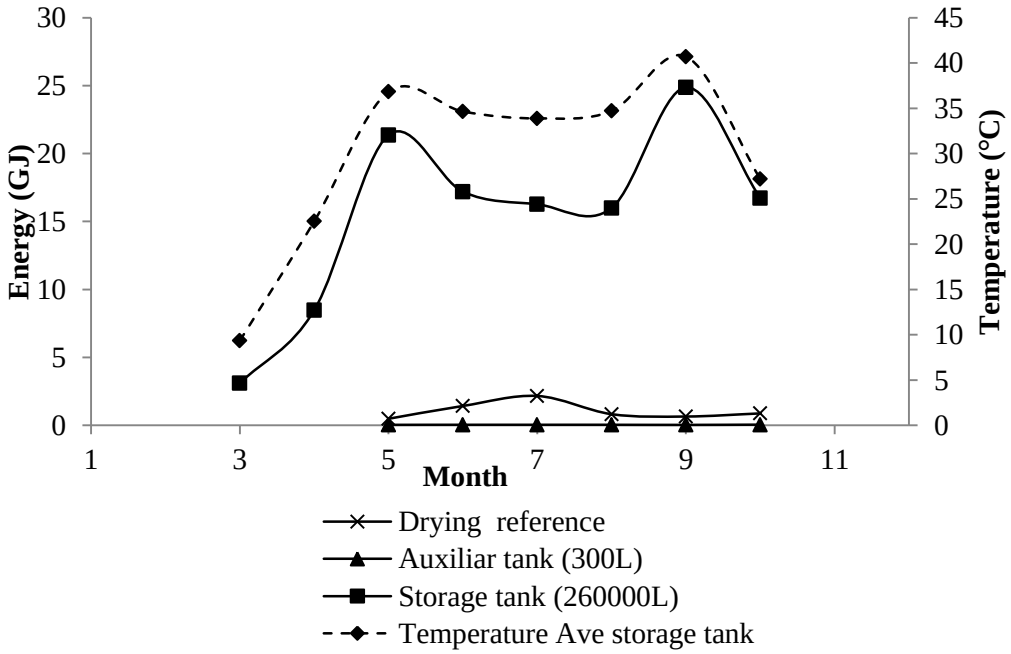

Fig. 27 Temperature and energy availability from the storage tank

4.2 Case B: exergy and energy

During the drying process, water as not fully saturated wet air is not used after the process even though its temperature is usually higher than the ambient temperature. This means that a large amount of energy is lost to the atmosphere [98]. This loss of energy was estimated between 70 and 90 kcal kg^{-1} of evaporated water [99] and 150-174 kcal kg^{-1} for walnut drying [100]. Basically all the energy from exhausted air could be recycled, which is usually mixed with fresh air and recirculated back to the system, and hence the exergy loss could be minimized [97]. Several authors have studied air recirculation for energy savings in dryers reporting reduction of energy requirements by 29.6% for orange drying, energy savings of up to 30% by recirculating 60% of the air in the drying of walnuts, savings of up to 15% and thermal efficiencies of 50% in tunnel dryer for fruits and average reduction of the energy requirements of 26% for peanuts ([101], [102], [100], [103]; respectively).

However, air recirculation increases the retention times and the drying potential is reduced, which in some cases can affect the quality of the final product. The retention of carotenoids is impacted by high rates of air recirculation, especially in the first stages when the elevated moisture content of the product facilitates the elimination of these. Other quality parameters affected by air recirculation are ascorbic acid retention and nonenzymatic browning [104].

Although heat recovery is a good solution, the cost of heat exchangers, fans, piping, etc. is excessive and the implementation requires broad expertise. The main objective is to research the easiest and, of equal interest, the cheapest way to recover the exhaust air from drying process.

The proposed interaction is depicted in Fig. 28. The exhaust air from the drying process is mixed through physical interaction with the greenhouse air.

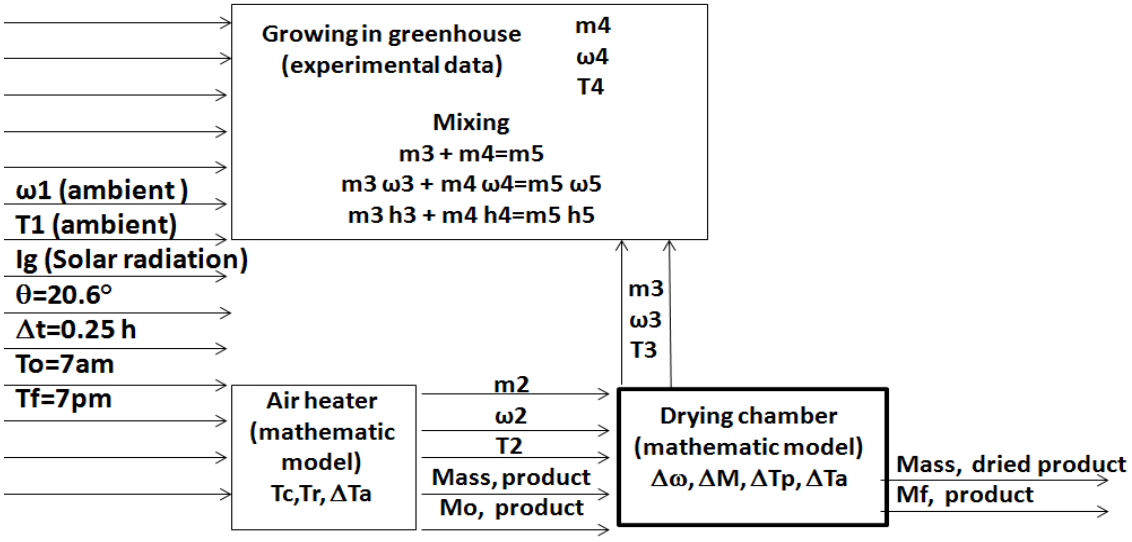

Fig. 28 Schematic interactions growing in greenhouse drying (states)

The states 1, 2 and 3 from Fig. 28 are described from Eq. 10 to 39. States 4 and 5 are determined by the following equations

State 4: Greenhouse

Experimental data for temperature T4 and relative humidity hr4 are taken from greenhouse data recording system.

State 5: Mixing

The thermodynamic mixture is determined by

$$m_3 + m_4 = m_5 \tag{49}$$

$$m_3\omega_3 + m_4\omega_4 = m_5\omega_5 \tag{50}$$

$$m_3h_3 + m_4h_4 = m_5h_5 \tag{51}$$

The mixing of the flow of exhaust drying air with the air of the greenhouse (state 5) was simulated based on the thermodynamic principle of evaporative cooling.

Fig. 29, 30, 31 and 32 summarizes the state changes along the process from the proposed energy interaction.

For both days, it is observed that the absolute humidity from the exhaust air of the drying, ω3 shows the highest values of all trends, being maximum at midday. The absolute humidity of the greenhouse, ω4, is raised, after the interaction, to ω5. So the temperature of the greenhouse, T4, is decreased.

On average the results show a decrease of greenhouse temperature, T4, of 12.8°C and 8.7°C and an increment of relative humidity, ω4, of 7% and 9%, for a spring day and winter day, respectively. These results are presented as averages, to enclose the overall impact of the air mixing and the variations of irradiation, absolute humidity, heat losses and transpiration of plants during daytime.

Hence, with the calculated new states T5, hr5 and ω5 the heat load to reach the set point of 27°C, is 2216 MJ and 10540 MJ for D1 and D2 respectively, so the change of cooling load from the base case of greenhouse (state 4) for D1 is 1265 MJ for heating and for D2 is 16932 MJ for cooling, considering the same time span observed in Fig. 22 and Fig. 23.

For the spring weather D2 (Fig. 31) the proposed flow interaction lowers the temperature, especially in the high irradiation hours, from a maximum of 40°C to around 20°C. However, for a winter day D1 (Fig. 32) such low temperatures are not desired.

The presented results are convenient for hot days within the plastic greenhouses where the targeted energy savings are focused on the heat load for the cooling utility. However, for cold days the proposed interaction lowers the temperature even more which derives in heating need.

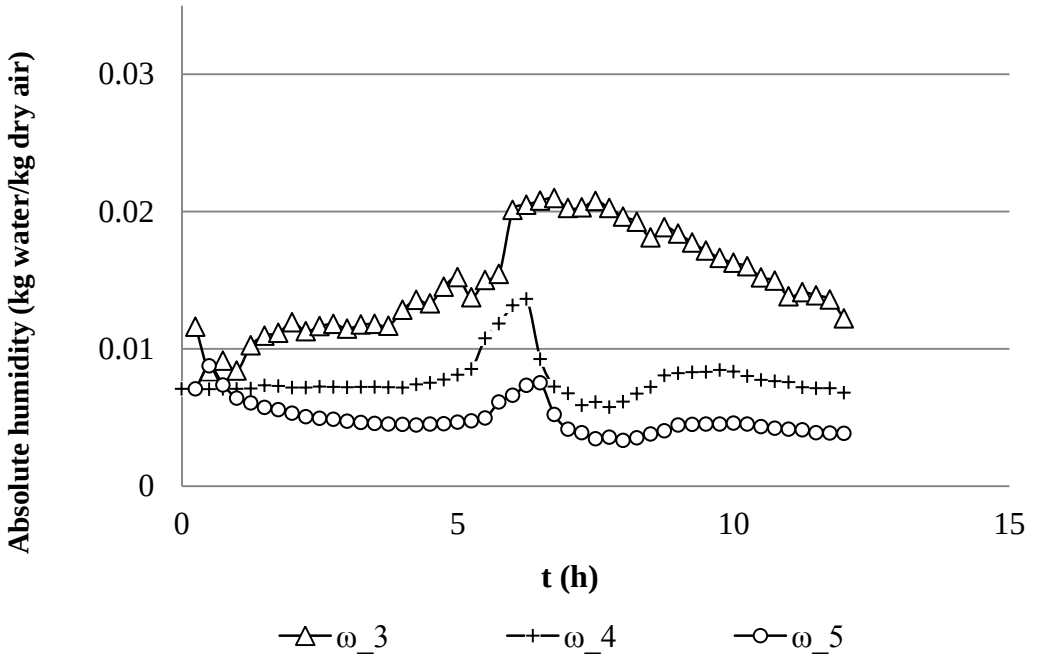

Fig. 29 Absolute humidity on a winter day (D1) at the dryer outlet (ω3), within the greenhouse (ω4) and from the mixing (ω5)

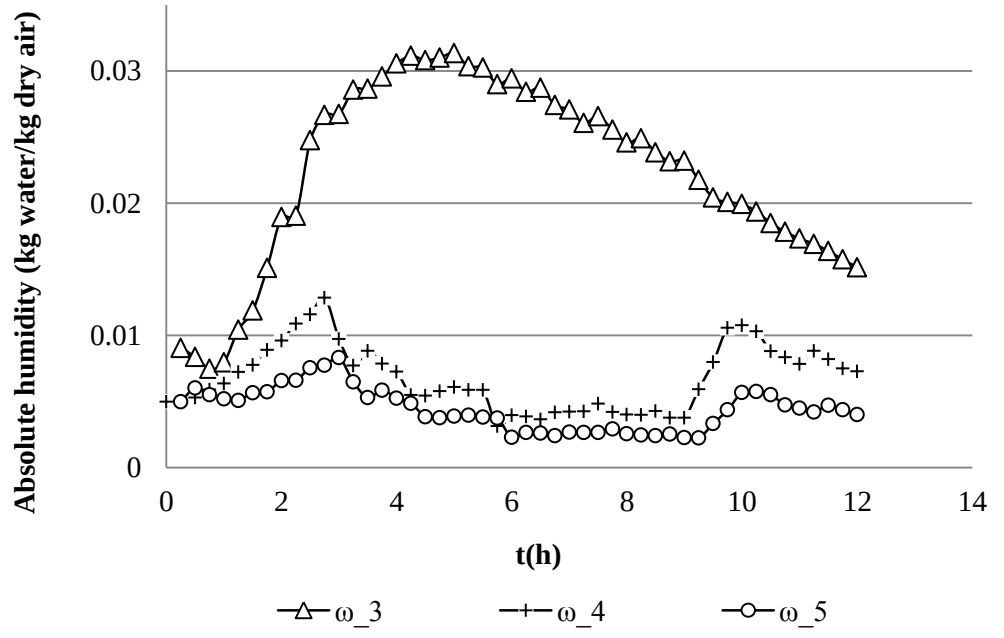

Fig. 30 Absolute humidity on a spring day (D2) at the dryer outlet (ω3), within the greenhouse (ω4) and from the mixing (ω5).

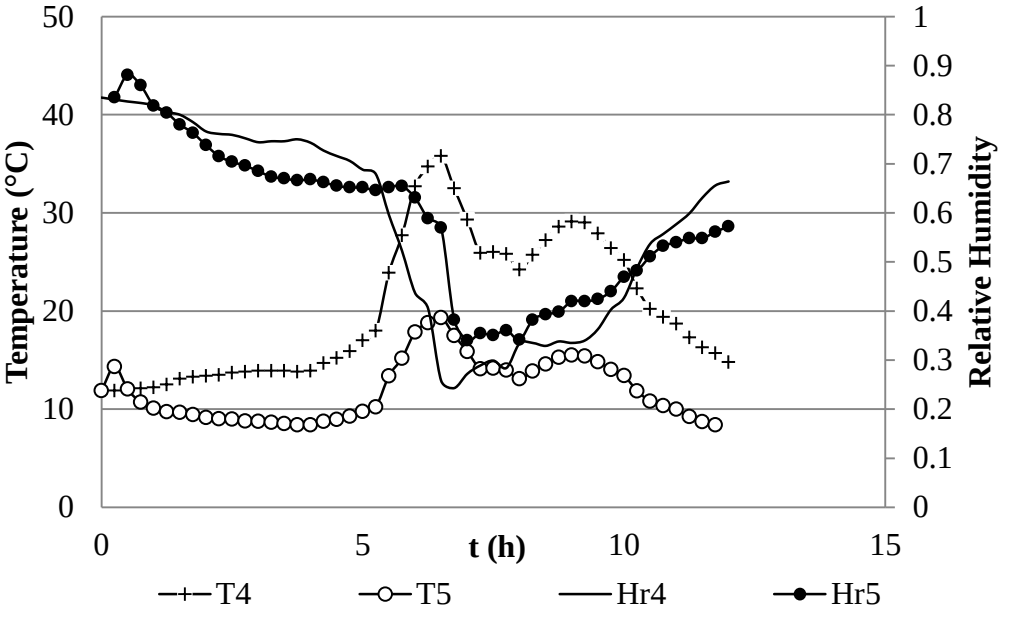

Fig. 31 Temperature and relative humidity on a winter day (D1) within the greenhouse (T4, hr4) and from the mixing (T5, hr5)

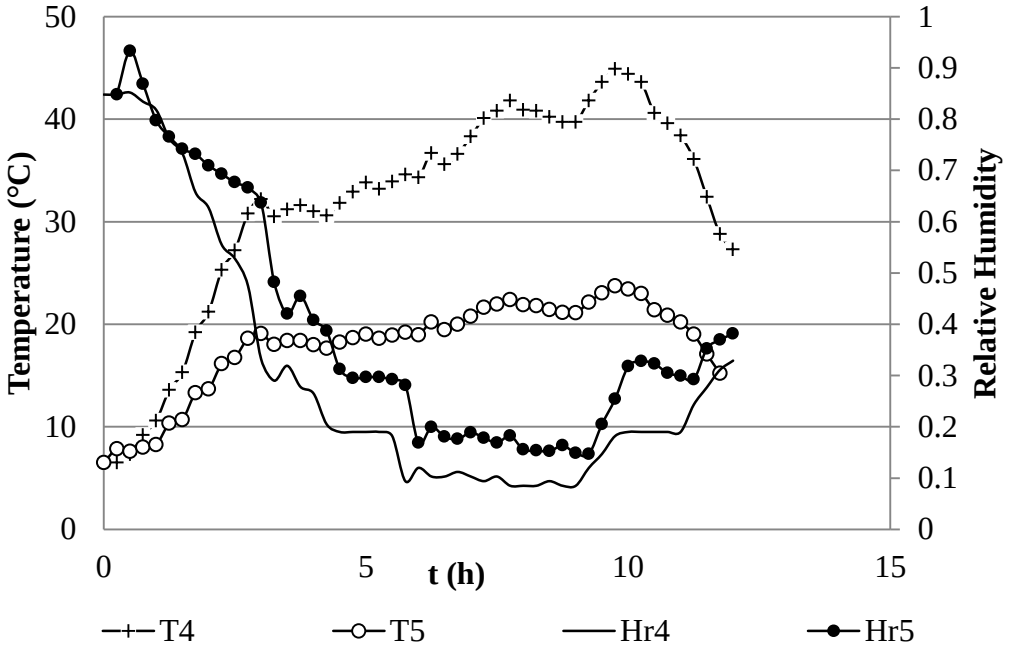

Fig. 32 Temperature and relative humidity on a spring day (D2) within the greenhouse (T4, hr4) and from the mixing (T5, hr5)

As mentioned, for industrial drying processes, energy and water amounts become significant. Thus, energy interaction thermodynamic results between greenhouses and drying process show the possibility of energy savings by using exergy from exhaust drying air, reducing the use of cooling systems within greenhouses in high temperature zones, and by retrieving water as absolute air humidity in the contained air. From this the positive potential of making use of the exhaust air, finding that for cooler days the energy interaction does not have such good benefits is observed. However, it is also clear that the energy savings during a day are not constant.

This interaction presents an economic solution for the problem of high temperature and low relative humidity within greenhouses in hot dry environments. In the following section the impact of this proposed solution is evaluated.

Chapter 5

Stage 4 and 5: implementation strategy and post-benchmarking

Due to the characteristics of the two cases study, i.e. ambient conditions, process configuration, economic restrictions, energy requirements, resource availability, operation conditions and operation time span, it is important to develop a specific **strategy for the implementation** of energy improvement measurements and programmes.

The optimum order of implementation may be different from the order in which the systems interactions have been analyzed [20], mainly because of the predominant relevance of economic type factors.

For both case studies, the growing phase in greenhouses are complete projects already developed in: case A, the Humboldt University of Berlin and case B, the Queretaro Autonomous University. The drying process is studied and integrated mainly to add value to the second quality products as well as to make use of the waste of energy and water. The drying simulation **(section 2.3.3.4)** has been used to design the energy enhancing measures proposed and to determine their impacts on water and energy consumption within the whole value chain.

For the case A value chain, the major funding portion is assigned to the growing phase in the already well established ZINEG project which aims to recover energy, reduce heat losses and optimize the use of the heating systems, and to keep the conditions within the greenhouse as constant as possible because of continual climate variation. The priority is the use of harvested energy in the growing phase for the post-harvest drying process.

For case B, the funding is applied to the post-harvest drying process to develop a dryer with industrial capacity. Due to continuous tomato production throughout

the whole year, the priority is to develop dried tomato of high quality. A solar-electric dryer is designed and tested to determine its thermal impact on the process; the potential savings and economic analysis are given. The obtained product is characterized in a complete way for different market purposes.

The **post-benchmarking** is based on the quantification of the benefits from the energy interaction analysis. In case A, the impact on the whole value chain is done in analytic form. For case B, the analysis of the impact is complemented with experimental results.

5.1 Case A: *collector* value chain

5.1.1 Implementation strategy

The implementation strategy in the case of Germany is based on the main problem and economic limitations of Table 2. As indicated, the greenhouse ZINEG project was established in 2009. In this work results are reported and reorganized according to the followed methodology.

The following measurements were identified by the interactions analysis once all possible resource reductions had been maximized. According to the raised research questions, two types of measurements were identified: the ones wherein the energy efficiency is improved (1 to 3 identified by Tantau et al. [69], or substituted by renewable energy (measures 1 to 5) and those wherein water use is optimized (measures 6 and 7):

1) use of the greenhouses as solar collectors in the growing phase
2) recovery of the latent energy of vapour water by fine pipe heat exchanger
3) use of the heat stored form the greenhouse system
4) changes in logistics by coupling growing and drying sites
5) use of solar energy to dry produce for the harvest time

6) recirculation of the condensed water to the system
7) recovery of rain water as water input record

In the current process configuration, the implementation of measurements 1 to 3, 6 and 7 required the installation and control of high-tech devices in the greenhouses, i.e. an electrically driven water-water heat pump, fine pipe heat exchangers, a condensate channel in the roof zone, tubular-film heat blowers, a vegetation heating system, double glass panes, thermal screen, aluminized energy screens in the roof zone, drip irrigation, a fog system and CO_2 enrichment, polystyrene rainwater storage tank [71], as well as all the required sensors, controllers and main computer system.

The main objectives of these measurements could be enclosed in:

1) water and carbon footprint improvements
2) enhancement of the value of second class tomato fruits
3) reduction of the resources used for product transportation
4) highlighting and reporting of the amount of water in plants residues and tomato wastages
5) reporting the monthly performance of a whole season

5.1.2 Post-benchmarking

In comparison with the *reference*, in the ***collector*** **value chain** the growing occurs in a semi-closed greenhouse which is set up as an energy recovery system and is partially ventilated; the solar drying process takes place in the same location through the energy interaction with the growing phase, making use of the stored energy, i.e. eliminating the need to transport the fresh product. The ZINEG *collector* greenhouse is equipped with a finned pipe condensation heat exchange system in the roof zone, a conditioning system of a foliage tube heat exchanger below the channels, a canopy radiation heat exchanger, aluminized energy screens in the roof and standing wall regions, a fog system and CO_2 enrichment.

The *collector* greenhouse is also a Venlo-glass type of 200 m^2 crop area with a set point temperature of 24°C and RH above 90%. The *collector* and the *reference* greenhouses are connected with a heat pump circuit (Schuch et al. [83]; Dannehl et al. [74]).

For the growing phase, in Table 10 the *collector* greenhouse conditions show higher relative humidity with less variation compared to the *reference* greenhouse (Table 4) and a 0.6°C temperature difference, behavior expected due to the ventilated operation.

Table 10. Thermodynamic states in *collector* greenhouse

	Mean value	Standard deviation
Temperature (°C)	23.1	1.4
Absolute humidity (g kg^{-1})	16.1	2.2
Enthalpy (kJ kg^{-1})	64.3	6.7
Relative humidity (%)	89.3	8.5

As observed in Fig. 33, regarding the total produce weight (classes A, B and C), the *collector* greenhouse has 22.25% more than the *reference* greenhouse. Additionally, it is observed that for the collector greenhouse, the production of tomato class A was 50.9% higher; while the production of tomato class B was 7.2% and C 4.3% higher for the reference greenhouse. In the case of the BER tomato class, the reference greenhouse produced 75.5% higher amount. It was observed that the conditions from the collector greenhouse impacted positively on the yield sold as fresh produce.

The crop residues represent in total a weight of 28.8% for the *reference* and 25.5% for the *collector*; when including the non-marketable products (BER) the values are 38.7% for the reference and 27.7% for the collector. These values are

in accordance with those reported as 30% [105] and 10-40% of total processed tomatoes ([106], [107]). However, when comparing both systems, the collector greenhouse reduces the residue generation by 10.9% total weight.

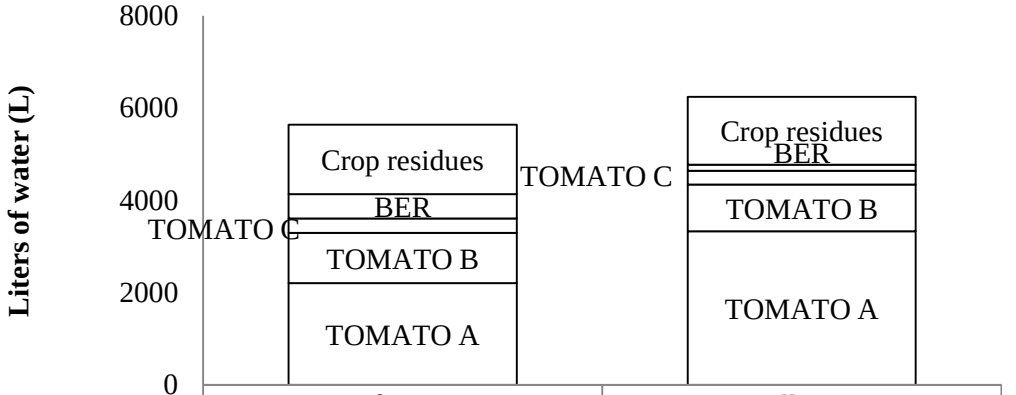

	Reference	Collector
Crop residues	1502.78	1471.06
BER	528.99	129.83
TOMATO C	313.53	299.97
TOMATO B	1087.62	1009.59
TOMATO A	2207.69	3332.27

Fig. 33 Water content considering tomato 94.6%, leaves 84% and stems 86% moisture content

5.1.2.1 Water and energy measurements impact

The total amounts of water per item over the 10 months are represented in the water flow diagram of Fig. 35. The percentage of water for each item is given with respect to the total water input in the *reference* configuration (100% = 242516 L of water) in order to make comparisons. However, the actual total water input to the *collector* is 72.9% (176994 L fresh water + rain water) of the water input to the *reference* greenhouse.

Fig. 36 For the *collector* water circuit in Fig. 34, the rain water collected represents 60.2% of the actual water input while the recirculation with nutrient solution represents 31.2% with respect to the *reference* water input. Page et al. [40] in comparison report values of 30% of rain water harvested from the

greenhouse roof and 30% for nutrient runoff. The transpiration is reduced to 27.2% in agreement to results from Dannehl et al. [75]. A significant 13.9% of transpired water is recovered by the fin pipe heat exchanger as condensed water. Class B and C tomatoes from the whole season are dried with solar energy in dryers installed next to the greenhouse. The exhaust air from the drying contains 1278 L of water as air humidity and the dried product contains 31.7 L of water, representing 105.75 kg of dried product at 0.43 kg kg^{-1} d.b. In order to reduce the moisture content of the residues, it is proposed that these are to be dried while no tomato harvest is available. The water content of the BER tomato is 130 L, of the pruned leaves it is 789 L, and from the plants after the season it is 682 L.

Fig. 35 and Fig 36 show the monthly trends of transpiration, irrigation, calculated ventilation and estimated water uptake per plant. The depicted curves show maximum values for summer time, an increase at the beginning of the season while the tomato plants start to develop, and a decrease at the end of the season. The comparison of the trends per month of water uptake by the plant is reduced by 28.6% on average for the *collector* greenhouse since the relative humidity is high. During the summer months, transpiration is decreased by 24% in the collector greenhouse. The seasonal average need for irrigation shows a 27% lower trend for the *collector* greenhouse, which is one of the main objectives addressed; during the summer months, irrigation is decreased by 34% on average.

In Table 11 the total amount of water used for the *collector* value chain is presented.

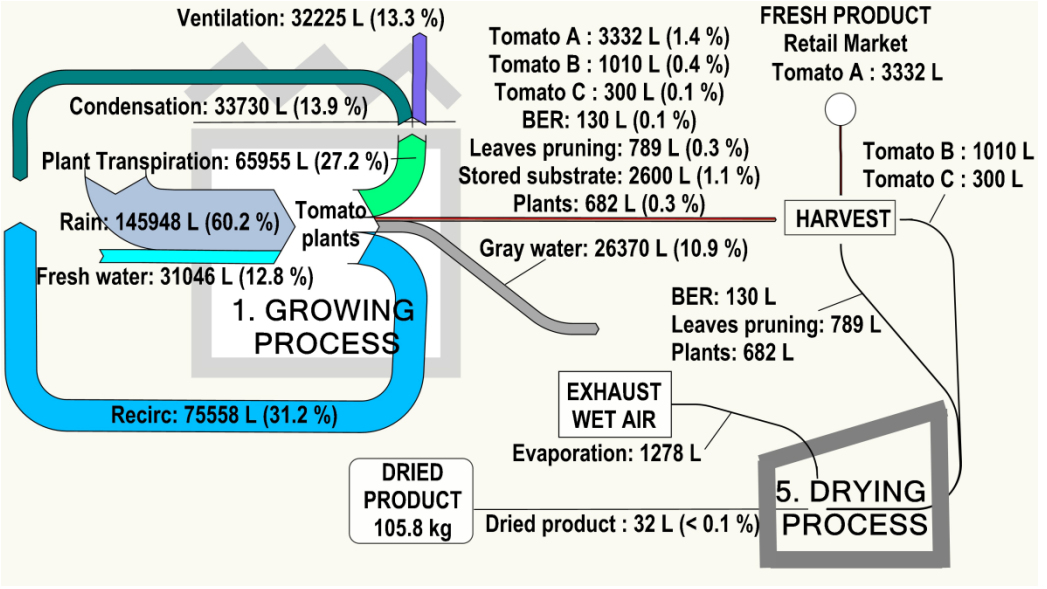

Fig. 34 Water flow for the *collector* configuration

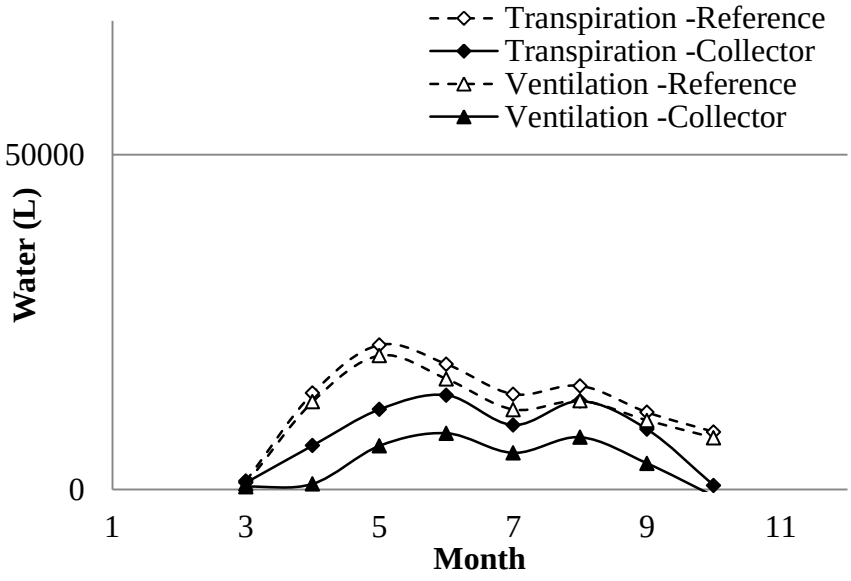

Fig. 35 Comparison of greenhouse transpiration and ventilation

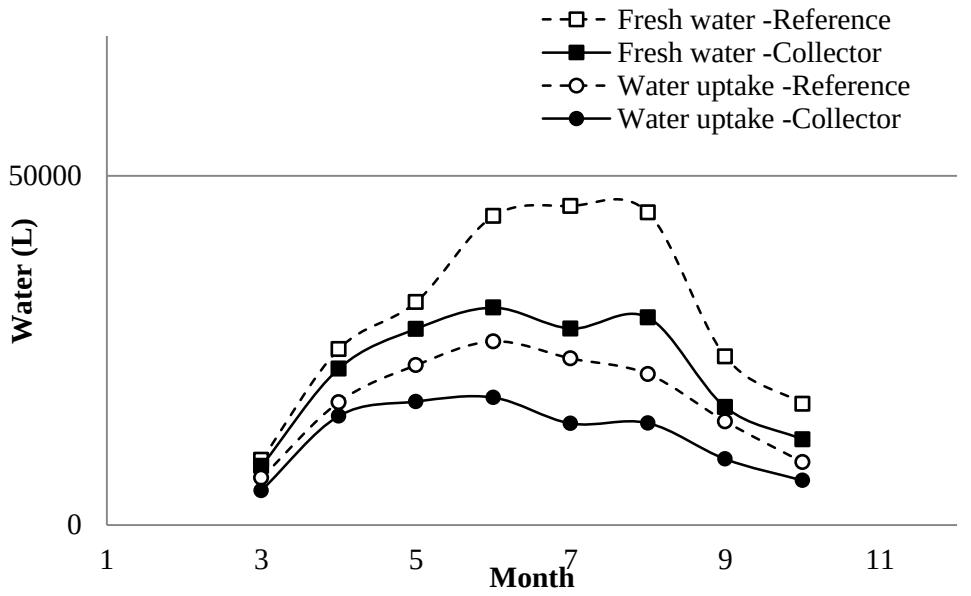

Fig. 36 Comparison of fresh water and plant uptake per month in greenhouses

Table 11. Water consumption for the *collector* value chain

	Month							TOTAL
Collector	5	6	7	8	9	10	End	
1. Growing (L kg^{-1} tomato)								
Green water	8.4	14.9	53.4	35.5	40.8	34.7		29.8
Blue water	19.2	25.5	-24.8	10.5	3.9	10.6		6.3
Grey water	4.4	11.7	10.7	14.7	15.1	15.4		10.8
Crop residues*	0.06	0.06	0.06	0.13	0.19	0.29	0.30	0.40
5. Drying (L kg^{-1} tomato)								
Blue water for washing	5	5	5	5	5	5		5
Grey water	10	10	10	10	10	10		10

* Including leaves, plants and BER

5.1.2.2 Energy measurements impact

The ZINEG arrangement is designed to supply heat to both greenhouses from the energy collected, with a maximum efficiency of 0.7 [74], thereby reducing the primary energy consumption by up to 81% [71].

In Fig. 37 the energy flow of the ZINEG system during the season is represented; 1.11 TJ of solar energy are received and for an average transmission of 0.65 there is a net input of 0.72 TJ. The overall electricity for cooling and heating required for the system is 0.22 TJ. 0.48 TJ are exchanged through the finned heat exchanger and 0.42 TJ are stored in the water tank. For greenhouse heating, 0.11 TJ are supplied to the *collector* and 0.17 TJ to the *reference* system. The available energy, sent to the cooling tower, is 0.38 TJ.

At night, the direction of heat exchange is reversed and 0.2 TJ from the storage tank are exchanged in the heat pump; since there is a low level of transpiration from the plants, the latent heat is not recovered. The total Heating Seasonal Performance Factor (HSPF) and the total Seasonal Energy Efficiency Ratio (SEER) are 2.9 and 3.3, respectively [71].

It is important to note that the process load is fed only by the supply of the two greenhouse systems and would be as shown in Fig. 37. However, usually commercial drying cluster facilities are fed by several growers and greenhouses or there is more than one product growth in a farm so the drying process occurs for different products according to the season.

For the incorporation of the heat pump, the range of electricity for heating/cooling is higher than the already reported values of 1.7 MJ m^{-2} [86], 0.32 and 0.29 MJ kg^{-1} tomato for med-tech and hi-tech systems, respectively [40], and 0.40 MJ kg^{-1} tomato with a standard deviation of 0.30 MJ kg^{-1} [87]. The heating system consumption is reported by [40] as 0.6 kg coal kg^{-1} for med-tech and 0.18 kg natural gas kg^{-1} and 0.43 kg coal kg^{-1} tomato for high-tech systems; when considering the heat content of coal as being in a range of 16.08

to 28.47 MJ kg^{-1} and for natural gas as 49 MJ kg^{-1} the energy consumption for med-tech is from 9.65 to 17.08 MJ kg^{-1} and for high-tech from 15.73 to 21.06 MJ kg^{-1} tomato.

The use of solar drying next to the growing site represents savings in energy consumption per transport, which reduces GHG emissions. As Poritosh et al. [11] state, transport energy consumption varies depending on truck quality and age, as well as transport logistics and the type of road. The variation of produce of classes B and C impacts the transport energy consumption from 2.8 to 11.8 MJ kg^{-1} tomato. These values are in the range of the ones reported by Karakaya and Özilgen [12], as 8.08 MJ kg^{-1} with associated carbon dioxide emissions of 11.2 kg CO_2 kg^{-1} tomato.

Table 12 presents the used solar energy and the still required auxiliary energy for the *collector* case. These values are depicted in Fig. 38 which shows the energy for *drying collector + reference produce* (circles) and the energy for drying *collector produce* (crosses). Also shown is the *energy available* from the tank (squares) and the energy from the *auxiliary source* (triangles) supplied to heat an auxiliary tank of 300 L to 70°C to preheat the air (via a heat exchanger) for the drying process.

Table 13 then collects all energy estimations. In this, it is observed that the *reference* greenhouse requires more thermal energy due to its ventilated operation, therefore losing more energy via the wet air. The *collector* drying process requires slightly less energy than the *reference* drying process (6.34 GJ as opposed to 6.44 GJ in Table 9 and Table 12). However, it is important to consider that the different tomato produce per month impact on the values of energy per kg tomato. The *collector* greenhouse requires less total growing energy for the whole production than the *reference* greenhouse (0.98 TJ as opposed to 1.07 TJ).

Table 14 shows the water and carbon footprint with a standard deviation for the collector value chain of 12.4 L kg^{-1} of tomato for the water footprint and 11.4 kg CO_2 kg^{-1} of tomato for the carbon footprint. The CO_2 per kilogram of tomato consumed in photosynthesis is reduced principally for the higher productivity.

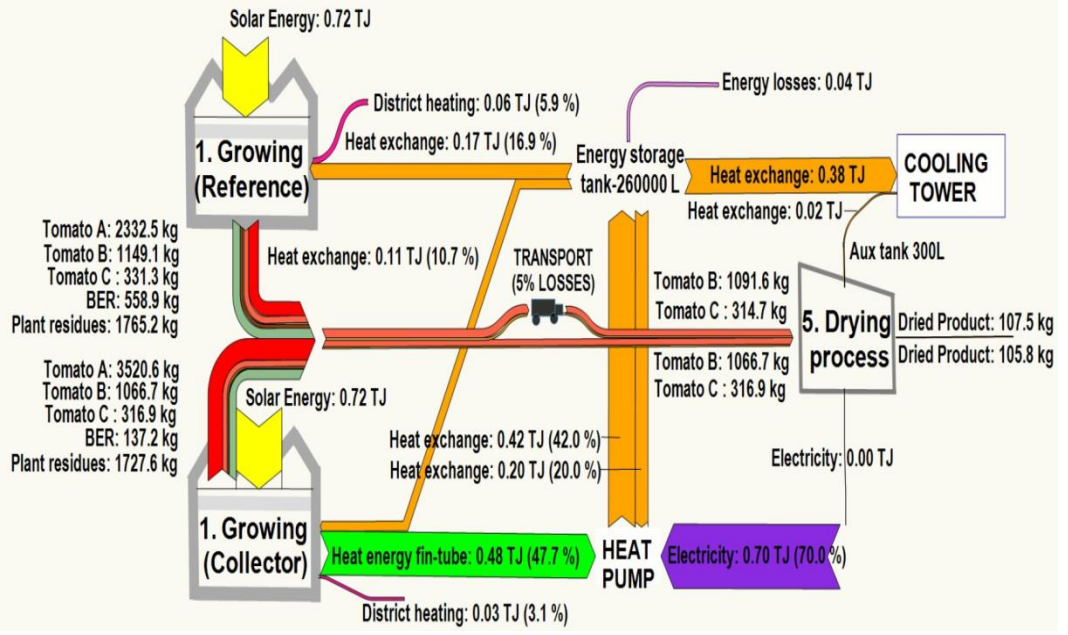

Fig. 37 Energy flow interaction for a coupled system

Table 12. Energy requirement for drying (tomato classes B+C) in the *collector* value chain

	Month						
Collector	5	6	7	8	9	10	Total
5. Drying							
Solar energy **(GJ)**	0.06	0.34	0.56	0.16	0.25	0.19	1.58
Thermal energy **(GJ)**	0.51	0.90	1.47	0.58	0.62	0.68	4.77
TOTAL per month **(GJ)**	0.58	1.24	2.04	0.75	0.87	0.87	6.34
Auxiliary tank **(GJ)**	0.04	0.04	0.05	0.04	0.04	0.05	0.27

[2] 300 L temperature 70°C

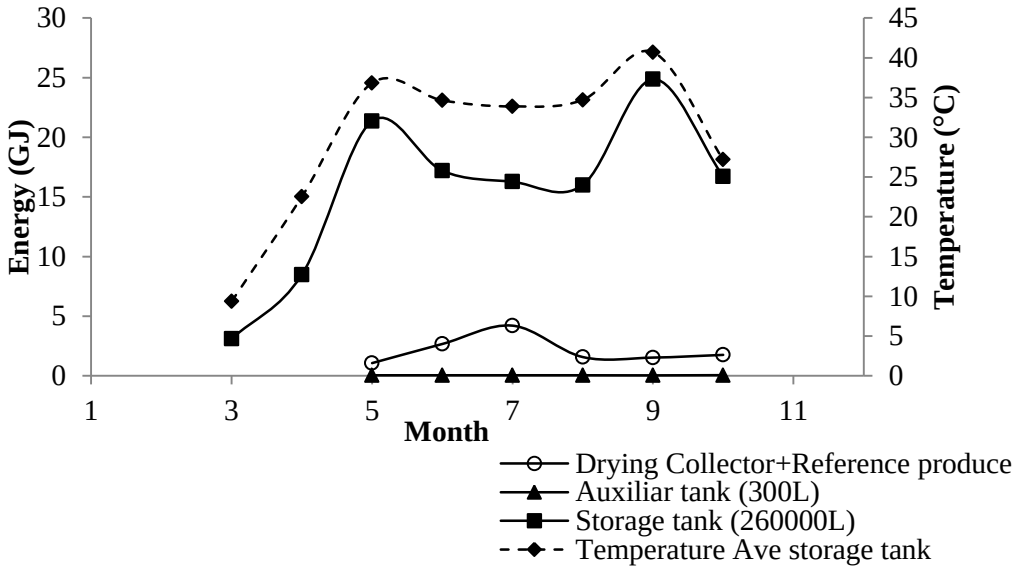

Fig. 38 Temperature and energy availability from the storage tank

Table 13. Energy flow (MJ kg^{-1} tomato) of the *collector* drying value chain

	Month						
Collector	5	6	7	8	9	10	TOTAL
1. Growing (MJ kg^{-1} tomato)							
Solar energy	131.79	170.70	104.11	159.24	204.23	180.09	147.63
Thermal energy	11.98	18.14	20.48	24.50	50.83	110.02	28.64
Electricity *	16.94	25.27	16.10	22.42	39.80	41.80	23.35
5. Drying (class B+C) (MJ kg^{-1} tomato)							
Solar energy	0.47	1.22	1.27	1.00	1.36	1.09	1.14
Thermal energy	3.83	3.23	3.31	3.63	3.34	3.78	3.45
Electricity	1.13	1.02	1.16	1.01	1.02	0.91	1.06

* Electricity of total ZINEG system, considered equally distributed to reference and collector

Table 14. Water and carbon footprint of the *collector* value chain

	Month						
Collector value chain	5	6	7	8	9	10	TOTAL
Water footprint (L kg^{-1} tomato)	46.9	67.1	54.3	75.7	74.8	75.7	51.1
CO_2 footprint (kg CO_2 kg^{-1} tomato)	6.52	9.04	8.62	10.55	19.81	36.43	10.99
CO_2 photosynthesis (kg CO_2 kg^{-1} tomato)	0.93	0.62	0.67	0.89	0.82	0.88	0.19
Residual water** (L kg^{-1} tomato)	0.37	0.61	0.63	0.65	1.04	1.35	0.66

** Water from greenhouse residues and drying evaporation not reutilized

As some of the referred authors of this section state, to include temporal factors in agricultural practices results in differences in the CO_2 and water footprint. However, most of the available information still indicates solely the average resource consumption per total production excluding the variations due to multiple factors according to the time of season. The work presented by Khoshnevisan [87], alone includes a standard deviation in the reported values of used resources, but not directly associated to temporal factors.

These results support the proposal to report resource values involving temporal factors, so that statistics and agribusiness project evaluations can offer better indicators. This, as observed in this research, is because a broad variation exists even for a process using fixed devices and procedures.

Even the use of renewable energy is in direct proportion to the resources supplied by the natural elements, giving additional value to the introduction of analyses of uncertainty levels involving temporal factors.

5.2 Case B: *solar dryer*

5.2.1 Implementation strategy

The implementation strategy is based on the main problem of Table 3 for the case in México. As mentioned the UAQ-campus Amazcala greenhouse is an ongoing project of the Biosystems group.

Three types of measurements have been identified: those of economic type (measure 5), those wherein the energy efficiency is improved or substituted by renewable energy (measures 3 and 4), and those wherein moisture from the air is re-utilized (measures 1 and 2):

1) recovery of water content in the exhaust air from the drying process
2) use of air humidity after drying chamber to estimate exergy profiles
3) coupling of growing and processing sites
4) reduction of cooling load
5) reduction of the electricity consumption in the drying process by solar energy contribution
6) fostering of economic advantages through value chain improvements

The main objectives of these measurements could be enclosed in:

1) enhancing the value of dried tomato fruits
2) reduction of the resources used for product transportation
3) highlighting and reporting the amount of water in the drying exhaust air
4) reporting of monthly performance of whole season

The increment in the added value of the tomato is one of the priorities in this case study. For this it is convenient to make use of a dryer which provides the conditions to reach a good dried product quality, that is to say, with airflow homogeneity inside the drying chamber, homogeneity of the heat transfer, industrial capacity, long life cycle, made of food grade materials, well isolated

from dust and animals, and including control and measurement devices for better performance monitoring.

In order to apply all measurements, the balance of the techno-economic limitations yields **1) to design and incorporate a solar assisted dryer for industrial load,** but **2) to apply low cost solutions for the energy interaction**.

5.2.2 Post-benchmarking

The *baseline* for this case is based on the results from the simulation in Matlab from the model for the solar dryer already described in **section 2.3.3.5**. The ***solar dryer*** of 100-200 kg capacity is designed and simulated in collaboration with the engineer Oscar Farias (CIDETEQ). As the first approach in the designing iterative process, this section presents an experimental part of drying the tests. The experiment took place in the community Amazcala, Queretaro. This represents the beginning of the evolution of continuous improvement of the dryer until there is a complete technological package.

The potential benefits are classified in product quality, energy renewable substituting electricity costs, water reuse and economic effect.

5.2.2.1 Drying experimental prototype

For construction and comparative evaluation of dryers some important considered points from an all literature review are summarized and highlighted. The first ones listed are from the study of Augustus León et al. [15], the sources of the following are indicated individually. These are:

1. Uniformity of drying in dryers with long or tall drying chambers to be obtained.

2. Floor space requirement in certain locations, especially in hilly terrain – identifying flat land for installing dryers may often be difficult, and may be an important consideration in the selection of dryers.

4. Ease of construction: availability of skilled manpower for construction.

5. Safety and reliability.

6. As a rule of thumb, the solar collector surface must be approximately three times the surface of the bed.

7. Pengpad and Rakwichian [108] note that loading/unloading of drying/dried products is important in commercial dryers due to possibilities of contamination and cost of labour.

8. Optimum airflow rate for solar dryers has been reported to be about 0.75 m^3/min per square metre of tray area [109] .

9. With a reference parameter of dry tomato slices to moisture content of 11%: the drying time at 38°C, 44°C, 50°C, 57°C, and 64°C with an airflow rate of 1ms-1 is, respectively, 22 h, 18.5 h, 16.7 h 13.5 h and 9.9 h. An increase of airflow rate 1ms^{-1} to 3ms^{-1} causes a relative decrease in drying time, for T = 50°C, the drying time is 16.7 h, 14.2 h and 11.7 h, respectively, for airflow velocity equal to 1 ms^{-1}, 2 ms^{-1} and 3 ms^{-1} [110].

10. Solar dryers having various input parameters can often be controlled by individual controllers [17].

11. An artificial dryer with a similar performance has a capacity of 120 kg/batch, a voltage of 380V/220V, power of 15 KW and weighs 800 kg.

According to Araya-Farias and Ratti [2], in this experiment the dryer prototype is 1) of batch mode operation; 2) the operating pressure is atmospheric; and 3) the heat transfer is a combination of convection and radiation. According to Ímre [17] is a solar-assisted artificial dryer which operates by using a conventional (auxiliary) energy source if needed.

The benefits of a hybrid solar/electrical are: 1) the stability of the air temperature; and 2) the use of renewable energy. The working fluid selected is water in a vacuum tube solar collector considering its higher heat capacity value in comparison with air (Cp = 4.18 kJ kg^{-1} K^{-1} versus 1.005 kJ kg^{-1} K^{-1}).

The general array of the drying systems with a capacity of 200 kg of fresh tomato is depicted in Fig. 39.

5.2.2.1.1 Heat storage and solar collector

The selection of the vacuum tubes solar collector system was influenced by its current ratio price/efficiency. The heat storage is a stainless steel tank of 305 L (isolated with polyurethane 0.05 m) directly connected to the vacuum tubes arrangement; the latter is a compound of 28 vacuum tubes (1.8 m long per 0.058 m diameter), with a selective surface 3 target (Cu-SS-Al). The auxiliary resistance of 1.5 kW is installed inside the storage tank with a control on/off at a set point of 65°C. The detail of the resistance is depicted in Fig. 40

5.2.2.1.2 Heat transfer

The heat transfer to the air is made by an indirect copper tube (¾ inches) heat exchanger designed specifically for the dryer depicted in Fig. 40. The single pass heat exchanger is integrated with the drying chamber to avoid the use of an extra device for reducing heat losses. This is located inside the drying chamber and the airflow is perpendicular to the water flow.

5.2.2.1.3 Air distribution

The air distribution chamber is comprised of a shared section to which the air from a centrifugal blower is inserted, and also air deflectors which mobility allow the transversal compensation to the drying chamber inlet. At the opposite side the air gathering chamber is installed. The flow distribution occurs in an homogenous way guaranteeing proper formation of current lines and allowing the proper water mass transfer from the tomato.

The use of the two chambers, at the inlet and the outlet from the drying chamber, permits the use of a blower and a suction-blower, or the use of the recirculation via and connecting duct which allow the increase of the operation

temperature. Fig 41 and 42 show images of the air circulation system as well as a detail of the deflectors.

5.2.2.1.4 Drying chamber and tray trolley

The drying chamber is the space assigned for carrying out the drying or dehydration process. This is designed with simple geometry and all walls are isolated with sheets of synthetic rubber based foam Armaflex™ (thickness ¾ inches).

The tray trolley is made of stainless steel, which in this case uses 20 Teflon™ tray meshes of 1.2x1.2 m with a mesh size of 3 mm. The trays are removable and built with wood frames making them light and easy to handle by operators. There are 20 cm between trays.

5.2.2.1.5 Design simulation

A fluids dynamic simulation was run for the design validation. Through this it is possible to predict the current lines inside the drying chamber. In the first phase of these results the simulation was done for the airflow distribution alone.

The following assumptions were considered: 1) steady state; 2) velocity defined at the distribution chamber inlet (1 m s^{-1}); 3) direct outlet to surroundings (no recirculation); 4) simple coupling between pressure and velocity; 5) turbulence model k-ε; and 6) wall functions in the hydrodynamic boundary layer. The results from this pre-simulation are shown in Fig.43.

The airflow distribution was evaluated experimentally with just one repetition, but as it was a fairly good match with the simulation no further detail took place. The function of the deflectors was successfully performed. Nevertheless it is necessary to achieve a better alignment in the deflector's curvature. The test was done with 20 trays and partially charged load in the final stage of drying. The function of the deflector is to distribute the airflow, and this can be confirmed

with the measured flow Fig. 44, which presents an average of 0.45 m s^{-1} in the horizontal central part or the dryer.

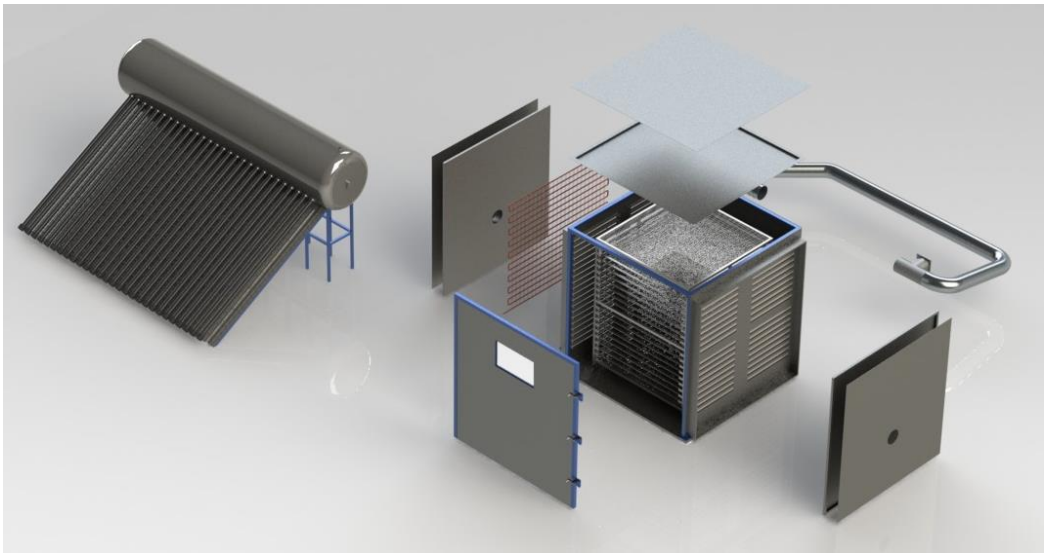

Fig. 39 Array of the drying system

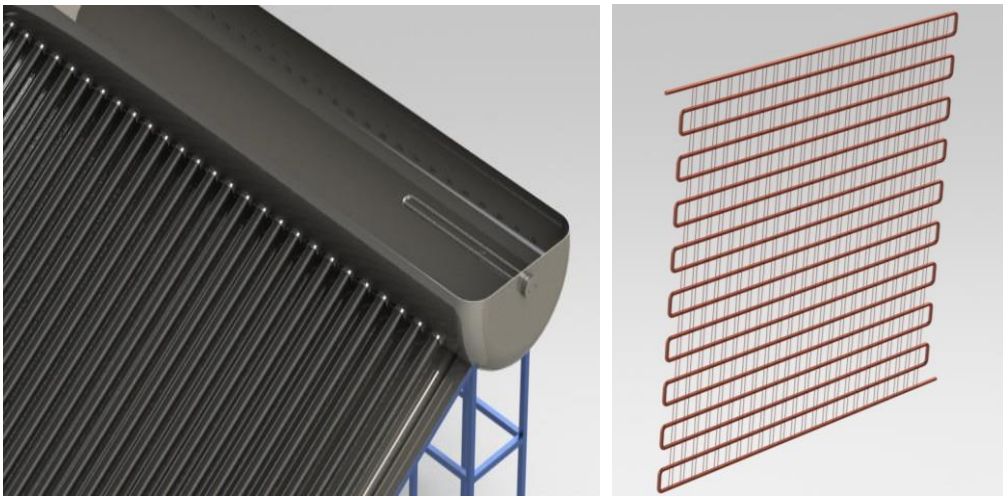

Fig. 40 a) Detail of the resistance inside the storage tank and b) heat exchanger

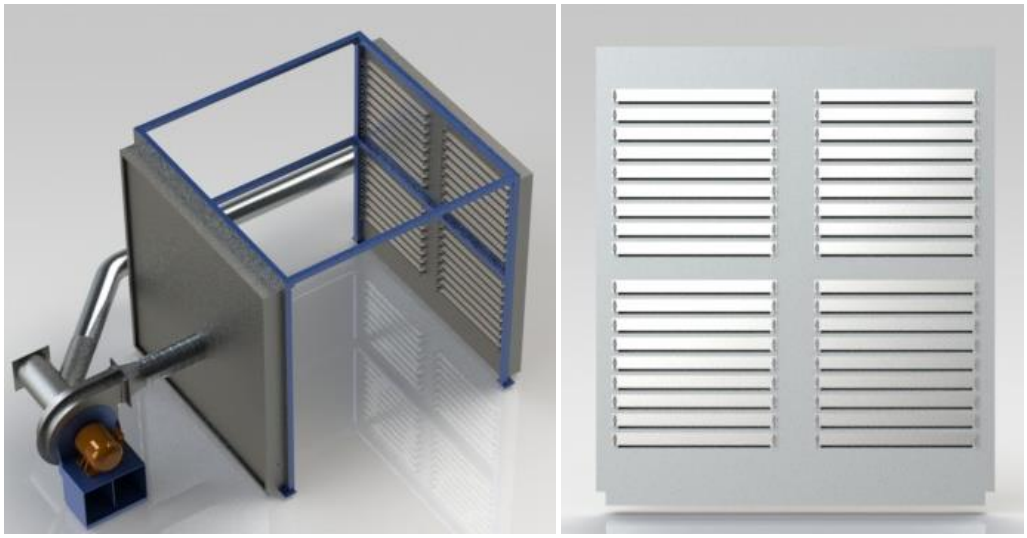

Fig. 41 a) Air circulation system and b) air deflector

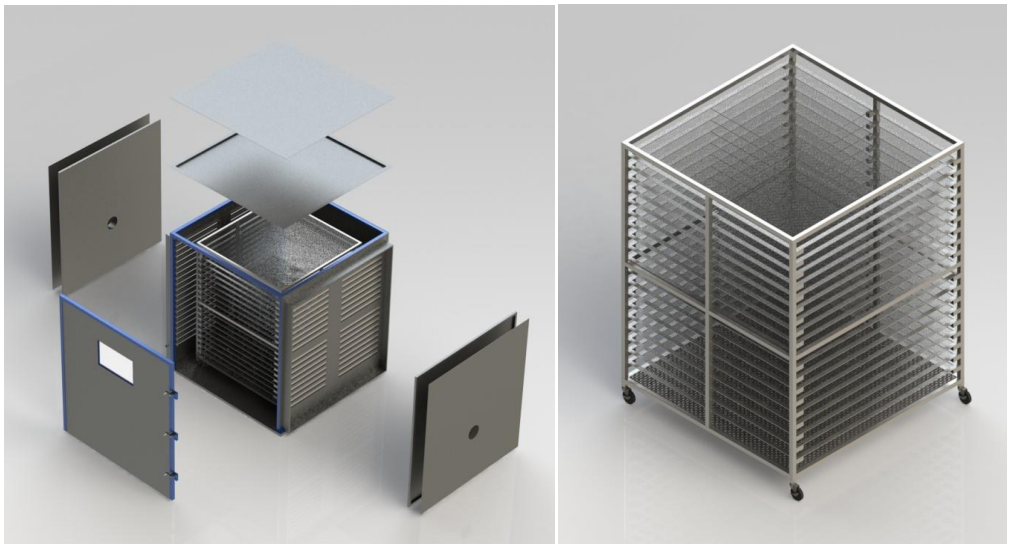

Fig. 42 a) Parts of the drying chamber and b) tray trolley with wheels

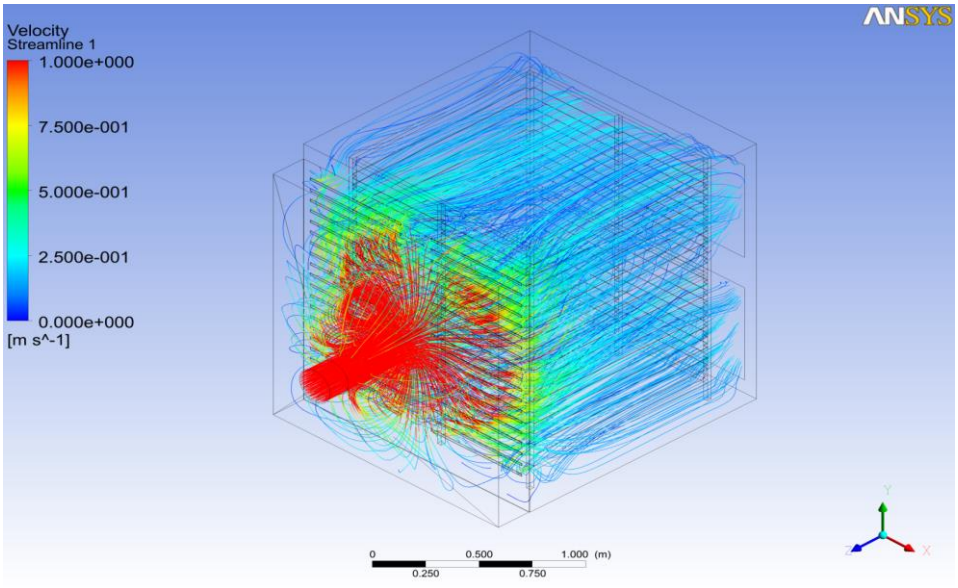

Fig. 43 Trajectory lines from the air inlet

Fig. 44 Velocity distribution of flow

5.2.2.1.6 Photo voltaic energy supply

The electricity requirement is supplied by a solar photovoltaic array. Considering at least 8 hours of operation, the following devices in Table 15 yield a total power of 4.6 kW, and so with a safety factor of 30% the required power for the PV is 5.9 kW; in comparison, a commercial dryer for a 120 kg load requires 15kW.

The characteristics of the PV inter-connected grid system are shown in Table 16. This system permits the use of energy from the grid to complement the required energy and also for use during the night.

Table 15. Electricity requirements of *solar dryer*

Component	Model	Voltage	Current	Power
Blower	1	220VAC	12.7/5.8A	560 W
Recirculation pump	1	220VCA		34W
Electric resistance	1	220VCA		1500W
Electric heaters	2	127VCA		2500W
			Total	5972W

5.2.3 Test under case B conditions

The experiments are: **1) *pre-test 27.01.15*** took place in winter during 9 days of January 2015. The examinations were done on an empty load working with solar and a drying test of 21.8 kg of product; and **2) *test 25.06.15*** took place in summer during 4 days with a 80 kg load (Table 17). The result of a drying cycle of 24 hours (started at 10 am) with the measurements of the product quality taken every 2 hours reported in the following section.

Table 16. Characteristics of the photovoltaic system

PV panels (250W)	9
Tilt	20°
Invertor (24 Vcd 120 Vca 2.75 kW)	1
Surface (m^2)	14.6
Global power generator (Wp)	2027
Performance factor	77.3

Table 17. General characteristics of test A 25.06.2015

Parameter	**Value**	**Control**
Drying time (t)	30	Manual
Load (kg) (max. 200 kg)	80	
Slice thickness (m)	0.005	
Set point electric heater (°C)	65	On/Off intermittent.
Air outlet aperture (%)	40	Manual
Air recirculation (on/off)	off	Manual
Air heaters (on/off)	on	Manual
Blower (on/off)	off	Manual

5.2.3.1 Temperature and relative humidity profiles

For the analysis the results from *25.06.2015* are complemented with the pre-test Fig.45 showing an average temperature of 50°C and relative humidity of 53%. Fig 45 shows the values at the final stage of the drying with average values of 55°C and relative humidity of 6%.

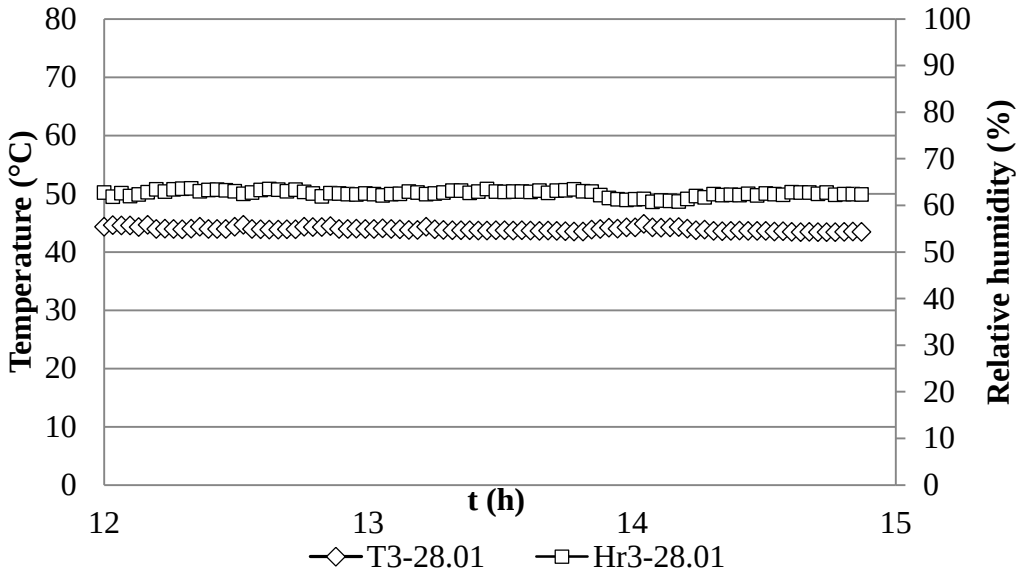

Fig. 45 Partially charged dryer 22 kg *28.01.2015*

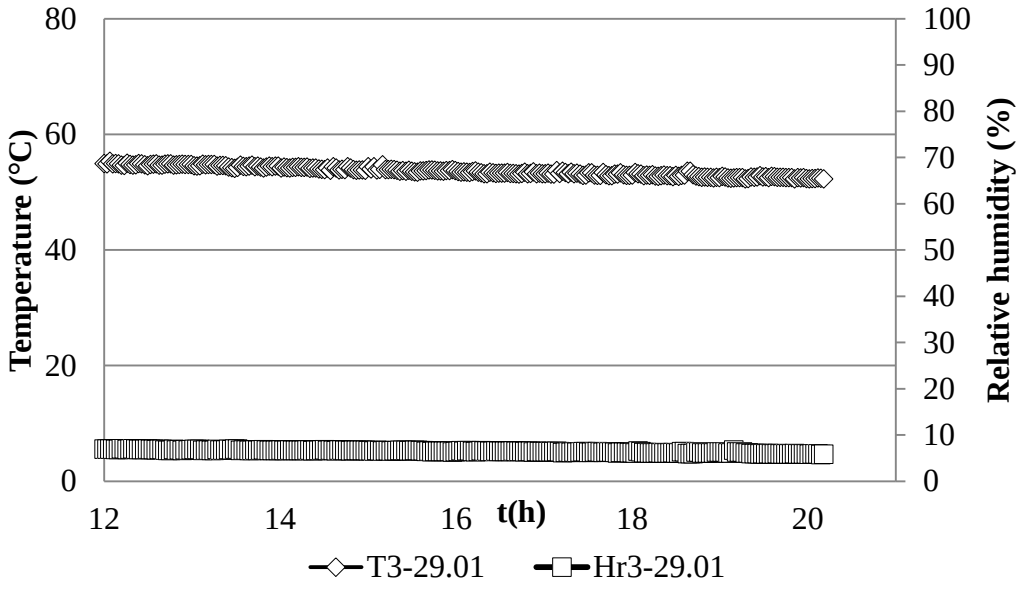

Fig. 46 End of the test partially charged dryer *29.01.2015*

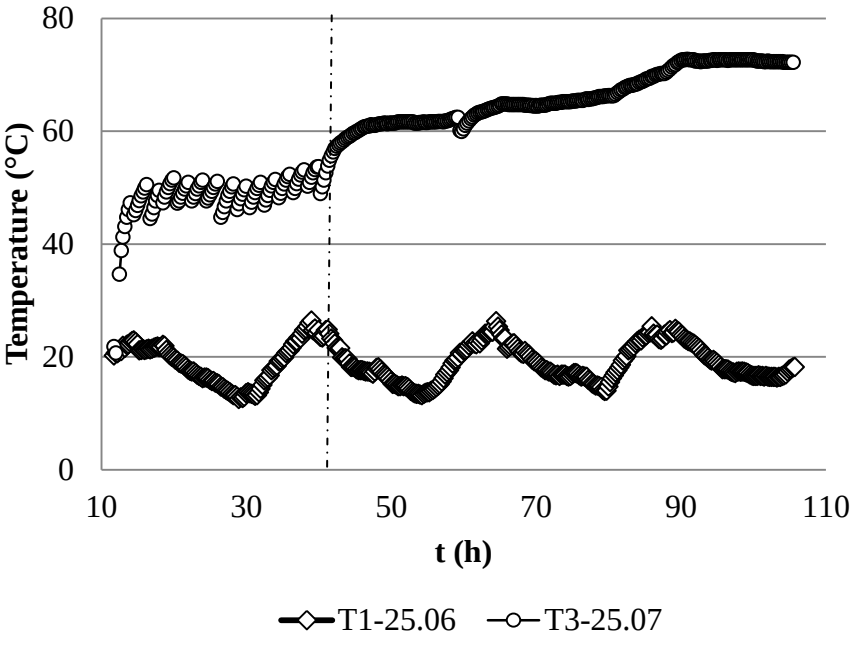

Fig. 47 Temperature and humidity inside the drying chamber for 4 days. Starting at 10 am

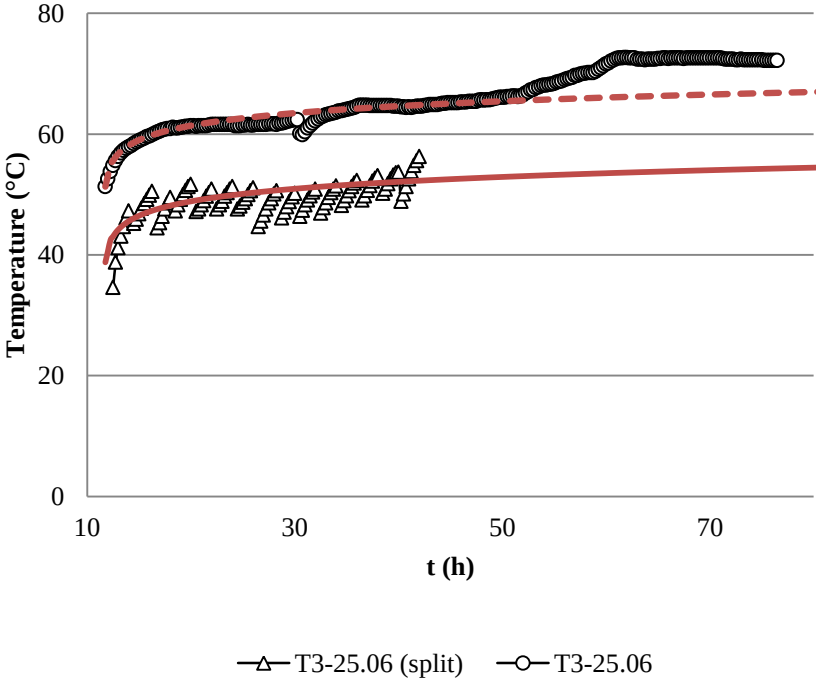

Fig. 48 Adjustment for temperature results

Fig. 47 is the representation of 4 days of measurements inside the drying chamber; the test started at 10 am and measurements of product quality were recorded over 30 hours. As observed, the two clear trends (divided by a line in the image) show behaviour **a) with regular peaks** and **b) with a smooth trend**. Trend a) is the result of opening the door or the dryer to take samples, while in b) no measurements took place.

The analysis of the impact was assessed, the procedure consisted of a comparison between both trends first, and then with the trends of an empty load. The *25.06.2015* test was divided as observed in Fig. 48 where the segment b) has a displacement to the left.

To determine the model for the temperature in function of time, segment a), b) and with empty load *27.01.2015* are compared. The adjustment for segment a) was made with polynomial form of 4^{th} grade. However, when observing the behaviour of segment b) with load and no occurrence of the opening door, the curve is seen with a logarithmic approximation given by

$$T = 2.6675 \ln(t) + init \quad (52)$$

To complement the approximation of the model, the line is compared with a run of empty load from the pre-test *21.01.2015*. Fig. 49 observes the response curve of the dryer.

The values were determined as 42.47 for segment a), 55 for segment b), and 38 for empty load. This observed displacement with certainty depends on the other operation conditions. As it is appreciated in Fig. 48 the door opening lowers the trend by around 13°C.

In the case of relative humidity, the behavior of the empty load conditions from Fig. 49 are compared with an expected decreasing trend due to no tomato load where the highest point is not more than 20% relative humidity during the day, while in Fig. 50 and Fig. 51 it is 60%.

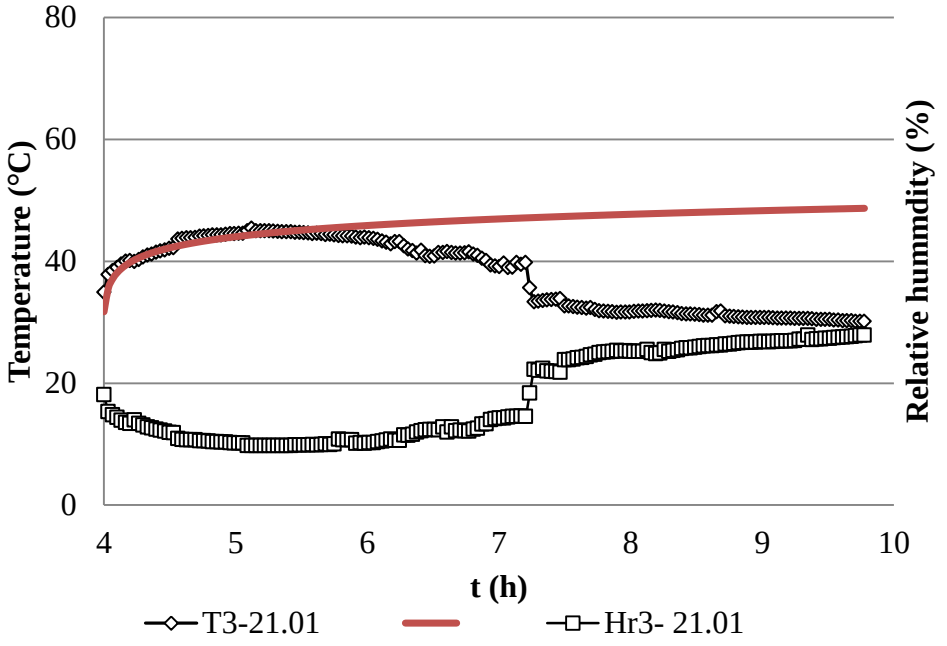

Fig. 49 Result of run with empty load for a span of 10 hours *21.01.2015*. Starting at 4pm

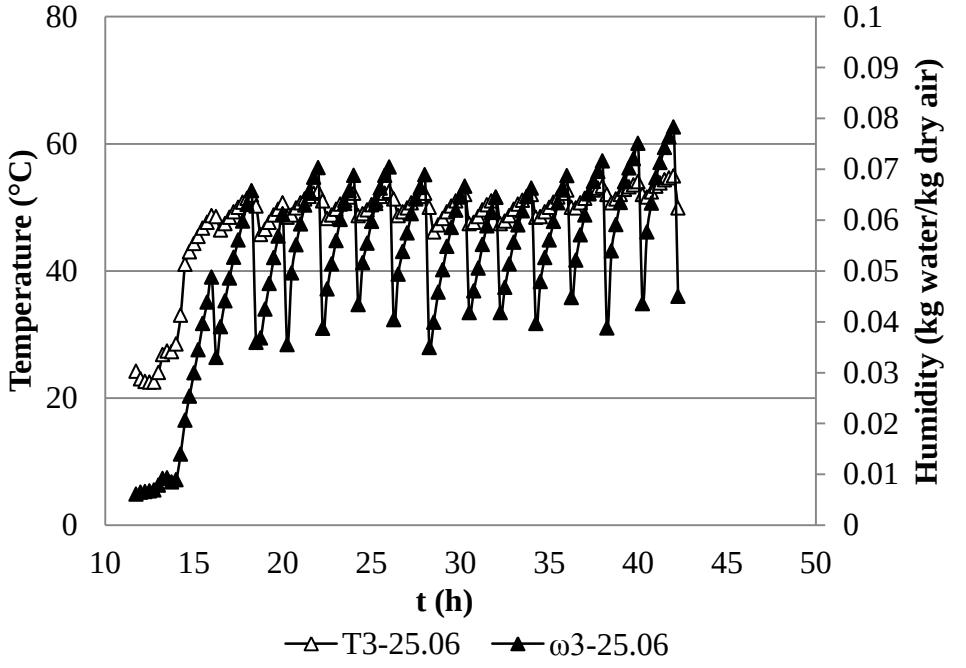

Fig. 50 Temperature (T3) and absolute humidity (ω3) inside the drying chamber on *25.06.2015*

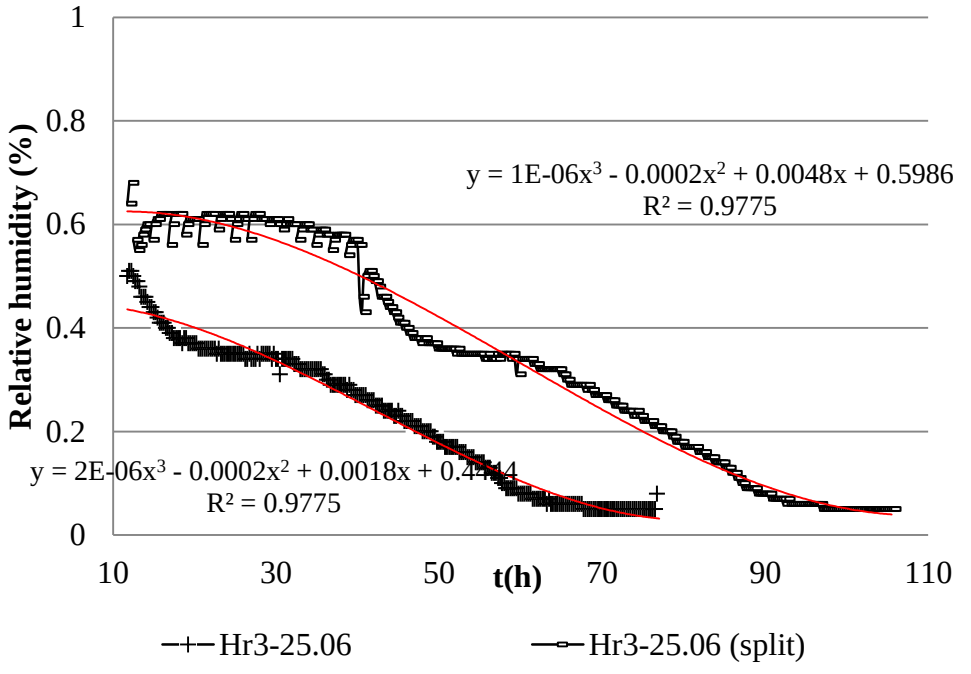

Fig. 51 Humidity (Hr3) trend inside the drying chamber *25.06.2015*. The main curve is split and displaced to the left. The first part corresponds to the measurement

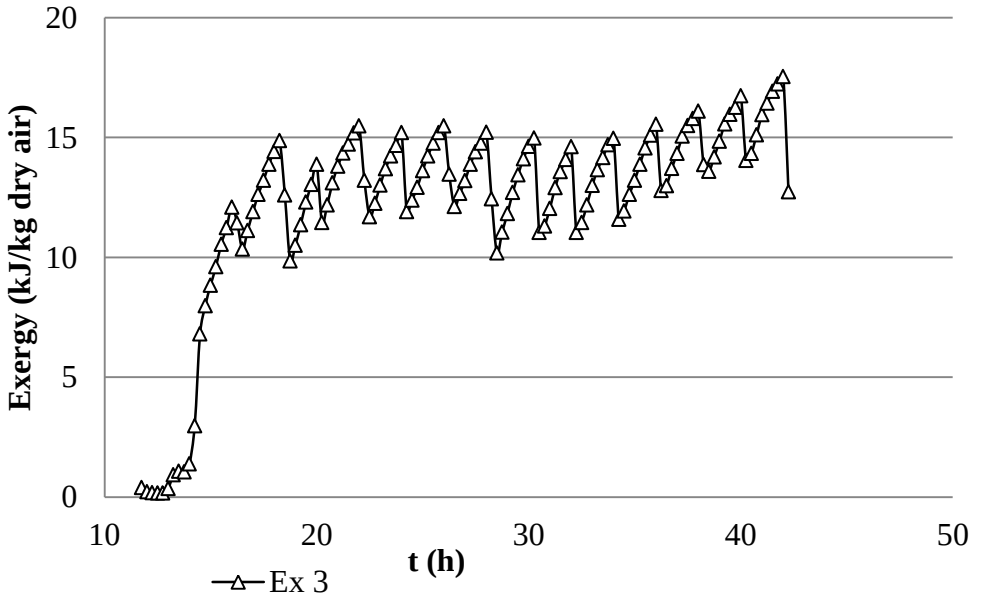

Fig. 52 Exergy use potential from the drying air inside the drying chamber

5.2.3.2 Exergy and energy

In Fig. 52 the exergy from the exhaust air according to Eq. (48) is lost to the environment. As the results from the analysis of the simulation of the *baseline* show, this exergy could be connected to the greenhouse on hot days. The range of exergy is from 10-15 kJ kg^{-1} dry air. Thus, the humidity of the wet air for industrial quantities represents a good amount of energy.

It should be emphasized that the solar energy utilized by the solar dryer is not equal to the energy collected by the solar collector and transferred into the drying air but the energy effectively used in the drying process [17].

In Fig. 53 the Mollier diagram of operation zones drying occurs on a day-basis. The arrow indicates the trajectory during the day. Here the energy required to change the ambient conditions to the drying conditions related to humidity is depicted. The growing trend reaches the furthest point in the diagram with 220 kJ kg^{-1}. The increment of absolute humidity added to the air coming from the tomato fruits is also observed.

In Fig. 54 the energy for drying is compared with the solar energy available to highlight the actual fraction of solar energy used. The effective energy that is finally transmitted to heat the air inside the drying chamber is plotted in Fig. 53 and Fig. 54.

It is observed in Fig. 55 that the overall efficiency of the solar dryer in regards to solar input is from 0.3 to 0.8, an average of 0.6, though over just a few hours. The complementary energy during the night and inconvenient conditions is given by other sources, like a PV system or grid electricity.

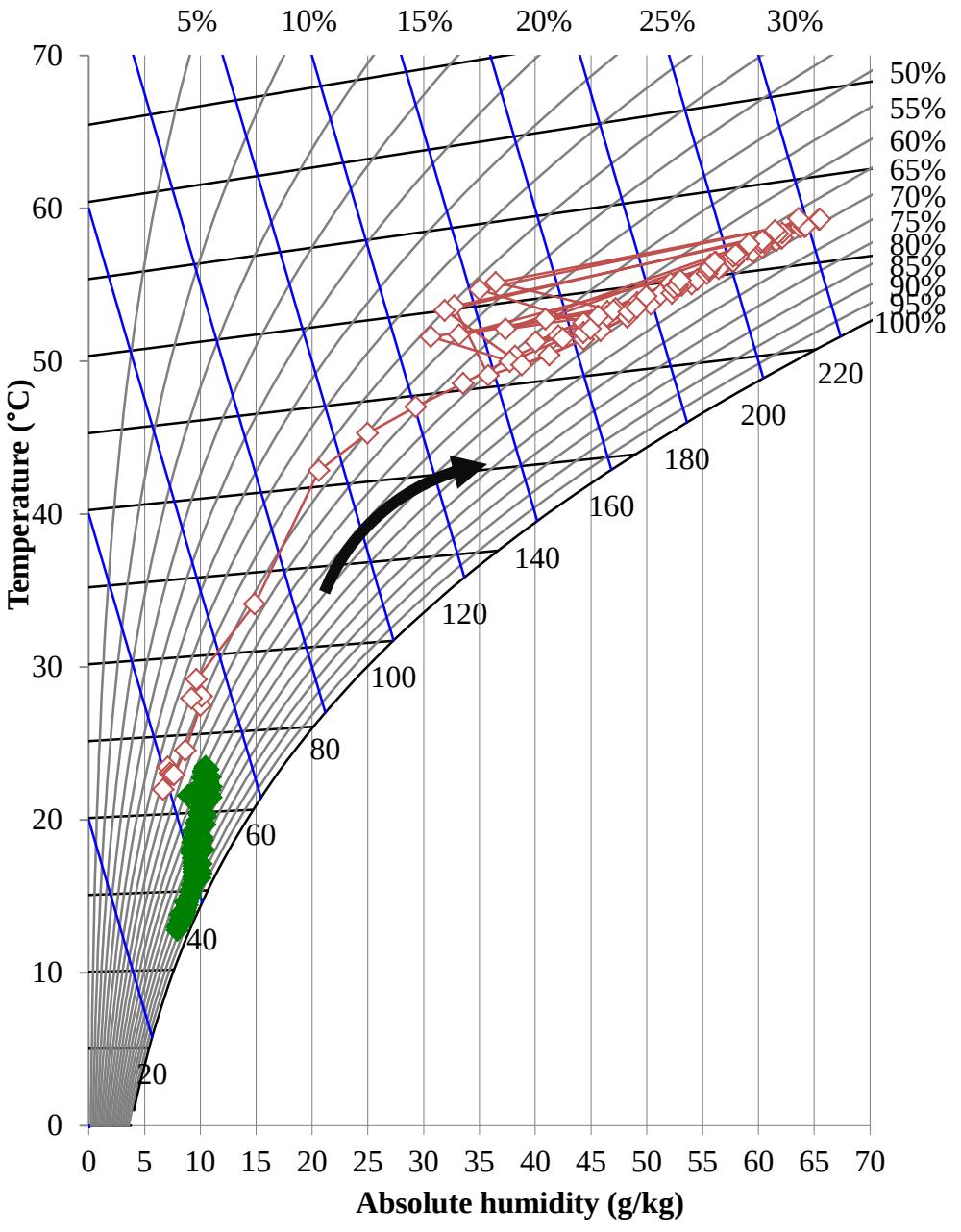

Fig. 53 Mollier diagram for test *25.06.2015* ambient conditions (T1) and inside drying chamber (T3)

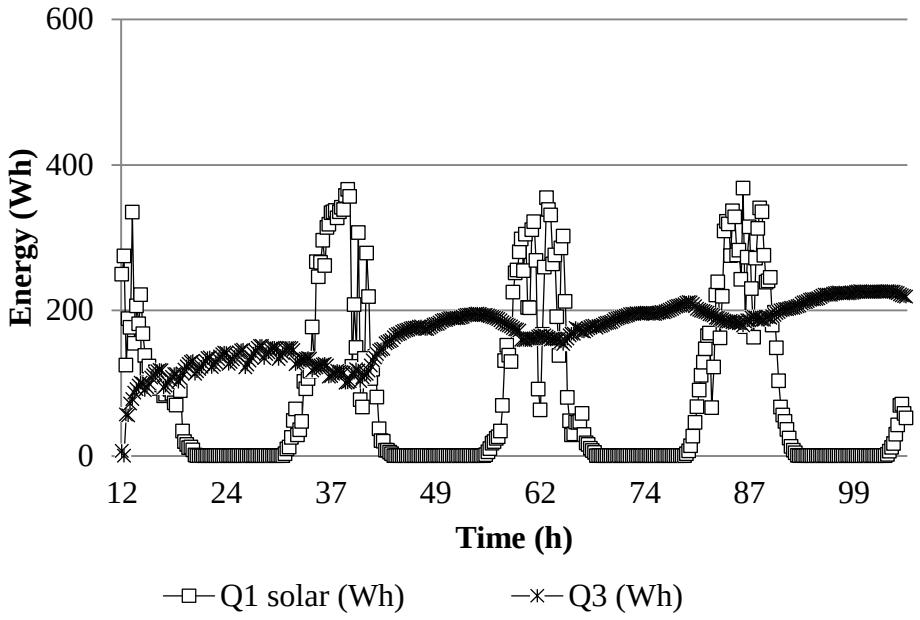

Fig. 54 Energy from solar source (Q1) and effectively used in air heating (Q3), test *25.06.2015*

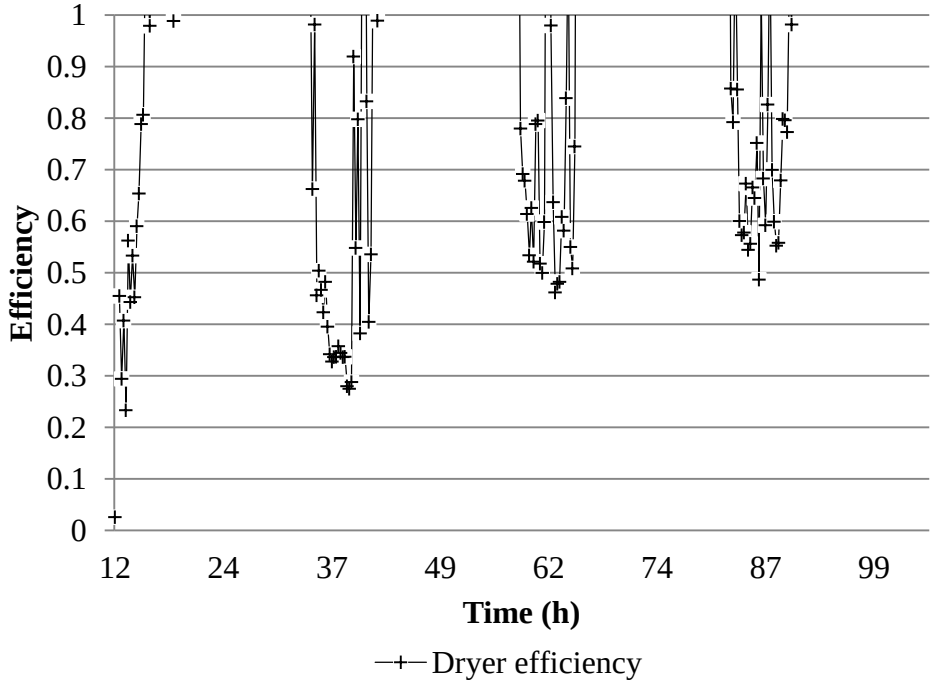

Fig. 55 The efficiency obtained from the solar resource and the real heating of the air, test *25.06.2015*

5.2.3.3 Product quality

A report of physical and chemical analyses of the effect of solar assisted drying was made at the UAQ in the Laboratory of Bioengineering in the Faculty of Engineering at the Amazcala campus.

Eight series of measurements of tomato shell and pulp were taken systematically each four hours until values of humidity were stabilized. For the measurements all chemicals used were of analytical grade. Sodium nitrite, (+) -catechin, aluminum chloride, sodium carbonate, sodium hydroxide, methanol, hexane, acetone, Gallic acid, lycopene, 2,2-diphenyl-1-picrylhydrazyl (DPPH), butyrate hydroxyanisole (BHA), a-tocopherol and Folin–Ciocalteu reagent. The parameters measured were

- Moisture content: measured with forced convection at 60°C following the procedure established in the NMX- 116-SSA1-1994.

- Lycopene content of tomatoes extracts was determined using a colorimetric method which has been validated with HPLC by Rao, Waseem, and Agarwal [111], to ensure the specificity sufficiently high for lycopene measurement. Lycopene from tomato products was extracted with hexane, methanol, and acetone together with a volume ratio of 2:1:1 for 1 h. Absorbance of the extract at 502 nm was measured using UV/vis against the blank extract solvent. Concentration of lycopene was calculated using the extinction coefficient (E%) of 3150.

-Ascorbic acid content: measured following the NMX- NOM-131-SSA1-2012. B13

- Acidity measured with an HQ40 from HACH Company with a potenciometric sensor.

- Colour: measured with a colorimetric instrument CANNON.

- Brix grades were measured with a refraction instrument.

As a control to the drying test *25.07.2015,* simultaneous drying of three non-replaced samples of 1 kg took place in the laboratory in an oven at 60°C while three samples of 1 kg were placed inside the solar dryer. The comparison of the drying trends is observed in Fig 56. In the oven, the final moisture of the product was 9% and in the solar dryer it was 20% after 30 hours of measurements every 4 hours. In the pre-test *21.01.2015* with 21.8 kg, the final moisture was 8% after 30 hours.

Fig. 57 depicts the lycopene content results. In this, it is observed higher values at the end of the test from initial average value of 13.27 to 14.9 mg $(100\ g)^{-1}$. However, after 8-10 hours the trend drops, and the standard deviation (dashed lines) is considerable. This could be related to the changes that the tissue is having for the lost of water, and finally the dried product has an enhancement of lycopene content. The obtained values are lower than the ones reported by Goméz-Gómez [31] and CernÎsev and Sleagun [34].

In Fig 58 and Fig. 59 the results of the analysis show that there is an increment of vitamin C because of its bio availability; simultaneously the tissue degrades and the Brix grades increase constantly.

The acidity, in Fig. 60 presents no clear trend, however, after 13-15 hours diminishes. The average pH is 4.34.

Regarding the colour components in Fig. 61, the values of L, a*, b*, the presented degradation of all parameters in the measurements at 20 and 24 hours of drying changes, presenting higher values, attributable to changes in ambient conditions. However, in comparison with data from **section 2.2.2.2** all parameters present higher values than the ones already reported.

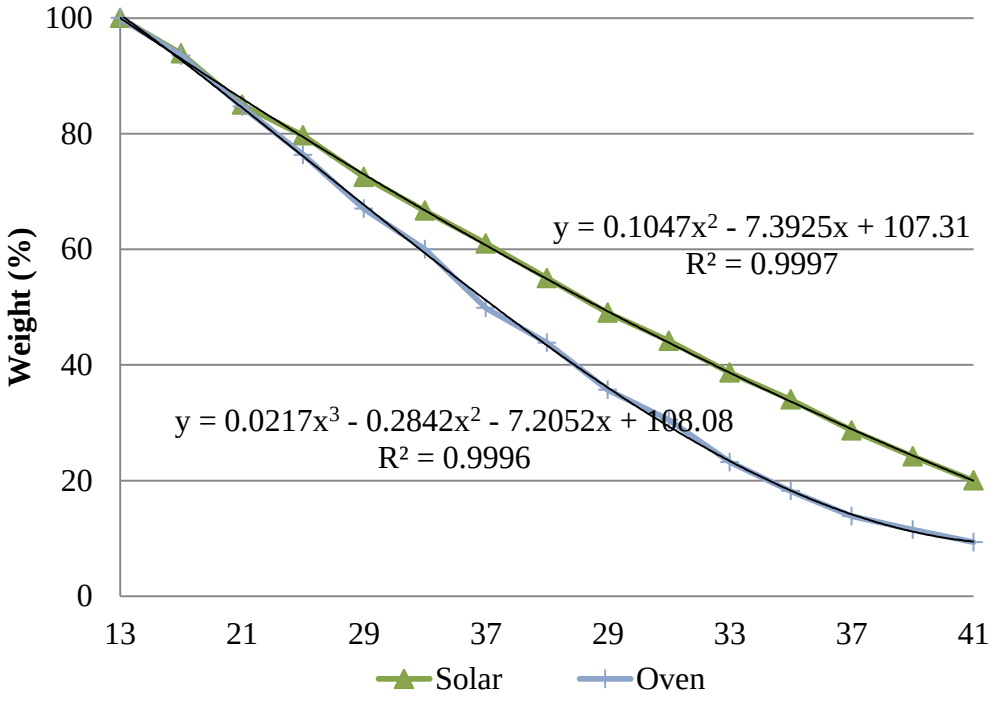

Fig. 56 Drying process comparison of solar and oven conditions, test *25.06.2015*

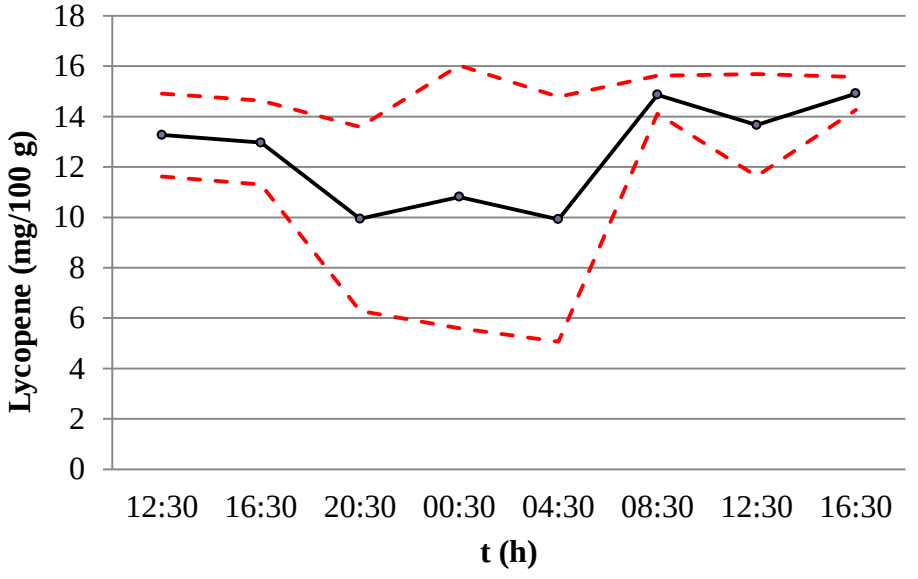

Fig. 57 Lycopene content in the solar drying process, test *25.06.2015*

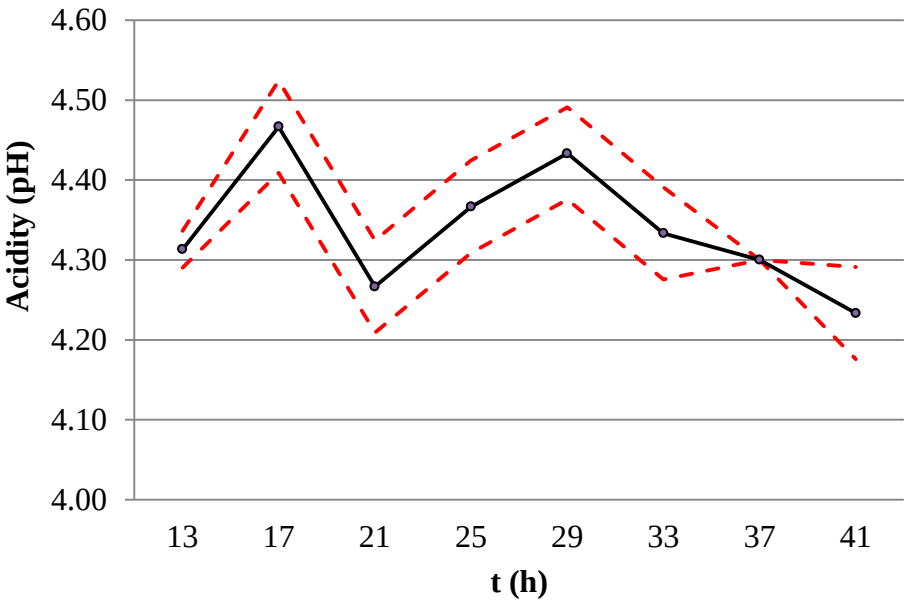

Fig. 58 Acidity of the dried tomatoes, test *25.06.2015*

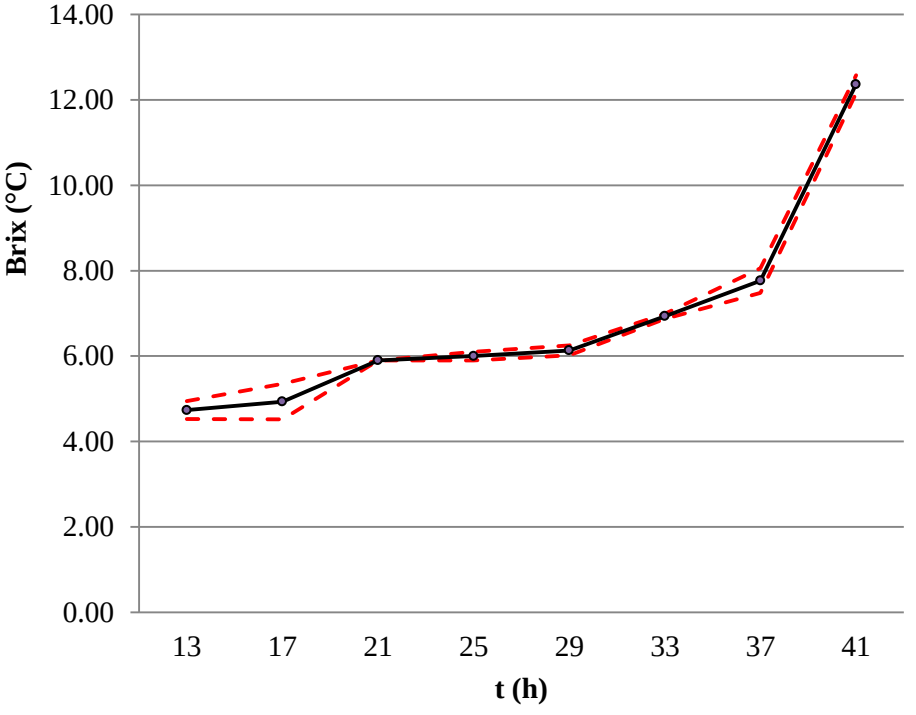

Fig. 59 Brix grades of dried tomatoes, test *25.06.2015*

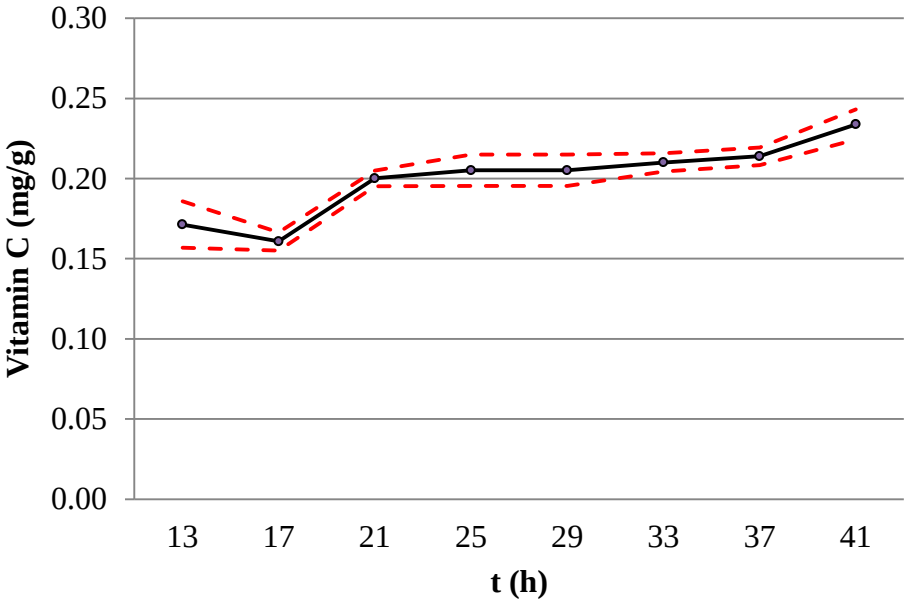

Fig. 60 Vitamin C content of dried tomatoes, test *25.06.2015*

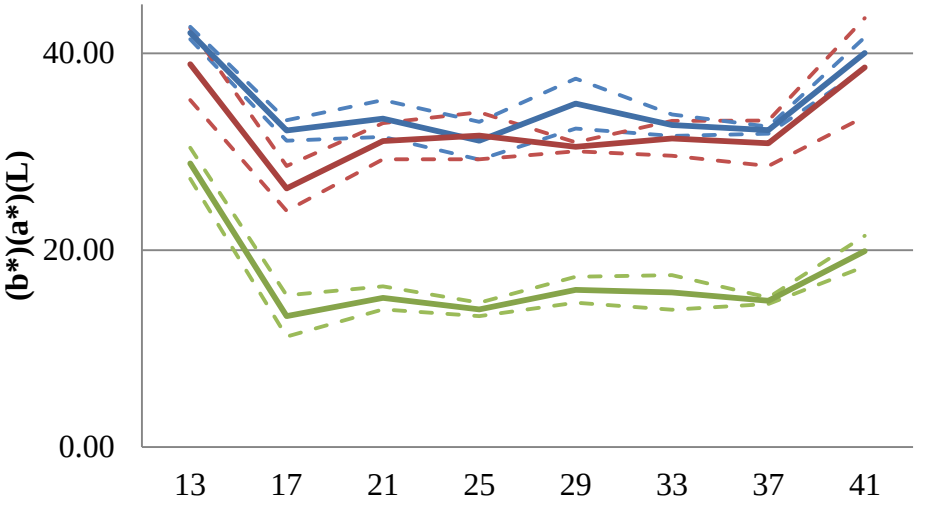

	12.50	16.50	20.50	24.50	28.50	32.50	36.50	40.50
L	42.08	32.17	33.39	31.13	34.89	32.71	32.20	40.04
a*	38.91	26.30	31.08	31.64	30.51	31.37	30.86	38.57
b*	28.83	13.32	15.17	13.99	15.99	15.72	14.87	19.91

Fig. 61 Colour of dried tomatoes in its values (L) (a*) (b*), test *25.06.2015*

5.3 Economic evaluation

The substituted electric energy in Table 18 with the solar-assisted artificial dryer – thermal and with photovoltaic - is equal to the addition of values from Table 15 and 16. According to the energy source, there is a variation of the amount of total hours per year considering drying cycles of 20 hours 6 months per year. These conditions consider a drying cluster where drying is not dependent on harvesting times from a specific greenhouse.

In the proposed system, 65.3% of the electricity for a year comes from renewable energy and 34.7% from the public electricity grid.

Table 18. Energy distribution in the system

	kWhr year
Solar energy	30950
Electricity	21500
Substituted with solar thermal (46.8%)	10080
Produced with PV (18.4%)	3953
Renewable (65.3%)	14033
Consumed from the grid (34.7%)	7467

The steel construction makes it possible to estimate the lifetime of the dryer at 15 years as a minimum. As Ímre [17] states, even when the cost of the device is high, its effect on economics can be balanced by the better quality of the product and by better energy effectiveness.

Table 19 collects the values from the economic dynamic method according to Böer [111] to describe the financial part considering inflation. In Fig. 61 in the examination for this period of time it is identified that payback occurs at 6 years where the savings cover the price of the sum of investment capital I, plus yearly interest and the accumulated costs.

The values of the equipment inflation, i, the prices of energy and the annual fixed rate are considered equal to the 2015 inflation year rate of 2.88%. However, these values are not constant during the lifetime of any dryer.

In this estimation the market price of the dried products and the economic benefits of transport reduction are not considered. The elimination of losses from the growing phase by the implementation of the drying post-harvest process adds value to the final product by itself.

Table 19. Economics of solar energy system. Values of 08.07.2015 in Mexican economy.

	Life time (15 years) n=6	Euros
C	Investment cost	14604,811
D	Price of the substituted conventional energy	2160,723
	Average retail electricity prices USD/MWh [112]	173.005
	$S = I + E$	20356,073
S	Accumulated savings $S = \frac{(1+r)^n - (1+e)^n}{r-e} D$	16837,66
I	Investment cost $I = C(1+r)^n$	17438,9081
E	Accumulated yearly costs $E = \frac{mC(1+r)^n - mC(1+i)^n}{r-i}$	2917,16498
m	Annual fixed charge rate m	0.0288
i	Equipment inflation rate i	0.0288
e	Yearly inflation rate for the prices of energy	0.0288
r	Interest rate (%)	0.03

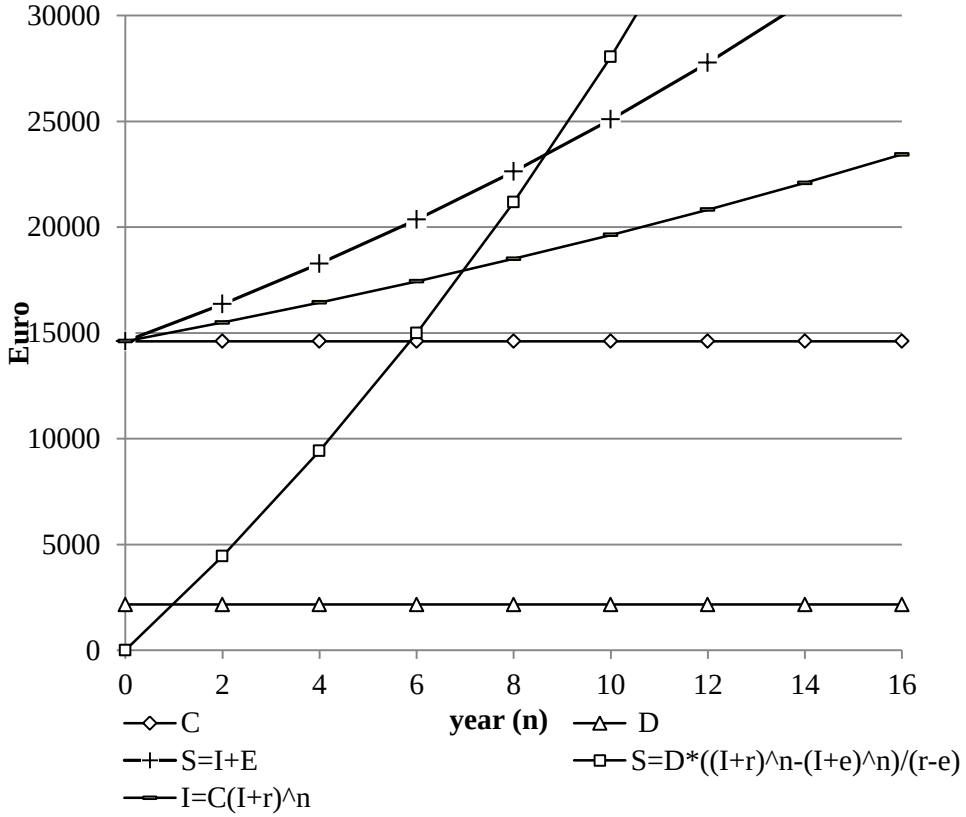

Fig. 62 Payback time of *solar dryer* proposal

5.3.1 Cost and community

Amazcala is a community of 4955 habitants (where there are 1090 housing units of which 0.57% has a computer and 0.16% of adults speak an indigenous language). According to SEDEA [113], there are two growing seasons in Queretaro: spring-summer and autumn-winter. In 2006, for the first season 202 Ha were harvested with a productivity of 61.87 Ton Ha^{-1} and in the second season 24 Ha were harvested with productivity of 301.29 Ton Ha^{-1}.

The use of this technological package of drying systems in the whole value chain is of general positive impact. Initially, the benefit is economic and still has areas of opportunity for savings. Also, this creates community benefits in the

income either for the owner, consumer or other members of the community for labour and better prices. Additionally the coupling of drying and growing systems – at the location of the greenhouses – eliminates prices from the growing to drying processing site. In general, the community is benefited when the product is consumed locally. This reduces indirect costs added to the price of the product through the elimination of the cost of transport and consumption of electricity substituted by renewable source. Furthermore, in the high level long-term, the social cost of carbon impact and future taxes on emissions is positively impacted.

In terms of marketing to the external market it is important to highlight that the efficiency of the dryer impacts directly on the quality of the dried products. The better the quality, the higher the energy consumption but also the better the marketing and shelf live.

In any case, drying has always been a method for reducing losses and consequently representing savings.

Chapter 6

6.1 General conclusions

The originality and impact of this work is the **application of a methodological scientific analysis to the whole dried tomato value chain**. Therefore, the result emerging from this research is a **high relevance contribution to resource efficiency for complete food processing value chains**.

The raised research questions and the objectives are fulfilled. Different ways to reduce water and energy consumption along the value chain for the two different temporal and location conditions were identified and assessed.

Through the followed methodology tools, models and best practices are applied in the selected sub-processes of the value chain. By the use of **renewable energy** (solar energy), **water saving practices** (reutilization) **and new energy interaction methods** (growing and drying interaction process) the improvements derive a **more efficient use of available resources**.

The analysis done by **thermodynamic operation zones**, makes it feasible to link the growing phase with the post-harvest processing in the drying value chain. This is researched by applying **changes in logistics** and **coupling processing sites**. In this way, it is observed that from the overall high level perspective, common industries share the same building capacity giving support to the introduction of the concept of "compound industries".

Presenting the quantities in visual form of water and energy highlights the real consumption of the value chain. Also, this study reveals the **relevance of the implementation in the agribusiness sector of seasonal statistics** for the better sizing of processes and equipment.

In the comparison of the **two cases** a different trajectory towards finding a solution was determined. As a consequence, the quantitative impact is reported in **case A in terms of the reduction of the water and carbon footprint and,**

for case B, in terms of energy savings. The nutritional value of the dried products is reported in terms of lycopene content, vitamin C and Brix grades, as well as evaluation of colour.

Case A

For the **cold weather case study**, the technology and environment themselves entirely determined the implementation strategies to improve the value chain.

The seasonal analysis showed that a broad variation contingent on time exists even for a process using fixed devices and procedures. In particular, the results of the monthly record of a season showed that the **water footprint was reduced by 43.8%** from 91 to 51.1 L kg^{-1} with a standard deviation from 53.2 to 12.4 L kg^{-1}. The **carbon footprint was reduced by 72.6%** from 40.2 to 11 kg kg^{-1} with a standard deviation from 23.9 to 11.4 kg carbon dioxide kg^{-1}.

Case B

For the **warm weather case study**, the availability of resources and economic factors determined the task application.

The impact of the energy supply on the system was observed on a daily basis while the drying procedure itself determined the product characteristics obtained. The result of an energy consumption drying test in partial load yielded **65% of electricity use substituted by renewable energy**. The device built for the purpose presents a payback of 6 years. The product presented a final moisture content of 0.25 kg kg^{-1} d.s. or 20% water content, with 30 hours drying during summer at 55°C. At the end of the test of the nutrient content, lycopene content was 14.9 mg $(100\ g)^{-1}$, vitamin C was 0.23 mg g^{-1} and Brix grades were 12.37°.

6.2 Further research

In order to complement this research report future actions with regards to the following lineaments are recommended:

- An improvement of the system used to measure the properties of the products that are being dried, i.e. not to open the door and affect the operation of the dryer.
- The construction of detailed profiles of air humidity describing a time dependent curve will complement the analysis of exergy waste utilization. The variation of conditions in the sample size is increased for better statistics prediction.
- For optimum conditions of mixing air, it is necessary to include in the calculation the variation of flow conditions of the incoming air.
- Developing the drying kinetics of the process with intermittent temperature to simulate solar behavior.
- The study of recirculation needs to determine optimal values of damper aperture and scheduling times for drying in different conditions.
- Complementing all the improvements with a complete control module is of interest, where the devices work at best operation standards.
- An improvement of heat transfer and aperture reflectors.
- Construction of the model that rules the dryer performance.

Appendix 1. Basic concepts used for drying

Water activity

A key parameter for drying processes is water activity (a_w), which corresponds to the ratio of water vapour pressure (p) of the food system to the vapour pressure of pure water (p_0) at the same temperature.

$$a_w = \frac{p}{p_0}$$

Saturation vapour pressure of water

$$p_{vs} = 6.11 * 10^{\left(\frac{7.5*T_1}{(T_a+237.3)}\right)}$$

Relative humidity

Relative humidity (Hr) is defined as the ratio of p_v to p_{vs} at the same temperature. It is a relative measure of the amount of moisture that wet air can hold at a given temperature:

$$p_v = p_{vs} Hr$$

Absolute humidity

The mass ratio of water to dry air is known as absolute humidity, which can be defined as the amount of moisture in the air at any condition. Equilibrium is reached when the partial pressure of water vapour in the air equals the water saturation pressure at a given temperature. Thus, the mass ratio of water to air is called the saturation absolute humidity. This is the maximum amount of moisture that the air can carry at that temperature, which can be expressed as

$$\omega_1 = 0.622 \frac{p_v}{P}$$

Wet bulb temperature

A wet tissue is added at the tip of the common thermometer to make this temperature measurement. The water from the tissue evaporates to the air,

reducing the water temperature in the tissue and so the final temperature reached depends on the air humidity. The dryer the air, the lower the wet bulb temperature.

Appendix 2. Tools

Mollier diagrams

The Mollier diagrams are generated using the DesireTOOL Mollier h,x-Diagramm (Version 1.0 - 30.03.2009) © 2008 by ATB Leibniz-Institut für Agrartechnik Potsdam-Bornim e.V. und HTW Hochschule für Technik und Wirtschaft Berlin.

These diagrams are used for a given ambient pressure; the temperature (°C) is on the y-axis, the absolute humidity (g kg^{-1}) on the x-axis, the enthalpy (KJ kg^{-1}) is shown in diagonal lines and the relative humidity (%) in curved lines.

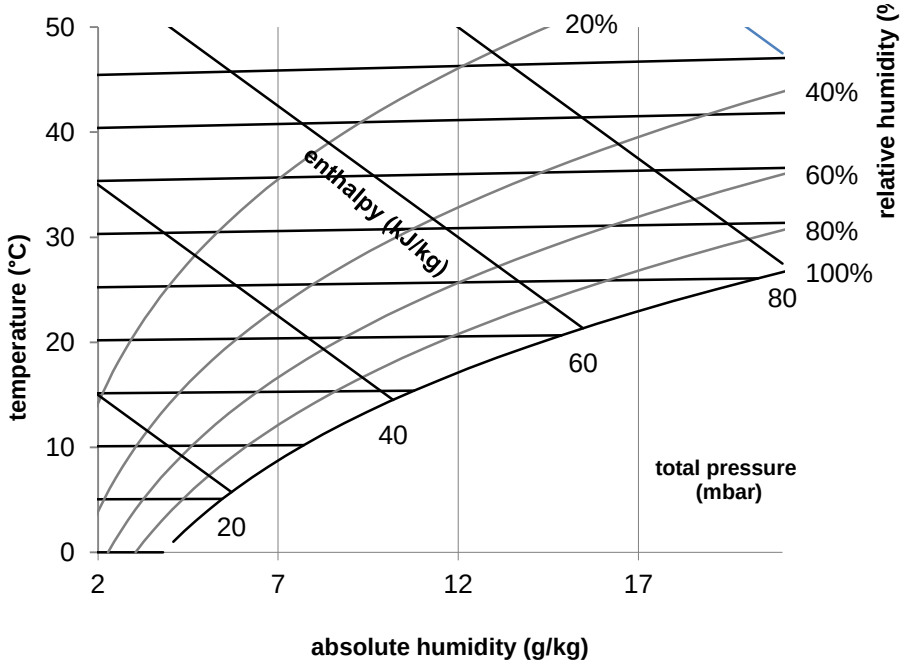

Sankey diagrams

The water and energy flows are described with Sankey diagrams (e!Sankey™) in which it is easy to follow the quantities of the materials represented because the thickness of the arrows are proportional to the quantity they represent. In this case are the growing process and the post-harvest drying process are represented and the following image uses the scale of the arrow to represent liters of water.

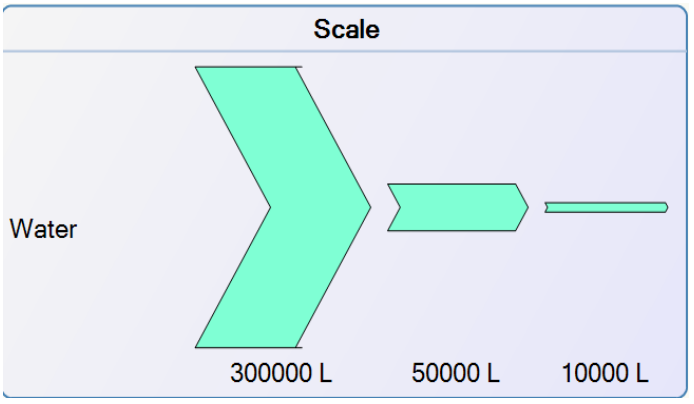

Matlab tool

Matlab™ Simulink™ is the environment where the solutions of the coupled system are given. The code of the script is inserted in the Simulink objects, which are variables that can be manipulated in equation form in their interaction with the other variables. The equation M1=M+DM is represented as follows:

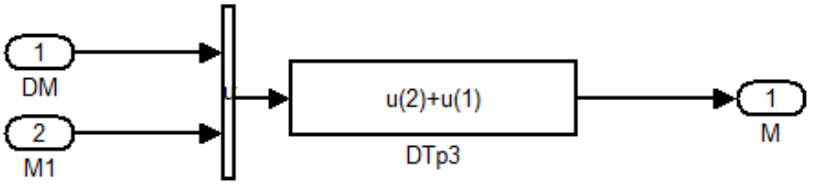

Appendix 3. Statistiscs

a	Collector			Reference			t test			
	$\bar{X}$	σ	cont	$\bar{X}$	σ	cont	t test	Freedom grades	t limit	
3	351,285	236,946	24	208,729	590,636	24	-1,097	46	1,679	H0
4	745,823	378,980	30	542,150	917,195	30	-1,124	58	1,671	H0
5	906,041	265,694	31	774,573	616,150	31	-1,091	60	1,671	H0
6	1037,152	362,304	30	1103,002	972,534	30	0,348	58	1,671	H0
7	907,449	342,162	31	-462,425	3663,760	31	-2,073	60	1,671	H0
8	958,522	252,672	31	646,711	1563,997	31	-1,096	60	1,671	H0
9	562,722	137,090	30	207,591	1284,443	30	-1,506	58	1,671	H0
10	490,400	88,032	25	250,064	1056,809	25	-1,133	48	1,677	H0

b	Collector			Reference			t test			
	$\bar{X}$	σ	cont	$\bar{X}$	σ	cont	t test	Freedom grades	t limit	
3	88,171	234,715	27	201,993	316,649	26	1,482	51	1,676	H0
4	374,848	1285,702	30	240,729	362,913	30	0,550	58	1,671	H0
5	37,255	375,268	31	65,187	250,138	31	0,345	60	1,671	H0
6	152,250	534,220	30	194,283	877,483	30	0,224	58	1,671	H0
7	188,209	333,876	31	421,646	445,797	29	2,284	58	1,671	-
8	159,603	493,032	31	206,881	1498,992	31	0,167	60	1,671	H0
9	85,913	357,293	30	244,841	363,005	30	1,709	58	1,671	
10										

c	Collector			Reference			t test			
	$\bar{X}$	σ	cont	$\bar{X}$	σ	cont	t test	Freedom grades	t limit	
5	404,720	274,900	4	376,352	322,853	4	0,134	6	1,943	H0
6	294,858	131,863	4	322,554	98,748	4	0,336	6	1,943	H0
7	338,253	88,823	4	269,217	195,713	4	0,642	6	1,943	H0
8	242,461	87,260	5	197,133	54,000	5	0,988	8	1,860	H0
9	163,677	89,736	4	96,894	47,868	4	1,313	6	1,943	H0
10	133,865	37,155	4	109,377	28,072	4	1,052	6	1,943	H0
leaves total	62,288	22,744	5	68,065	24,854	5	-0,383	8	1,860	H0
plants total	1,971	0,132	3	1,847	0,095	3	1,322	4	1,960	H0
BER	21,639	11,724	5	88,166	73,552	5	-1,997	8	1,860	H0

a. blue water foot print , b. grey water footprint and c. total production.

d	Collector			Reference			z test		
	$\bar{X}$	σ	cont	$\bar{X}$	σ	cont	z test	z limit	
3	0,00096236	0,003094	4030	0,00181641	0,00328128	4030	12,0217	2	-
4	0,00033679	0,00106	4680	0,00032855	0,00094035	4680	-0,39755	2	H0
5	-0,00040877	0,001486	5549	0,00010533	0,00050118	5549	24,4229	2	-
6	-0,00015424	0,001016	5760	8,1466E-05	0,00047333	5760	15,9639	2	-
7	0,00016141	0,001087	6324	0,00043303	0,0009872	6324	14,7097	2	-H0
8	7,947E-06	0,001087	5952	0,0002029	0,00074314	5952	11,4217	2	-
9	0,00024461	0,000883	5040	0,00039707	0,00102099	5040	8,01789	2	-
10	0,00051828	0,00122	4464	0,00097414	0,0019458	4464	13,262	2	-

e	Collector			Reference			z test		
	$\bar{X}$	σ	cont	$\bar{X}$	σ	cont	z test	z limit	
3	0,00253942	0,00222	5642	0,00390052	0,00313547	5642	26,6117	2	-
4	0,00099764	0,00119	4680	0,00146735	0,0012735	4680	18,4346	2	-
5	0,00053654	0,000867	4123	0,00051613	0,00089003	4123	-1,05538	2	H0
6	0,00037236	0,000498	3600	0,00015696	0,00046004	3600	-19,071	2	H0
7	0,00045808	0,000783	3348	0,00049496	0,00094767	3348	1,73616	2	-
8	0,00027612	0,000496	3720	0,00029015	0,00076155	3720	0,9417	2	H0
9	0,0004162	0,000767	3960	0,00058516	0,00101441	3960	8,36045	2	-
10	0,00102611	0,001088	5208	0,00136688	0,00164607	5208	12,4643	2	-

d. thermal energy day time and e. thermal energy night time

Appendix 4. Values of parameters

Values of assumed parameters in models

Parameter	Definition (Dimension)	Value
α_c	Absorbency for cover, (dimensionless)	0.1
Γ	Capture fraction, (dimensionless)	0.8
ρ_r	Reflectance for receiver, (dimensionless)	0.05
ρ_c	Reflectance for cover, (dimensionless)	0.1
τ_c	Transmittance for cover, (dimensionless)	0.8
α_r	Absorbency for receiver, (dimensionless)	0.85
ρ	Reflectance for reflector, (dimensionless)	0.9
Δx	Distance between two points along the dryer, (m)	5 cm
σ	Stefan-Boltzmann constant, ($W/m^2 K^4$)	5.67×10^{-8}
ε_c	Emittance for cover, (dimensionless)	0.1
ε_r	Emittance for receiver, (dimensionless)	0.1
Δy	Thickness of receiver, (m), (Amer et al., 2010)	0.002
Cp_a	Specific heat of air ($kJ\ kg^{-1}\ K^{-1}$)	1,007
Cp_l	Specific heat of liquid ($kJ\ kg^{-1}\ K^{-1}$)	4,179
Cp_p	Specific heat of product ($kJ\ kg^{-1}\ K^{-1}$)	3,97746
Cp_v	Specific heat of water vapour ($kJ\ kg^{-1}\ K^{-1}$)	1,82
Cp_w	Specific heat of water ($kJ\ kg^{-1}\ K^{-1}$)	4,179
$h_{conv,\ c\text{-}a}$	Convective heat transfer coefficient between cover and inlet air, (W/m^2K), (ASHRAE, 2009)	15
$h_{conv,\ c\text{-}am}$	Convective heat transfer coefficient between cover and	15

	environment, (W/m^2K), (ASHRAE, 2009)	
$h_{conv,\ r\text{-}a}$	Convective heat transfer coefficient between receiver and inlet air, (W/m^2K), (ASHRAE, 2009)	15
K_{cond}	Thermal conductivity for receiver, (W/m.K), (Baher and Stephan, 2006).	81
L	Length of cover, (m), (Amer et al., 2010)	2.8
R	$kJ\ kg^{-1}\ K^{-1}$	8,31
R_a	$kJ\ kg^{-1}\ K^{-1}$	0,287
R_v	$kJ\ kg^{-1}\ K^{-1}$	0,4615
θ	Latitude, (degree), (Anon, 2012a)	52.4, 20.6
ρ_a	$kg\ m^{-3}$	0,98
P_p	$kg\ m^{-3}$	900
P_w	$kg\ m^{-3}$	1000

Appendix 5. Complementary images

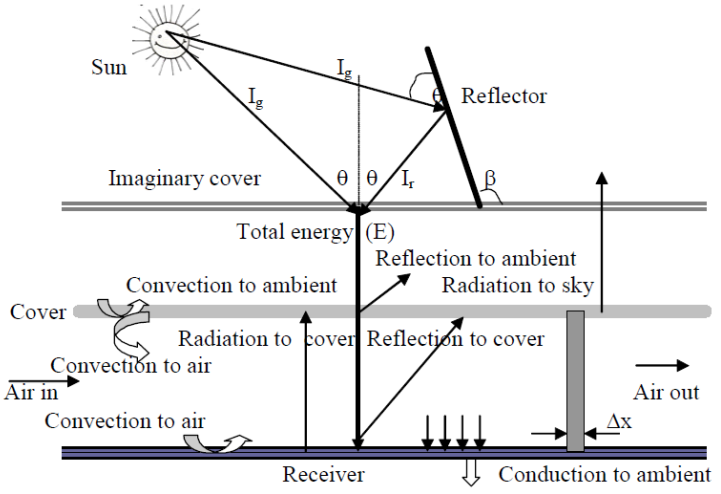

A4.1. Schematic for energy balances taken from Hossain [65]

A4. 2. Drying chamber interior

1. Producto fresco

2. Se pesa

3. Se rebanó

4. Rebanadas finas

5. Distribución de producto

6. Carga

7. Espiguero en cámara

8. Remover producto

A4.3 Pictures of the drying process

References

[1] C. Ratti, “Hot air and freeze-drying of high value foods: A review,” *Journal of Food Engineering,* p. 311–389, 2001.

[2] M. Araya-Farias and C. Ratti, “Advances in food dehydration,” in *Chap 1. Dehydration of food: General concepts*, Taylor & Francis Group, LLC, 2009, pp. 1-32.

[3] A. S. Mujumdar, "Chap.1 Principles, classification and selection of dryers," in *Handbook of Industrial drying (Third Edition)*, Boca Raton,FL, Taylor & Francis, 2007, pp. 3-32.

[4] M. Bazilian, H. Rogner, M. Howells, S. Hermann, D. Arent, D. Gielen, P. Steduto, A. Mueller, P. Komor, R. S.J.Tol and K. K. Yumkella, “Considering the energy,water and foodnexus:Towards an integrated modelling approach,” *Energy Policy,* vol. 39, p. 7896–7906, 2011.

[5] S. Grabowski, M. Marcotte and H. Ramaswamy, "Cap 23. Drying of Fruits, Vegetables and Spices," in *Handbook of postharvest technology*, NY USA, CRC Press Book Taylor and Francis group, 2003, pp. 654-656.

[6] T. Kudra, “Chapter 14 Energy Aspects in Food Dehydration,” in *Advances in food dehydration*, vol. 5, 2009, p. 423.

[7] C. Strumillo and T. Kudra, Drying: Principles, Applications and Design., Gordon and Breach Science Publishers., 1986.

[8] G. Chen, “Enciclopedio of energy engineering and technology,” in *Drying Operations: Agricultural and Forestry Products*, Taylor and Francis GRoup, 2007, pp. 332-338.

[9] I. Dincer, “On energetic, exergetic and environmental aspects of drying systems,” *International Journal of Energy Resources,* no. 26, p. 717–727., 2002.

[10] E. Mateos-Espejel, L. Savulescu, F. Marechal and J. Paris, “Unified Methodology for Thermal Energy Efficiency Improvement: Application to

Kraft Process," *Chemical Engineering Science,* vol. 66, no. 2, pp. 135-151, 2011.

[11] R. Poritosh, N. Daisuke, O. Hiroshi, N. Nobutaka, O. Takahiro and S. Takeo, "Life cycle inventory analysis of fresh tomato distribution systems in Japan considering the quality aspect," *Journal of Food Engineering,* vol. 86, no. 2, pp. 225-233, 2008.

[12] A. Karakaya and M. Özilgen, "Energy utilization and carbon dioxide emission in the fresh, paste, whole-peeled, diced, and juiced tomato production processes," *Energy,* vol. 36, no. 8, pp. 5101-5110, 2011.

[13] E. Riggi and G. Avola, "Quantification of the waste stream from fresh tomato packinghouses and its fluctuations: Implications for waste management planning," *Resources, Conservation and Recycling,* vol. 54, p. 436–441, 2010.

[14] R. Toor, G. Savagea and C. Listerb, "Seasonal variations in the antioxidant composition of greenhouse grown tomatoes," *Journal of Food Composition and Analysis,* vol. 19, pp. 1-10, 2006.

[15] M. Augustus Leon, S. Kumar and S. Bhattacharya, "A comprehensive procedure for performance evaluation of solar food dryers," *Renewable and Sustainable Energy Reviews,* vol. 6, p. 367–393, 2002.

[16] A. Fudholi, K. Sopian, M. Ruslan, M. Alghoul and M. Sulaiman, "Review of solar dryers for agricultural and marine products," *Renewable and Sustainable Energy Reviews,* vol. 14, pp. 1-30, 2010.

[17] L. Ímre, "Chap. 13," in *Handbook of industrial drying, Third Edition,* EU, Taylor & Francis Group, LLC, 2006, pp. 308-309.

[18] M. Hossain and K. Gottschalk, "Determination of Optimum Conditions for Half Fruit Drying Kinetics of Tomato," *Bornimer Agrartechnische Berichte,* vol. 55, 2006.

[19] K. Sacilik, R. Keskin and A. Konuralp, "Mathematical modelling of solar tunnel drying of thin layer organic tomato," *Journal of Food Engineering,*

vol. 73, no. 3, pp. 231-238, 2006.

[20] Mateos-Espejel, Development of a strategy for energy efficiency improvement. PhD Thesis, Montreal, Canada: Department of Chemical Engineering, École Polytechnique de Montréal, 2009.

[21] W. Stahl and H. Sies, "Uptake of lycopene and its geometricalisomers is greater from heat-processed than from unprocessed tomato juice in humans," *Journal of Nutrition,* vol. 122, p. 2161–2166, 1992.

[22] R. Y. Chen, J. J. Wu, M. J. Tsai and M. S. Liu, "Effect of storage and thermal treatment on the antioxidant activity of tomato fruits," *Journal of the Chinese Agricultural Chemical Society*, vol. 38, p. 353–360, 2000.

[23] H. Wang, G. H. Cao and R. L. Prior, "Total antioxidant capacity of fruits," *Journal of Agricultural and Food Chemistry,* vol. 44, pp. 701-705, 1996.

[24] C. I. Nindo, T. Sun, S. W. Wang, J. Tang and J. R. Powers, " Evaluation of drying technologies for retention of physical quality and antioxidants in asparagus (Asparagus officinalis, L.).," *Lebensm. Wiss. Technol.,* vol. 36, pp. 507-516, 2003.

[25] C.-H. Chang, H.-Y. Lin, C.-Y. Chang and Y.-C. Liu, "Comparisons on the antioxidant properties of fresh, freeze-dried and hot-air-dried tomatoes," *Journal of Food Engineering*, p. 478–485, 2006.

[26] S. St. George and S. Cenkowski, "Dehydration processes for nutraceuticals and functional foods," in *Advances in food dehydration*, CRC Press, 2009, pp. 286-309.

[27] S. Sokhansanj and D. Jayas, "Handbook of industrial drying," in *Drying of Foodstuffs*, USA, Taylor and Francis, 2006, pp. 541-544.

[28] M. Krokida, Z. Maroulis and G. Saravacos, "The effects of the method of drying on the colour of dehydrated products," *Int. J. Food Sci. Technol*, vol. 36, pp. 53-59, 2001.

[29] N. Kerkhofs, C. Lister and G. Savage, "Change in colour and antioxidant content of tomato cultivars following forced-air drying," *Plant Foods*

Human Nutr., vol. 60, pp. 117-121, 2005.

[30] J. Shi, M. Le Maguer, Y. Kakuda, A. Liptay and F. Kiekamp, "Lycopene degradation and isomerisation in tomato dehydration.," *Food Research International,* vol. 32, pp. 15-21, 1999.

[31] M. Gómez-Gómez, "Deshidratado de tomate saladette en un secador de charolas giratorias," Mexico, 2009.

[32] A. Unadi, R. Fulle and R. Macmillan, "Strategies for drying tomatoes in a tunnel dehydrator," *Drying technology,* vol. 20, no. 7, pp. 1407-1025, 2007.

[33] W. Hayes, P. Smith and A. Morris, "The production and quality of tomato concentrates," *Crit. Reviews Food Science and Nutrition,* vol. 7, pp. 537-564,, 1998.

[34] S. CernÎsev and G. Sleagun, "Influence of dehydration technologies on dried tomato biological quality and value," *Agronomical research in Moldovia,* vol. 3, no. 131, pp. 63-68, 2007.

[35] T. Ramírez-Jiménez, Y. Meas, D. Dannehl, I. Schuch and L. Miranda, "Water and carbon footprint improvement for dried tomato value chain," *Journal of cleaner production,* no. 104, pp. 98-108, 2015.

[36] A. Hepbasli, "A comparative investigation of various greenhouse heating options using exergy analysis method," *Applied Energy,* vol. 88, no. 12, pp. 4411-4423, 2011.

[37] T. Ramírez, Y. Meas and K. Gottschalk, "Energy interaction of sub processes in drying value chain using exergy waste. Study case: drying and greenhouse growing of tomato," *Energy Procedia,* no. 57, pp. 1437-1446, 2014.

[38] D. Pimentel and M. Pimentel, "Chapter 11 Energy use in Fruit, vegetable and forage production," in *Food, Energy and Society,* CRC Press , 2007, pp. -400.

[39] “Food and Agricultural commodities production,” FAOSTAT, 2011.

[40] G. Page, B. Ridoutt and B. Bellotti, “Carbon and water footprint tradeoffs in fresh tomato production,” *Journal of Cleaner Production,* vol. 32, pp. 219-226, 2012.

[41] E. Fitz-Rodríguez, PhD Thesis. Decision support systems for greenhouse tomato production, THE UNIVERSITY OF ARIZONA, 2008.

[42] F. Bronchart, M. De Paepe, J. Dewulf, E. Schrevens and P. Demeyer, “Thermodynamics of greenhouse systems for the northern latitudes: Analysis, evaluation and prospects for primary energy saving,” *Journal of Environmental Management,* vol. 119, p. 121, 2013.

[43] J. Bakker, "Energy saving greenhouses," *Chron.Hortic.,* vol. 49, pp. 19-23, 2009.

[44] D. Dannehl, I. Schuch, T. Rocksch, S. Huyskens-Keil, U. Schmidt and A. Rojano-Aguilar, “Climate conditions in a closed greenhouse affect plant growth and secondary plant compounds of tomatoes (Solanum lycopersicum L.),” *Acta Horticulturae*, 2012 b.

[45] O. Jolliet, “Hortitrans a Model for Predicting and Optimizing Humidity and Transpiration in Greenhouses,” *Journal of Agricultural Engineering Research,* vol. 57, no. 1, pp. 23-37, 1994.

[46] G. N. Tiwari, Solar Energy Technology Advances, Nova Science Publishers Inc., 2005, p. 88.

[47] J. Bakker, “The effects of air humidity on flowering, fruit set, seed set and fruit growth of glasshouse sweet pepper (Capsicum annuum L.),” *Scientia Horticulturae,* vol. 40, no. 1, pp. 1-8, 1989.

[48] O. Jolliet and B. Bailey, “The effect of climate on tomato transpiration in greenhouses: measurements and models comparison,” *Agricultural and Forest Meteorology,* vol. 59, no. 1-2, pp. 43-62, 1992.

[49] O. Körner and H. Challa, “Process-based humidity control regime for greenhouse crops,” *Computers and Electronics in Agriculture,* vol. 39, no.

3, pp. 173-192, 2003.

[50] J. R. Duflou, J. Sutherland, D. Dornfeld, C. J. Herrmann and K. S. Jeswiet, “Towards energy and resource efficient ma-nufacturing: A processes and systems approach,” *CIRP Annals - Manufacturing Technology,* vol. 61, no. 2, pp. 587-609, 2012.

[51] N. Bansal and H. Garg, “Solar crop drying,” in *Advances in drying, Vol. 4*, Washington DC, Hemisphere, 1987, pp. 279-299.

[52] Y. H. Hui, Handbook of Food Science, Technology and Engineering, Volumen 3, Taylor & Francis, 2006.

[53] C. Ratti and A. S. Mujumdar, “Cap. 7 Drying of Fruits,” in *Processing fruits science and technology*, CRC Press LLC, 2005, pp. 1-33.

[54] M. N. A. Hawlader, M. S. Uddin, J. C. Ho and A. B. W. Teng, "Drying Characteristics of Tomatoes," *Journal of Food Engineering,* pp. 259-268, 1991.

[55] I. Doymaz, “Air-drying characteristics of tomatoes,” *Journal of Food Engineering 78,* p. 1291–1297, 2007.

[56] M. Colina Irezabal, Deshidratación de alimentos, Mexico: Trillas, 2010.

[57] Y. Jannot and Y. Coulibaly, “The "evaporativecapacity" as a performance index for a solar-drier air-heater,” *Solar Energy,* pp. 387-391, 1998.

[58] D. Marinos-Kouris and Z. Maroulis, “Cap 4. Transport Properties in the Drying of Solids,” in *Handbook of industrial drying*, Boca ratón FL, Taylos and Francis Group, 2006, pp. 82-83.

[59] M. Krokida, V. Karathanos, Z. Maroulis and D. Marinos-Kouris, “Drying kinetics of some vegetables,” *Journal of Food Engineering,* vol. 59, no. 4, pp. 391-403, 2003.

[60] Z. Maroulis, G. Saravacos and A. S. Mujumudar, “Ch. 5 Spreadsheet-Aided dryer design,” in *Handbook of Industrial Drying*, Taylor & Francis Group, 2006, pp. 121-134.

[61] K. Chua, A. Mujumdar, S. Chou, M. Hawlader and J. Ho, "Convective drying of banana, guava and potato pieces: Effect of cyclical variations of air temperature onconvective drying kinetics and color change," *Dry. Technol,* vol. 18, pp. 907-963, 2000.

[62] Y. Pan, L. Zhao, Z. Dong, A. Mujumdar and T. Kudra, "Intermittent drying of carrots: Effect on product quality," *Dry. Technol.,* vol. 17, p. 2323–2340, 1999.

[63] J. Bon and T. Kudra, "Enthalpy-driven optimization of intermittent drying," *Dry. Technol,* vol. 25, p. 523–532, 2007.

[64] A. S. Mujumdar, Handbook of industrial drying, 3. Edition ed., CRC Press, 2006.

[65] M. A. Hossain, K. Gottschalk and M. A. Amer, "Mathematical modelling for drying of tomato in hybrid dryer," *The arabian journal for science and engineering*, vol. 35, no. 2b, 2010.

[66] R. Stull, "Wet-bulb temperature from relative humidity and air temperature," *Journal of applied meteorology and climatology.*

[67] G. Zhen-Xiang and A. S. Mujumdar, "Software for Design and Analysis of Drying Systems," *Drying Technology*, pp. 884-894, 2008.

[68] J. B. Guinée, Handbook on Life Cycle Assessment: Operational Guide to the ISO Standards (Eco-Efficiency in Industry and Science), 1st ed., Springer, 2002.

[69] H.-J. Tantau, U. Schmidt, J. Meyer and B. Bessler, "Low Energy Greenhouse - a system approach," *Acta horticulture,* vol. 893, pp. 75-85, 2011.

[70] D. Dannehl, C. Huber, T. Rocksch, S. Huyskens-Keil and U. Schmidt, "Interactions between changing climate conditions in a semi-closed greenhouse and plant development, fruit yield, and health-promoting plant compounds of tomatoes," *Scientia Horticulturae*, no. 138, pp. 235-243, 2012 a.

[71] I. Schuch, D. Dannehl, L. Miranda-Trujillo, T. Rocksch and U. Schmidt, "ZINEG Project - Energetic Evaluation of a Solar Collector Greenhouse with Above-Ground Heat Storage in Germany," *Acta Horticulturae,* vol. 1037, pp. 195-201, 2014.

[72] D. Dannehl, M. Josuttis, S. Huyskens-Keil, C. Ulrichs and U. Schmidt, "Comparison of Different Greenhouse Systems and Their Impacts on Plant Responses of Tomatoes.," *Gesunde Pflanzen,* 2014 a.

[73] D. Dannehl, I. Schuch and U. Schmidt, "Plant Production in Solar Collector Greenhouses - Influence on Yield, Energy Use Efficiency and Reduction in CO2 Emissions," *Journal of Agricultural Science,* vol. 5, no. 10, pp. 34-45, 2013.

[74] D. Dannehl, J. Suhl, S. Huyskens-Keil, C. Ulrichs and U. Schmidt, "Effects of a special solar collector greenhouse on water balance, fruit quantity and fruit quality of tomatoes," *Agricultural Water Management,* vol. 134, pp. 14-23, 2014 b.

[75] J. Jaramillo, V. Rodríguez, M. Guzmán, M. Zapata and T. Rengifo, "Manual Técnico: Buenas Prácticas Agrícolas en la Producción de Tomate Bajo Condiciones Protegidas.," Organización de las Naciones Unidas para la Agricultura y la Alimentación -FAO-, Medellín, colombia, 2007.

[76] C. Pagella, R. Galli and D. Faveri, "Water reuse in industrial food processing," *The journal of food technology in Africa,* vol. 5, no. 1, pp. 25-29, 2000.

[77] OECD SIDS, "Citric Acid CAS No:77-92-9," UNEP Publications, Orlando, Fl, 2001.

[78] Federal Environmental Agency, "National Inventory Report Germany 2014," 2014.

[79] Country reports, "Trends in global energy efficiency 2011. Germany Energy efficiency report," Enerdata and the Economist Intelligence Unit., 2011.

[80] Energy Agency International, "CO2 emissions from fuel combustion Highlights," OECD-IEA, Paris, France, 2012.

[81] R. Tomás, F. Ramoa Ribeiro, V. Santos, J. Gomes and J. Bordado, "Assessment of the impact of the European CO2 emissions trading scheme on the Portuguese chemical industry," *Energy Policy,* vol. 38, no. 1, pp. 626-632, 2010.

[82] J. Gomes, J. Nascimento and H. Rodrigues, "Development of a Local Carbon Dioxide Emissions Inventory Based on Energy Demand and Waste Production," *Journal of the Air & Waste Management Association,* vol. 57, pp. 1032-1037, 2007.

[83] I. Schuch, D. Dannehl, T. Rocksch and R. Salazar Moreno, "The closed solar collector greenhouse- application concept and energetic examination for heat energy earning in summer 2010," *DGG-Proceedings,* vol. 1, no. 10, pp. 1-5, 2011.

[84] T. Blom, W. Straver, F. Ingratta, S. K. -. OMAF and W. B. -. OMAF, "OMAF Factsheet Carbon Dioxide in Greenhouses, Order No. 94-055," Queens printer for Ontario, Ontario, 2002.

[85] D. Pimentel, B. Berger, D. Filiberto, M. Newton, B. Wolfe, E. Karabinakis, S. Clark, E. Poon, E. Abbett and S. Nandagopal, "Cap. 14 Water Resources:Agricultural and Environmental Issues," in *Food, energy and Society (Third edition)*, FL, Taylor & Francis Group, LLC, 2008, pp. 183-184.

[86] S. A. Hatirli, B. Ozkanb and C. Fertb, "Energy inputs and crop yield relationship in greenhouse tomato production," *Renewable energy,* vol. 31, pp. 427-438, 2006.

[87] B. Khoshnevisan, S. Rafiee, M. Omid and M. H. Mousazadeh, "Environmental impact assessment of tomato and cucumber cultivation in greenhouses using life cycle assessment and adaptive neuro-fuzzy inference system," *Journal of Cleaner Production,* vol. Article in press, pp. 1-10, 2013.

[88] M. Mekonnen and A. Hoekstra, “The green, blue and grey water footprint of crops and derived crop products,” *Hydrol. Earth Syst. Sciences,* vol. 15, pp. 1577-1600, 2011.

[89] F. Correa Rodríguez and C. Uribe Saracho, “Reporte de actividades de cultivo de jitomates y zanahoria para Proyecto-CIDETEQ en el campus Amazcala de la Facultad de Ingeniería de la Universidad Autónoma de Querétaro,” 2014.

[90] I. Kemp, “Chapter 7 - Batch and time-dependent processes,” in *Pinch Analysis and Process Integration (Second Edition),* Oxford, Butterworth-Heinemann, 2006, pp. 257-287.

[91] T. Kotas, The Exergy Method of Thermal Plant Analysis., Fl, U.S.A.: Krieger, 1995.

[92] J. Szargut, D. R. Morris and F. R. Steward, Exergy analysis of thermal, chemical and metallurgical processes, New York: Hemisphere Publishing, 1988.

[93] M. J. Moran and H. N. Shapiro, Fundamental of Engineering Thermodynamics, 3 ed., New York.: John Wiley & Sons, 1995.

[94] I. Dincer and M. Rosen, “Chapter 8. Exergy analysis of drying processes and systems,” in *Exergy,* Amsterdam, Elsevie, 2007, pp. 103-126.

[95] E. Cook and H. DuMont, Process drying practice, McGraw-Hill, 1991.

[96] S. Sami, N. Etesami and A. Rahimi, “Energy and exergy analysis of an indirect solar cabinet dryer based on mathematical modeling results,” *Energy,* vol. 36, no. 5, pp. 2847-2855, 2011.

[97] M. Aziz, T. Oda and T. Kashiwagi, “Enhanced high energy efficient steam drying of algae,” *Applied Energy,* vol. 109, pp. 163-170, 2013.

[98] X. Liu, PhD thesis Energy Conservation by Recirculation of Drying Air, Knoxville: University of Tennessee, 1995.

[99] J. M. Flink, “Energy analysis in dehydration process,” *Food Technology,*

vol. 31, no. 3, p. 76–83, 1977.

[100] J. F. Thompson, M. S. Chhinnan, M. M. Miller and G. D. Knutson, " Energy conservation in drying of fruits in tunnel dehydrators," *Journal of Food Process Engineering,* no. 4, p. 155–169, 1981.

[101] W. M. Miller, " In plant study of potential for air recycling in fresh fruit drying," *Proceedings of the Florida State Horticultural Society,* no. 93, p. 332–333, 1980.

[102] T. R. Rumsey, J. F. Thompson and J. Young, "Simulation of fixed bed drying of english walnuts," *American Society of Agricultural Engineers,* pp. 281-354, 1980.

[103] J. Young, " Energy conservation by partial recirculation of peanuts drying air," *Transactions of the ASAE 1984 (3),* pp. 928-934, 1984.

[104] A. Iguaz, A. López and P. Vírseda, "Influence of air recycling on the performance of a continuous rotary dryer for vegetable wholesale by-products," *Journal of Food Engineering,* vol. 54, no. 4, pp. 289-297, 2002.

[105] K. Waldron, Handbook of waste management and co-product recovery in food processing, Boca Raton FL: Woodhead Publishing Limited, 2007.

[106] H. Al-Wandawi, M. Abdul-Rahman and K. Al-Shaikhly, "Tomato processing wastes as essential raw material sources," *Journal of Agricultural and Food Chemistry,* vol. 33, p. 804–807, 1985.

[107] U. Topal, M. Sasaki, M. Goto and K. Hayakawa, "Extraction of lycopene from tomato skins with supercritical carbon dioxide: Effect of operating conditions and solubility analysis," *Journal of the Science of Food and Agriculture,* vol. 54, no. 15, p. 5604–5610, 2006.

[108] S. Pengpad and W. Rakwichian, "Development of an air recycle solar drying system for continuous banana drying.," *Paper presented at the Asian Seminar and Workshop on Solar Drying Technology, 3–5 June, Phitsanulok, Thailand, ,* p. 27–34, 1998.

[109] G. Tokar, “Food drying in Bangladesh.,” Agro-based industries and technology project (ATDP), IFDC, Dhaka, 1997.

[110] M. Sana Ben and M. Salah Ben, “Drying Characteristics of Tomato Slices and Mathematical Modeling,” *International Journal of Energy Engineering*, vol. 4, no. 2A, pp. 17-24, 2014.

[111] A. Rao, Z. Waseem and S. Agarwal, " Lycopene content of tomatoes and tomato products and their contribution to dietary lycopene," *Food Res. Int*, vol. 31, p. 737–741, 1998.

[112] K. Böer, “Payback of solar systems,” *Solar Energy*, vol. 20, no. 3, p. 225–232, 1978.

[113] “http://global-climatescope.org/en/country/mexico/#/details,” [Online].

[114] SEDEA , “Censo agropecuario 2007,” Secretaría de Desarrollo Agropecuario, Querétaro, 2007.